UNIVERSITÀ DEGLI STUDI DI MILANO

PhD Course in Molecular and Cellular Biology

XXX Cycle

FUNCTIONAL CHARACTERIZATION OF SOX TRANSCRIPTION FACTORS IN ZEBRAFISH ANGIOGENESIS AND LYMPHANGIOGENESIS: KNOCKDOWN AND KNOCKOUT APPROACHES

Donatella D'Angelo

PhD Thesis

Scientific tutor: Monica Beltrame

Academic year: 2016-2017

SSD: BIO/18

Thesis performed at:
Dipartimento di BioScienze
Università degli Studi di Milano

Part I

Part I

ABSTRACT

My laboratory is interested in studying Sox (Sry-related HMG box) proteins, a family of transcription factors (TFs) present throughout the animal kingdom and important for the regulation of several fundamental processes during development (Pevny and Lovell-Badge, 1997; Wegner, 1999; Bowles et al., 2000). In particular, we focused on SOX18 that, together with SOX7 and SOX17, belongs to the SoxF subgroup (Bowles et al. 2000). In humans, mutations in *SOX18* are associated with the Hypotrichosis-Lymphedema-Telangiectasia (HLT) syndrome, combining defects in hair, blood vessels and lymphatic development (Irrthum et al., 2003). In zebrafish, Sox18 and Sox7 have a redundant role in regulating arterio-venous differentiation (Cermenati et al. 2008; Herpers et al. 2008; Pendeville et al. 2008; Hermkens et al. 2015), while only Sox18 is involved in lymphatic development (Cermenati et al., 2013). However, a recent article questioned the relevance of Sox18 role in zebrafish lymphatic vessel development, because a *sox18* mutant did not show a lymphatic phenotype (van Impel et al. 2014). To clarify Sox18 role in zebrafish lymphangiogenesis, we made use of a new, independent mutant allele: $sox18^{sa12315}$. In vivo analyses show that *sox18* mutant behaves as a null, indeed *sox18* mutation, associated with *sox7* perturbation, causes the absence of trunk tail circulation, the same phenotype observed in *sox7/sox18* double partial morphants and in *sox7/sox18* double mutants (Cermenati et al., 2008; Hermkens et al. 2015). Our data also point out that Sox18 has a conserved role in zebrafish lymphangiogenesis, with an interplay with VegfC in the formation of the thoracic duct (TD). The analyses of $sox18^{sa12315}$ mutation in two transgenic backgrounds reveal that, even if the mutation does not cause strong alterations of lymphatic system development, TD defects are statistically significant in homozygotes. Perturbation of Vegfc signaling exacerbates TD defects in a genotype-dependent manner; TD defects are highly enhanced in homozygotes, but even heterozygotes show statistically significant alterations when *vegfc* is slightly perturbed. The ectopic expression of *sox7* in the posterior cardinal vein (PCV), from which lymphatic precursors originate, can explain the only subtle lymphatic defects observed in *sox18* mutants transgenic line used for TD analyses. However, *sox7* ectopic expression is not seen in all the fish lines we have analyzed, suggesting that also in zebrafish, as in mouse, the fine regulation of *soxF* genes depends on the genetic background.

On the other hand, we are interested in studying the complex interplay between Sox and Notch signaling. This year we published a collaborative article showing, with knockdown and knockout approaches, that SoxF transcription factors positively regulate *notch1b* and *Notch1* vascular expression in zebrafish and mouse, respectively (Chiang et al., 2017). This work identifies SoxF responsive enhancers in *Notch1* and *notch1b* loci in mouse and in

zebrafish, respectively. SoxF binding to the zebrafish *notch1b* enhancer is functionally relevant: arterial ISV defects are indeed found in enhancer mutants under experimental conditions, which slightly perturb Notch signaling.

My laboratory is also interested in studying the role of *sox13* (subgroup D), a gene vaguely linked to angiogenesis in different models (Roose et al., 1998; McGary et al. 2010). We have the evidence that Sox13 is implicated in zebrafish angiogenesis and that SoxF positively regulate *sox13* (subgroup D) endothelial expression. In particular, *sox13* morphants show ISV defects and an upregulation of some genes implicating in the Notch pathway. In vivo SPIM time lapse was used to characterize in a dynamic way, through long-term time lapse analysis, the ISV defects observed in *sox13* morphants. With a combination of knockdown approaches in zebrafish and overexpression studies in vitro on ECs, we gathered evidence of an involvement of Sox13 in promoting endothelial cell migration.

Finally, we confirmed that SoxF positively regulate *sox13* by performing ISH analyses both in morphants and mutants.

Since SoxF positively regulate the Notch signaling and positively regulate the expression of *sox13,* a negative regulator of the Notch pathway, we can speculate the existence of a complex regulatory network between SoxF and Sox13 in fine-tuning vascular development.

STATE OF THE ART

Each organism develops through a series of events that lead to the formation of a complex multicellular system starting from a zygote. These processes require delivery of nutrients, oxygen, cellular and humoral factors to the developing organs and structures; all these functions are conducted by a functional cardiovascular system that is fundamental for a correct embryogenesis. For these reasons the establishment of a functional cardiovascular system is one of the earliest events that occur during organogenesis.
An accurate knowledge of the players, the signaling pathways and the mechanisms that regulate the correct patterning of the cardiovascular system is really relevant, especially because the molecular mechanisms involved in pathological processes could be sometimes similar or identical to those used during embryogenesis (Folkman, 1995).

In the past centuries, different animal models were used to examine the anatomy, the physiology and the development of the heart and the vascular vessels. The first description of the vascular network was performed in 1661 by Marcello Malpighi using a chicken embryo, while in 1905 M. Hoyer illustrated the lymphatic system in early tadpoles (Carmeliet, 2005). In the last two decades, the zebrafish has emerged as an innovative model system to go deeper into the mechanisms of cardiovascular development and the players that regulate this process in vertebrates since it provides a series of advantages (Lawson and Weinstein 2002b). The external development and the optical clarity of the embryos make it possible to perform in vivo imaging of the vascular system using a variety of labelling techniques such as endothelial specific expression of fluorescent proteins and microangiography (Lawson and Weinstein 2002b).
Morpholino and mRNA injection in the embryo at very early developmental stages are powerful techniques for manipulating gene expression.
Moreover, in 2006, the existence of a lymphatic system has been demonstrated also in zebrafish through the characterization of the thoracic duct (TD) and other lymphatic vessels in developing and adult zebrafish (Kuchler et al., 2006; Yaniv et al., 2006). This system shares important features with the lymphatic vessels of higher vertebrates including conserved anatomy, characteristic morphology, expression and function of genes important for mammalian lymphatic development and functional features, such as lack of connection to the blood vasculature and ability to clear fluid and macromolecules from surrounding tissues (Yaniv et al., 2006).

1.1 KNOCKDOWN AND KNOCKOUT APPROACHES IN ZEBRAFISH

One of the great advantages of using zebrafish as a model system is the possibility to manipulate gene expression by using morpholinos (MOs). MO oligomers differ from standard nucleic acids because of the presence of a six-ring heterocycle backbone and non-ionic phosphorodiamidate linkages that makes MOs more stable when injected in vivo. Morpholinos have a high affinity for RNA and minimal off-target. They are injected into 1-2 cell stage zebrafish embryos and they can act by blocking translation or by interfering with splicing; some MOs can also block microRNA maturation (Kok et al., 2015).
Given their ease use in zebrafish, MOs have enabled widespread analysis of gene function. However, MOs can induce p53-dependent apoptosis and off-target cell-type-specific changes in gene expression that confound phenotypic analysis (Robu et al., 2007).

The recent development of new genome engineering techniques, such as TAL effector nucleases (TALENs) and, especially, clustered regularly interspaced short palindromic repeats (CRISPR/Cas9), has allowed the facile generation of a lot of mutants (Kok et al., 2015). In CRISPR/Cas9 knockout technique, an RNA is injected into one-cell stage embryos, where it binds to its target DNA and induces a double strand break. Non-homologous end joining imprecise repair of this break introduces small insertions or deletions that can lead to mutations when targeting coding sequence. Lesions that occur within the germline are inherited by the progeny (Kok et al., 2015).

The availability of so many mutants has opened a debate in the zebrafish community about morpholino validity and reliability. This happens because not all the zebrafish mutants show the same phenotype of the corresponding morphants (Kok et al., 2015). It is the case of *sox18* mutants that do not show lymphatic defects; this questions *sox18* role in zebrafish lymphangiogenesis (van Impel et al. 2014). Another example is provided by the zebrafish mutant in the endothelial extracellular- matrix (ECM) gene *egfl7* that does not show the same vascular defects of the corresponding morphants (Rossi et al., 2015).

Initially it was stated that the phenotypic difference between morphants and the corresponding mutants was the prove of MO unreliability and off-target effects (Kok et al. 2015). However, recent studies have proposed gene expression compensation in mutant, but not knockdown animals, as the reason for the observed differences (Mohamed and Stainier 2017).

The before mentioned article about the zebrafish *egfl7* mutant (Rossi et al., 2015) was the first work demonstrating the activation of a compensatory network to buffer against

deleterious mutations which was not observed after translational or transcriptional knockdown. The authors demonstrated that their TALENs mutant does not show the vascular phenotype of the corresponding morphant because of the upregulation of other ECM proteins, specifically Emilins. This upregulation occurs in the mutant but not in morphant embryos. Moreover, minor or no vascular defects were observed upon *egfl7*MO injections into *egfl7* mutants, indicating that the phenotypic differences are not due to MO toxicity.

Similarly, *vegfaa* mutants do not show the same phenotype of their corresponding morphants because of *vegfab* upregulation, that occurs only in mutants (Rossi et al., 2015).

Discrepant phenotypes between mutants and their corresponding knocked-down animals have been reported not only in zebrafish but also in many other model systems. For example, germline mutants for *Pkm2* are viable and fertile; however, conditional deletion of *Pkm2* in MEFs limits nucleotide synthesis, leading to cell-cycle arrest. Similarly, *Sirt1* mutant mice have no obvious liver defects, while hepatocyte-specific *Sirt1* mutant mice develop fatty liver. In all the cases the hypothesis is that a compensatory network becomes established during germline maturation or embryonic development, allowing the organism to adapt to the mutation (Mohamed and Stainier 2017).

Two possible triggers of the transcriptional adaptation response have been proposed (Mohamed A. et al., 2017): the DNA lesion and the mutant mRNA.

In the first case, in response to a lesion, global chromatin reorganization may positively affect chromatin accessibility around the compensating gene, thereby leading to increased expression levels. Part of such a model is consistent with the process of dosage compensation in *Drosophila* where the male-specific lethal (MSL) proteins, together with other proteins, form a complex on the male X chromosome leading to H4K16 acetylation and subsequent induction of an open chromatin configuration, which is more accessible for transcription (Mohamed A. et al., 2017).

Many studies have reported that small non-coding RNAs generate from regions spanning a double-stranded break (DSB). These DSB-induced RNAs may act as guides for specific transcription factors or chromatin remodelers. The transmission of the transcriptional adaptation response to the next generation could occur through genomic imprinting via histone modification (Mohamed A. et al., 2017).

In addition, induction of *GADD45A* expression following DNA damage has been reported to induce global DNA demethylation in HEK293T cells, leading to increased activation of methylation-silenced promoters (Mohamed A. et al., 2017).

Another explanation to the transcriptional adaptation could be the presence of aberrant RNA forming as consequence of the mutation. If RNA fragments are long enough, they act similarly to long non-coding RNAs and, for example, guide specific transcription factors or chromatin remodelers to the regulatory regions of compensating genes through homology-mediated base pairing.

In conclusion, today it is believed that some mutants do not show the same phenotype of the corresponding knocked-down models because of genetic compensation that occurs when a DNA lesion was generated but not after gene knockdown. So, morpholinos reliability is still recognized, but there are some recommendations to take into account when using MOs. One of these is to design MOs targeting exons encoding domains that are necessary for protein function (Kok et al., 2015); moreover, the use of two or more independent MOs is recommended. It is also important to use MO doses that do not induce *p53* expression and, if necessary, alleviate off-target phenotypes by simultaneously reducing *p53* levels. One should use the dose of MO that does not cause additional phenotypes in a null mutant background (Rossi et al., 2015). It is also proposed to perform rescue assay with both a wild-type and a mutated form of the RNA of interest; the mutated form should not to give a rescue. The comparison of chromatin accessibility and epigenetic changes at the upregulated genes' regulatory regions in wild-type, mutant, and knockdown samples will thus be interesting.
Eventually, whenever possible, the best way to be sure that a MO does not have off target effects is to compare the phenotype of the morphant with that of the corresponding mutant, if available, taking in consideration that in the mutant genetic compensation could occur.

1.2 VASCULAR DEVELOPMENT: VASCULOGENESIS AND ANGIOGENESIS

The external development, the optical clarity and the capacity to easily visualize the vascular tree and the blood circulation using a variety of labelling techniques make the zebrafish a useful model to study vascular morphogenesis *in vivo*. Furthermore, the small size of the zebrafish embryo ensures a sufficient supply of oxygen by passive diffusion for them to survive and develop for several days in condition of absence of blood circulation. This makes possible the *in vivo* study of conditions that alter considerably the cardiovascular system (Weinstein 2002).

Zebrafish has a closed circulatory system which shares many characteristics with those of humans and other higher vertebrates. In particular, the anatomical processes and the molecular mechanisms that regulate the assembly of a primary vascular network and its successive remodelling are highly conserved (Isogai et al., 2001; Isogai et al., 2003).

Two fundamental phases characterize vascular development in vertebrates: vasculogenesis and angiogenesis.

The primitive vascular network in vertebrate embryos forms by *vasculogenesis*. This process consists of *de novo* blood vessel formation by angioblasts aggregation and cavitation (Risau and Flamme, 1995). Angiogenesis is the process in which the primary vascular plexus remodels into an arborized network of large and small vessels by sprouting and branching (Risau, 1997). Lymphatic capillaries are mainly derived from veins (Sabin, 1902; Alitalo, 2011) (Fig. 1.1).

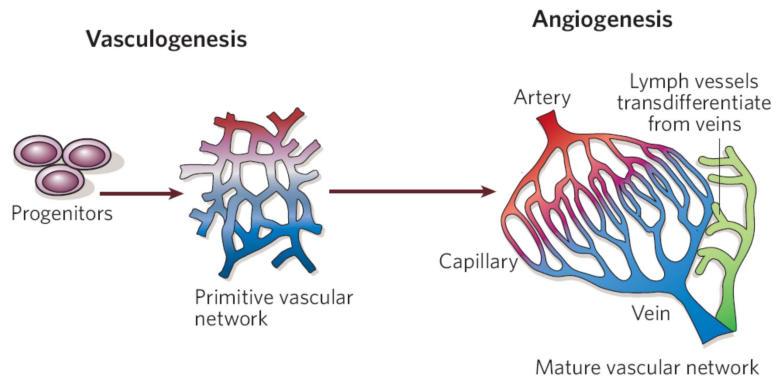

Fig. 1.1 Development of the vascular system in vertebrates. During vasculogenesis, endothelial progenitors give rise to a primitive vascular network, that will be remodeled and expanded during angiogenesis. Lymph vessels develop via trans-differentiation from veins. (Modified from Carmeliet, 2005).

1.2.1 Vasculogenesis in zebrafish

In zebrafish, as in other vertebrates, it has been hypothesized that endothelial and hematopoietic cells derive from a common progenitor, the hemangioblast, which originates from the lateral plate mesoderm (LPM) (Davidson and Zon, 2004).

The first evidence of the existence of these cells was provided from the *cloche* mutant, in which there is a great reduction of both endothelial and hematopoietic progenitors (Stainier et al., 1995). In addition, genes such as *stem cell leukemia -scl-* and *fetal liver kinase-1/vascular endothelial growth factor receptor 2 –flk1/vegfr2* are required for the formation of both lineages in both zebrafish and mouse (Kallianpur et al., 1994; Kabrun et al., 1997; Liao et al., 1998).

Endothelial specification occurs during early somitogenesis when angioblasts, endothelial cell precursors, begin to express genes specific of endothelial identity (Fouquet et al., 1997). Among these genes, a set of E26 transformation-specific (ETS) transcription factors are fundamental (Lelievre et al., 2001; Sumanas and Lin, 2006; Pham et al., 2007). Indeed, the simultaneous knockdown of four ETS genes (*fli1a, fli1b, ets1* and *ets-variant-2)* caused severe defects in vascular development (Pham et al. 2007).

Recently, it has been demonstrated that in zebrafish *etv2*/*etsrp* marks two different populations of angioblasts within the posterior LPM: medial angioblast and lateral angioblasts. These populations originate at different time points and are located at different distances from the dorsal midline. The former population corresponds to arterial progenitors of the dorsal aorta (DA), while lateral angioblasts give rise to the venous endothelial cells of the posterior cardinal vein (PCV) (Kohli et al., 2013).

Both vascular endothelial growth factor (Vegf) and sonic hodgehog (Shh) concentrations are important for the proper migration and contribution of both pools of angioblasts to the DA and the PCV (Lawson and Weinstein, 2002).

At around the 10 somite stage, *shh*, expressed by the notochord, induces the expression of *vegf* by the surrounding somites (Lawson and Weinstein, 2002) (Fig. 1.2). Vegf is important for medial angioblasts migration intersomitically to the midline over the endoderm in the anterior to posterior direction to form the DA. After the 15 somites stage, lateral precursors migration starts to give rise to the PCV with a migrational behavior similar to that of the medial angioblasts, (Kohli et al., 2013) (Fig. 1.2).

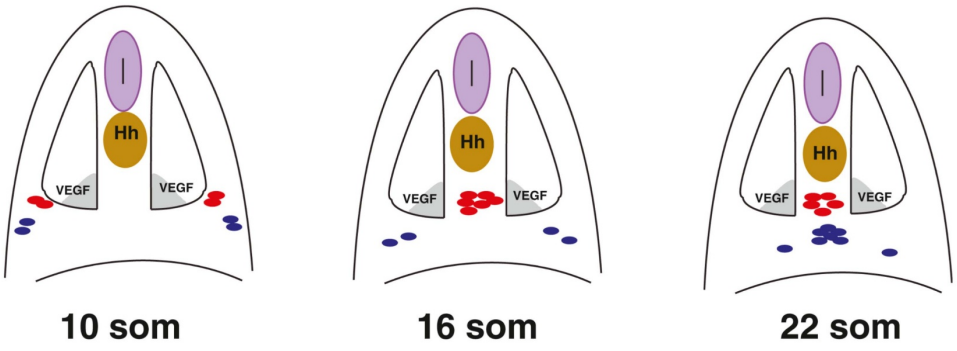

Fig. 1.2 Molecular control of vasculogenesis. During early somitigenesis *shh* expression by the notochord induces *vegf* expression in the somites (10 som). After the 10-somite stage, medial angioblasts migrate to the midline directly to the dorsal position where they differentiate as arterial cells. Shortly after the 15-somite stage, the lateral angioblasts migrate to the ventral position at the midline where they differentiate as venous endothelial cells. (Neural tube in purple, notochord expressing *shh* in brown, *vegf* expressed in the ventral somites, medial angioblasts in red and lateral angioblasts in blue) (Kohli et al., 2013).

In an alternative proposed model, the DA forms by classical vasculogenesis, whereas formation of the PCV involves a selective sprouting of venous-fated angioblasts from the DA; cell-cell segregation allows distinct arterial and venous vessels to form (Herbert et al., 2009).

At around 24 hours post fertilization (hpf), blood circulation starts and the main axial vessels are formed and luminized (Isogai et al., 2001). Initially, blood flows through a simple single circulatory loop which goes caudally from the heart through the DA and returns rostrally via the PCV (Lawson and Weinstein, 2002) (Fig.1.3).

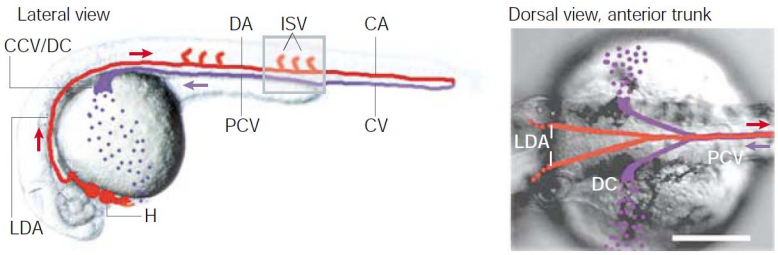

Fig. 1.3 Primary circulation in zebrafish embryo at 30 hpf. Blood leaves the heart (H) and enters the lateral dorsal aortae (LDA), which converge into the dorsal aorta (DA). The circulation flows into the caudal artery (CA), then into the caudal vein (CV) and returns rostrally through the posterior cardinal vein (PCV). Finally, it leaches through the Duct of Cuvier (DC), before returning to the heart (Lawson and Weinstein, 2002).

In the past, it was thought that arteries and veins acquired structurally and functionally distinct features in response to a different blood flow rates and pressure. Now we know that arteries and veins are specified by a complex genetic program before the onset of circulation (Lawson and Weinstein, 2002).

In mice, arterial-venous differentiation is driven by EphrinB2/Ephrin-ReceptorB4 signaling (Wang et al., 1998). In zebrafish, the Notch pathway activates an arterial while repressing a venous cell fate program within the presumptive DA. Embryos lacking Notch activity fail to induce arterial specific *efnb2a* expression, and exhibit ectopic expression of venous markers (Lawson et al., 2001).

Eventually COUP-TFII, a member of the orphan nuclear receptor superfamily, is specifically expressed in venous but not arterial endothelium. Ablation of COUP-TFII in endothelial cells enables veins to acquire arterial characteristics, including the expression of Notch signaling molecules. Thus, COUP-TFII has a critical role in repressing Notch signaling to maintain vein identity, which suggests that vein identity is under genetic control and is not derived by a default pathway (You et al. 2005; Aranguren et al. 2013; Swift et al. 2009).

1.2.2 Angiogenesis in zebrafish

The primary vascular plexus, formed by vasculogenesis, remodels in a mature and more complex network of vessels during angiogenesis.

If we focus our attention on the trunk/tail region of the zebrafish embryo, the main vessels which are formed through this process are: the intersomitic vessels (ISVs), the dorsal longitudinal anastomotic vessels (DLAVs), the sub-intestinal vein (SIV) basket, and the caudal vein plexus (CVP; Fig.1.4). Each structure is regulated by a specific interplay of different molecular pathways (Isogai et al., 2001).

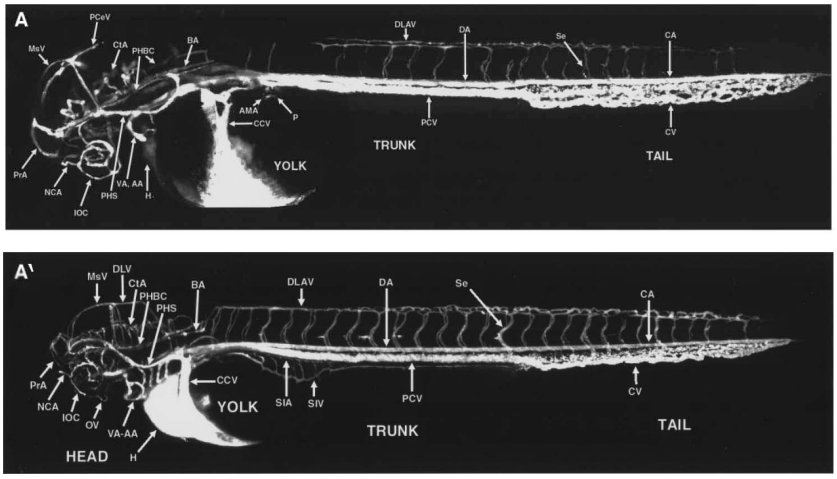

Fig.1.4 Microangiography of zebrafish embryos at 2 and 3 days post fertilization (dpf). (A and A'). Vessels of the trunk-tail region: dorsal longitudinal anastomotic vessel (DLAV), dorsal aorta (DA), intersomitic vessels (Se or ISV), caudal artery (CA), caudal vein (CV), posterior cardinal vein (PCV), sub-intestinal artery (SIA) and vein (SIV)(Isogai et al., 2001).

In zebrafish, as in other vertebrates, ISVs are among the first angiogenic vessels to form. Their formation requires two waves of endothelial cell migration that occur at different developmental stages, first from the DA and then from the PCV (Isogai et al., 2003).

At 22 hpf, a set of primary sprouts emerges from the DA and migrates towards the dorsal region of the embryo, following each vertical somites boundary (Fig.1.5A). These sprouts reach the dorsal portion of the embryo and branch rostrally and caudally to connect with their neighbors to form the DLAVs (Fig.1.5B-D) (Ellertsdottir et al., 2010).

At 32-34 hpf, secondary sprouts begin to emerge from the PCV, growing dorsally alongside the primary ISVs (Fig.1.5 C and D). About half of these secondary sprouts connects with the adjacent primary ISVs which loose the connection with the DA and become venous ISVs

(vISV; Fig1.5 D and E). The primary ISVs which are not attached by the secondary sprouts maintain an arterial identity and constitute the arterial ISVs (aISVs) (Isogai et al., 2003).

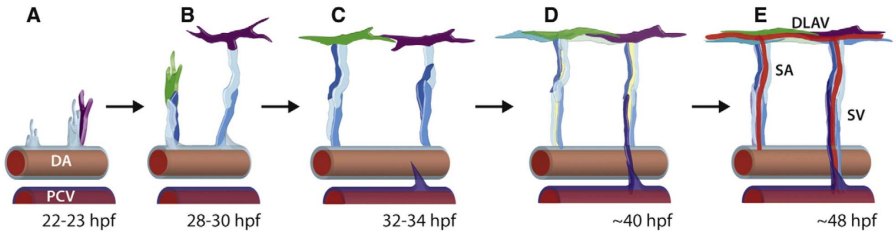

Fig.1.5 ISV and DLAV formation in the zebrafish trunk. Primary sprouts start from the DA and migrate dorsally to form aISV (or SA) and DLAV (A-C). Secondary sprouts originate from the PCV and a half of these connect to primary ISV, forming vISV (or SV; C-E) (Ellertsdottir et al., 2010).

The other half of the secondary sprouts stop at the horizontal myoseptum and give rise to a pool of lymphatic precursors, the parachordal lymphangioblasts (PLs) (Bussmann et al., 2010).

Both in mouse and in zebrafish, a single ISV sprout is formed by two different types of cells: the tip and the stalk cells. The tip cell is located in the apical portion of the sprout and it is characterized by long dynamic filopodial extensions, essential for the correct growth and migration of the vessel (Gerhardt et al., 2003; Siekmann and Lawson, 2007b). The stalk cells are behind the tip cells and are important to make up the base of the sprout and maintain the connection with the vessel of origin (Siekmann and Lawson, 2007a).

Regulation of the correct identity of each of these cells is essential for the proper patterning of the vasculature. As new vessels grow, migrating endothelial cells must also proliferate, which presents tip cells with a problem, as each daughter cell must acquire a different migratory profile dependent on their resultant position. The more distal daughter takes on tip cell identity, while the more proximal daughter becomes the trailing stalk cell. A very recent work reveals that tip cells use a form of asymmetric cell division to promptly generate daughters with distinct tip or stalk cell identity (Fig. 1.6). After tip cell division, the distal daughter immediately acquires tip cell- like motility whereas the proximal daughter displays motility near identical to a stalk cell (Costa et al., 2017). The motility of each daughter cell after division is positively correlated with their size: the larger distal daughter of tip cell division inherits a greater proportion of the Vegf signaling machinery and displays higher levels of Vegf signaling, establishing it as the leading tip cell (Costa et al., 2017).

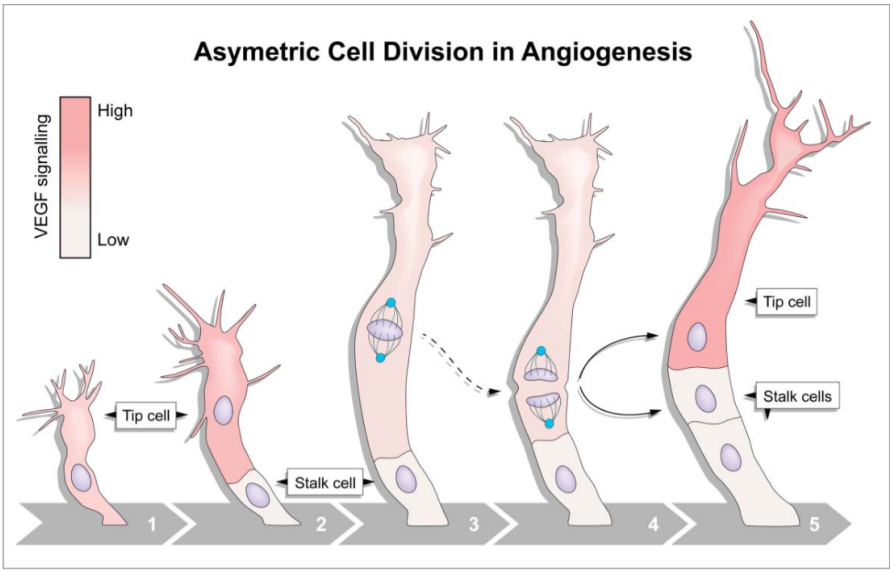

Fig. 1.6 Asymmetric endothelial cell division. Highly motile endothelial tip cells sprout from parental vessels (1) and lead stalk cells (2). Upon tip cell division, the mitotic spindle (3) is displaced to the proximal pole of the cell (4) before anaphase. This introduces cell size asymmetry and generates daughter cells with distinct Vegf signaling levels and behaviors (5). (Costa et al., 2017)

Vegfa signaling, which induces an endothelial cell to acquire a motile and invasive behavior, is required for tip cell differentiation (Gerhardt et al., 2003).

In the tip cell, Vegfr2 is active and stimulates the up-regulation of the Notch ligand Delta-like4 (Dll4) that up-regulates the Notch signaling in the neighboring cells, making them to acquire a stalk cell identity through a lateral inhibition mechanism (Fig. 1.7) (Leslie et al., 2007; Siekmann and Lawson, 2007b; Jakobsson et al., 2010). Notch activation in the stalk cells suppresses angiogenetic activity of Vegfr-3/Flt4 signaling (Siekmann and Lawson, 2007b; Tammela et al., 2008). Notch signaling inhibition, by DAPT (a γ-secretase inhibitor) or by genetic manipulation, causes hyper-sprouting both in zebrafish and in mouse (Siekmann and Lawson 2007; Hellstrom et al. 2007). The lateral inhibition mechanism has been recently questioned by Shane Herbert (DVB Meeting) because it takes too long to occur; the acquisition of stalk cell identity must be driven by a process faster than lateral inhibition.

The Wnt pathway is also important during angiogenesis. While in mice its role is well defined, indeed *loss-of-function* and *gain-of-funcion* mutants shows anomalous sprouting (Corada et al. 2010), there are only two articles describing its role in zebrafish (Cirone et al. 2008; Gore et al. 2011). However also in zebrafish, Wnt pathway alteration leads to defects in ISVs formation.

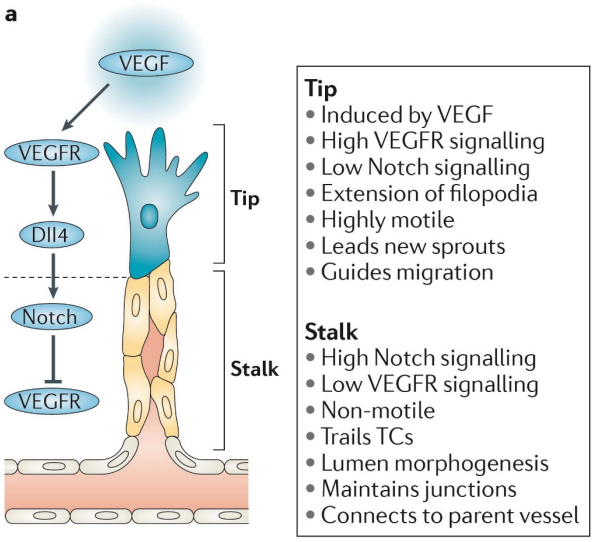

Fig. 1.7 Molecular mechanism of tip and stalk identity acquisition well reviewed in (Herbert and Stainier, 2011).

The caudal vein plexus is formed by a dorsal and a ventral vein interconnected by a series of sprouts which give rise to an honeycomb-like structure (Isogai et al., 2001). Sprouting from the axial vein is mainly regulated by bone morphogenetic protein (BMP) signaling (Wiley et al., 2011). However, also Vegfa, which is considered the typical regulator of arterial sprouting, seems to be involved in CVP remodeling (Rissone et al., 2012).

The SIVs run cranial ward along the yolk or the ventral walls of the intestine on both right and left sides (Isogai et al., 2001). These vessels originate from the duct of Cuvier at 2 dpf, however a partial contribution from the PCV has been recently proposed (Hen et al., 2015). During the next 24 hours, these vessels evolve in vascular plexus across most of the dorsal–lateral aspect of the yolk ball and will provide, together with the supra-intestinal artery, blood supply to absorb the yolk (Nicoli and Presta, 2007). The molecular mechanisms that regulate the SIV basket formation are not well characterized as in other districts, however an involvement of BMP signaling has been demonstrated , electing BMP as a main regulator of venous angiogenesis (Wiley et al., 2011). A recent work (Hen et al., 2015) show that other molecular pathways are important for the SIV formation. While the BMP signaling is essential for the ventral migration and expansion of the plexus (Wiley et al., 2011), the dorsal migration phase is driven by the *kdrl/plcg1* axis. The Notch signaling is dispensable for earlier phases of SIV formation, but it is essential for the late step, indeed Notch pathway participates in the remodeling of the subintestinal plexus involving retraction of venuos leading buds (Hen et al., 2015).

1.2.3 Lymphangiogenesis

The lymphatic system has a lot of important functions such as control of tissue fluid homeostasis, fat absorption and a role in the immune response; for this reason it is a very crucial part of the vascular system (Tammela and Alitalo, 2010).

In mammals, the lymphatic system has a venous origin, indeed, lymphatic precursors arise from the cardinal vein and give rise to the early lymph-sacs (Sabin, 1902; Oliver and Srinivasan, 2010). The remodeling of these structures, the ballooning from the cardinal vein and the migration as single cells allow the formation of the mature lymphatic vasculature (Francois et al., 2012; Hagerling et al., 2013).

The existence of a zebrafish lymphatic system has been demonstrated only in the last decade; lymphatic vessels derive mainly from veins also in zebrafish as in mammals (Kuchler et al., 2006; Yaniv et al., 2006).

As I mentioned above, lymphangiogenesis starts at 1.5 days post fertilization (dpf) when lymphatic precursors (PLs) originate from secondary sprouting, arising from the PCV, migrate along aISVs and transiently reside at the horizontal myoseptum at around 2-2.5 dpf. Then, some precursors migrate dorsally forming lymphatic intersomitic vessels (ISLVs) and the dorsal longitudinal lymphatic vessels (DLLVs), while other PLs migrate ventrally and give rise to the thoracic duct (TD; Fig. 1.8), the main trunk lymphatic vessel (Bussmann et al., 2010). The TD, located between the DA and the PCV, starts forming at 3.5 dpf and it is completely formed at 5 dpf.

Recently, it has been demonstrated that PLs derive from a specific subset of cells positioned in the ventral wall of the PCV and that express genes characteristics of both arterial and venous lineages such as *notch1b*, *nr2f2* and *fzd7a* (Nicenboim J. et al 2015).

In the last few years, new zebrafish transgenic lines allowed to uncover previously uncharacterised lymphatic vascular beds, such as the facial lymphatics (FLs), the lateral lymphatics (LL), the intestinal lymphatics (IL) (Koltowska et al., 2013) and the lymphatic vessels of the brain (Jung et al., 2017).

The molecular pathways driving zebrafish lymphangiogenesis are shared with mammals and the most important of them is the signaling driven by vascular endothelial growth factor VEGFC and its receptor VEGFR3/Flt4.

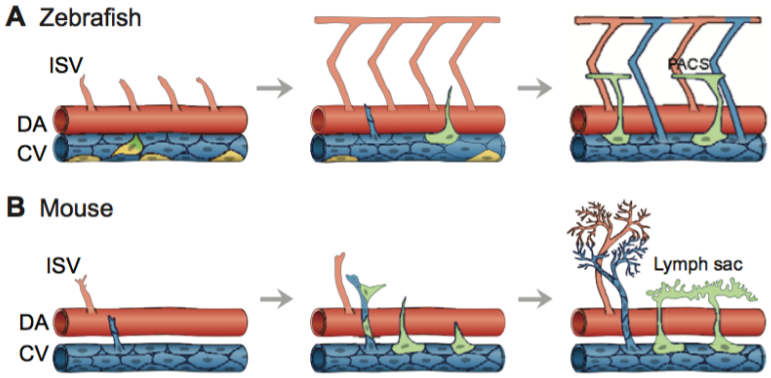

Fig. 1.8 An overview of lymphatic system development. Schematic model of early lymphatic development in zebrafish (A) and mouse (B). Arteries and veins are shown in red and blue, respectively. In both zebrafish and mouse, the cardinal vein (CV, blue) acts as a source of cells that become specified towards a lymphatic fate (green), giving rise to parachordal cells (PACs), which are the building blocks of the fish lymphatic system, or lymph sacs in the case of mouse. In mouse, lymphatic endothelial cells (LECs) also bud off from intersomitic veins (B, middle panel). In zebrafish, lymphatic progenitors are derived from a subpopulation of specialized angioblasts (yellow) within the posterior cardinal vein (PCV) through asymmetric cell division (Jung et al., 2017).

Mammalian VegfC is a potent inducer of lymphatic sprouting (Jeltsch et al., 1997; Saaristo et al., 2002) and Vegfc knockout mice die during embryogenesis due to lymphatic system alterations (Karkkainen et al. 2004). Analogously, in zebrafish, the *vegfc* knockdown affects TD formation, zebrafish *vegfc* mutants fail to establish a proper lymphatic system, developing lymphatic hypoplasia and lymphedema and zebrafish *flt4* mutant (*expando*) lacks lymphatics vessels and venous sprouting (Kuchler et al., 2006; Yaniv et al., 2006; Hogan et al., 2009).

Another gene important for zebrafish lymphatic development is *ccbe1* (*collagen and calcium binding EGF domain 1*). The story of this gene shows the importance of zebrafish as a model to study lymphangiogenesis, since *ccbe1* has been discovered for the first time in zebrafish in the *full-of-fluid* mutants lacking lymphatic vasculature (Hogan et al. 2009b). Then the murine counterpart has been studied and now we know that, in human, mutations in this gene cause the Hennekam syndrome, characterized by lymphedema and mental disabilities (Alders et al. 2009; Connell et al. 2010). *ccbe1* is expressed in non-endothelial cells and acts non-autonomously during embryonic lymphangiogenesis driving lymphangioblasts migration from the PVC during secondary sprouting (Hogan et al. 2009b). Moreover, *ccbe1* is involved in VEGF-C activation, indeed, together with ADAMTS3 metalloproteinase, it is essential for the cleavage of VEGF-C into its active form both *in vivo* and *in vitro* (Vaahtomeri et al., 2017). Importantly, *CCBE1*-inactivating mutations have been found in patients with Hennekam syndrome, which involves severe lymphedema (Alders et al. 2009,

2013; Connell et al. 2010). Furthermore, homozygous *Ccbe1* mutations prevent the formation of all primitive lymphatic structures both in mouse and zebrafish (Hogan et al. 2009b; Bos et al. 2011).

SoxF transcription factors are important for lymphangiogenesis. In mammals, Sox18, with Prox1 and Coup-TFII, is at the top of the molecular hierarchy of TFs that drive lymphatic development. In venous cells, Sox18 cooperates with the nuclear receptor Coup-TFII to activate the expression of the lymphatic master gene Prox1 (Fig. 1.9) (Watabe 2012).

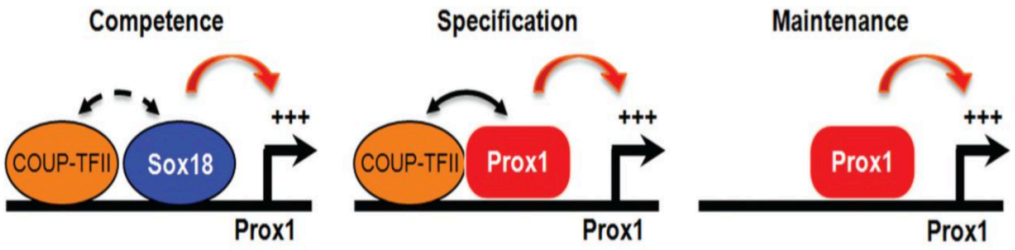

Fig. 1.9 Lymphatic transcriptional specification network. The hypothetical interaction between Sox18 and Coup-TFII (dotted line) activates Prox1transcription in a subset of venous endothelial cells that are committed in a lymphatic lineage. Prox1 is able to maintain its own expression in lymphatic cells (modified by Watabe 2012).

Venous cells expressing Prox1 are committed in a lymphatic lineage and start to migrate following Vegfc gradient to give rise to the early lymph-sacs (Oliver and Srinivasan 2010).

However, recent data published on zebrafish mutants have questioned the evolutionary conservation of the entire Sox18/Prox1/Coup-TFII regulatory axis because *prox1a*^{i278}, *coup-TFII*^{hu10330} and *sox18*^{hu10320} mutants were reported not to share lymphatic defects (van Impel et al. 2014).

Knockdown studies in my laboratory, instead, showed that Sox18 plays a conserved role in lymphatic development, indeed *sox18* morphants are not able to form a normal thoracic duct. Moreover, *sox18* genetically interacts with the central lymphatic growth factor *vegfc* in the early phases of lymphatic development since the combined partial knockdown of *sox18* and *vegfc*, using subcritical doses of specific morpholinos, causes defects in both venous and lymphatic sprouting (Cermenati et al. 2013). These data are in agreement with a recent work demonstrating that *prox1a* has a crucial role also in zebrafish lymphangiogenesis and suggest that Sox18/Prox1/Coup-TFII regulatory axis could be conserved also in this animal model (Koltowska et al. 2015).

1.3 THE SOX FAMILY

SOX (Sry-related-HMG box) proteins are a family of transcription factors found throughout the animal kingdom. They have been implicated in cell fate decisions in numerous developmental processes and they have diverse tissue-specific expression patterns during early development (Pevny and Lovell-Badge, 1997; Wegner, 1999; Bowles et al., 2000).

SOX proteins are characterized by the presence of a DNA-binding high mobility group (HMG) box domain (Bowles et al., 2000). The HMG box is 79 aa long and consists of three alfa helices which can bind the minor groove of the DNA to ATTGTT or related sequences motifs. This binding widens the minor groove and causes DNA to bend towards the major groove (fig. 1.10) (Lefebvre et al. 2007; Kamachi and Kondoh, 2013).

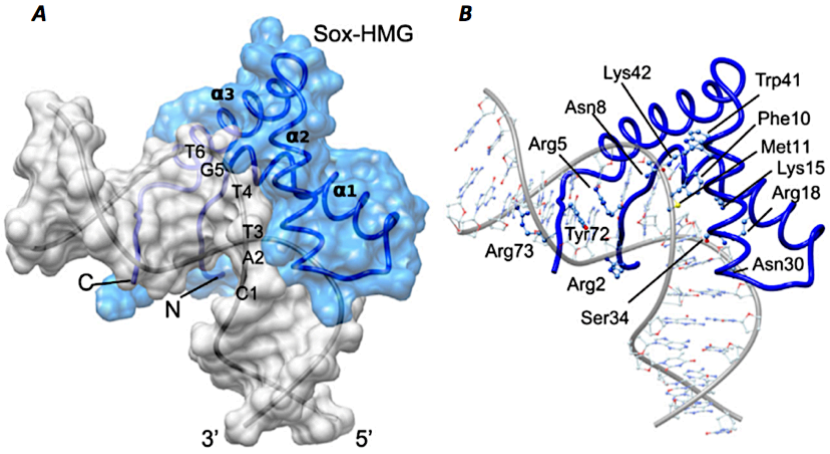

Fig. 1.10 Tridimensional representation of DNA/HMG-box interaction. A) Topological model of the Sox HMG (blue) bound to DNA (gray). Helices a1–a3, N-and C-termini and the position of the CATTGT core element are marked. B) The DNA bases and the DNA contact amino acids are shown as ball-and-sticks. (Modified from Hou et al. 2017).

In 1990, *SRY* (Sex determining region Y) was the first SOX family gene identified in humans and mouse where it is important for male sexual determination (Gubbay et al. 1990). By convention, HMG domains of SOX proteins are at least 50% identical to the HMG domain of SRY. However, over the years, new SOX genes, which do not confirm this rule, have been identified. For these reasons, recent studies classify SOX proteins on the base of the conservation of a key motif within the HMG box: the sequence RPMNAFMVW (position 5-13) that appears to be conserved in all SOX proteins but not in the most closely related outgroups (Bowles et al., 2000). In mouse and humans, the SOX family comprises 20 genes (Schepers et al., 2002) that have been divided into 8 groups (A-G) according to sequence similarity and genomic organization (Bowles et al., 2000) (Fig. 1.11).

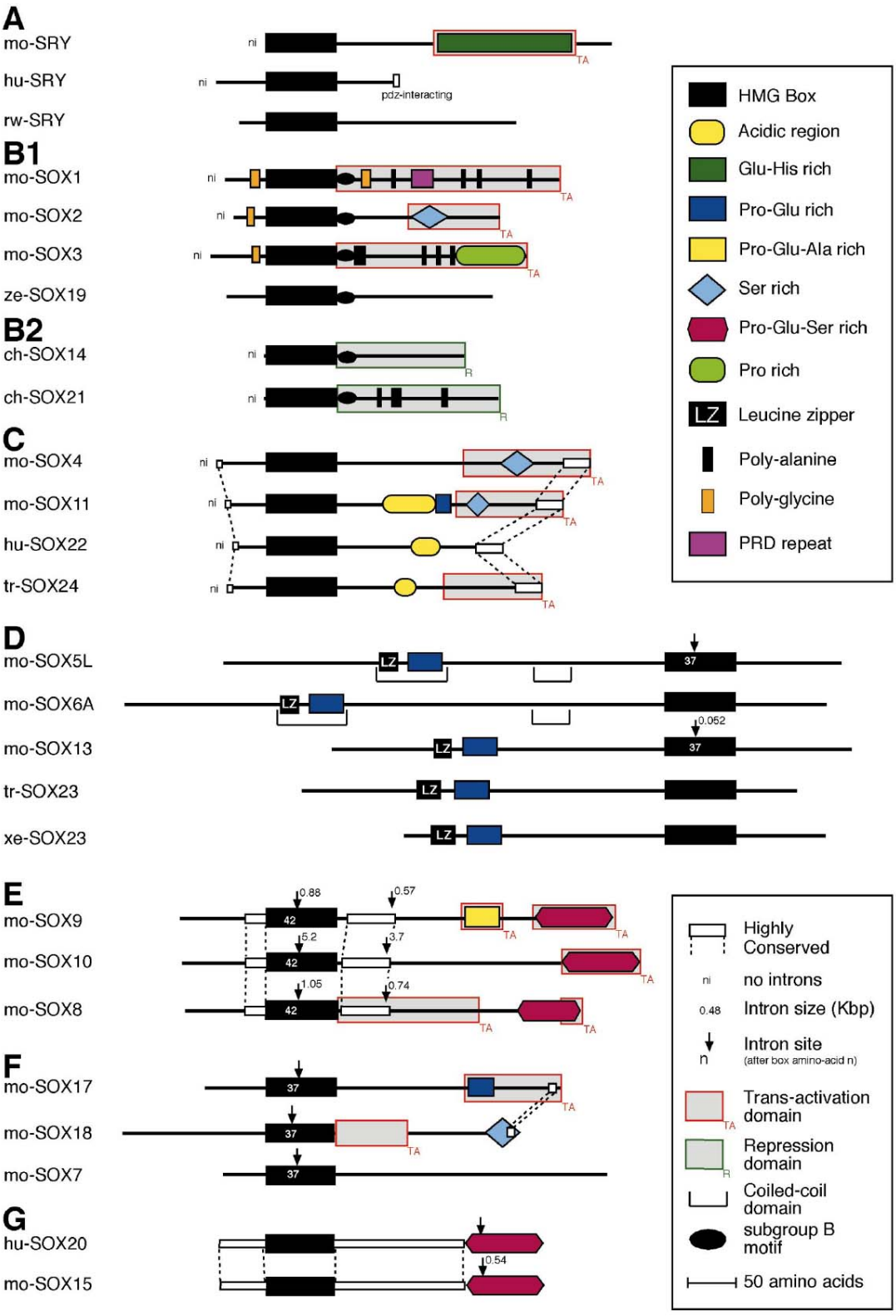

Fig.1.11 Schematic representation of SOX proteins highlighting conserved region and domain within SOX family groups. Proteins are arranged in groups as defined by HMG box domain sequence. Various structural features, motifs, and functional regions are shown along with intron positions and sizes where known (Bowles et al., 2000).

The identity of the HMG-box domain is very high (70-95%) among proteins of the same subgroup, while proteins belonging to different subgroups may show only a minor degree of identity both in the HMG-box and in other regions (Lefebvre et al. 2007).

It is not unusual that members of the same groups, when expressed in the same developing tissue, share equivalent functions, and so, many redundant roles between SOX proteins that co-regulate the same targets have been observed (Kamachi and Kondoh, 2013). The transcriptional activity of a SOX protein is strictly related to the necessity to form a complex with other partner transcription factors, thus, a Sox binding site in the DNA is accompanied by a second binding site for its partner (Kondoh and Kamachi, 2010). During the interaction with the partners, the HMG-box domain is important for protein-protein interaction, but the other domains of the SOX protein are fundamental both to stabilize and to give specificity to the interaction.

A three-step model has been proposed to explain the specificity of the interaction between SOX protein and their targets. In this model, the SOX proteins and the equivalent partner bind to adjacent sites on the DNA and interact through the HMG-box domain. The so formed protein complex is then influenced by not HMG-box domains of the SOX protein (Fig. 1.12) (Wilson and Koopman 2002).

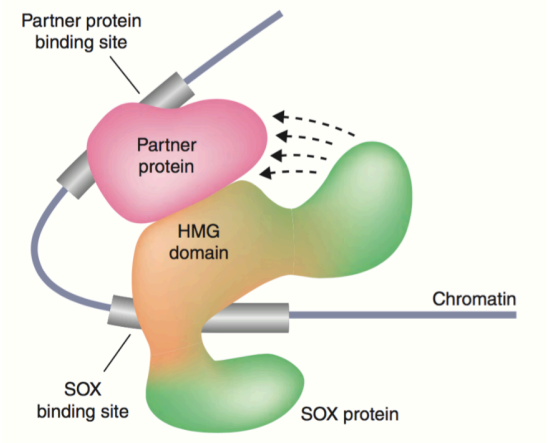

Fig.1.12 Model to explain the specificity of SOX protein transcriptional activity. The SOX protein and its partner (in pink) bind adjacent sites on the DNA and interact towards the HMG-box domains (in orange). Not HMG-box domains influence the complex by stabilizing it. (Wilson and Koopman 2002).

The correct shuttling nucleus-cytoplasm is very important to regulate SOX protein activity. Even in this case a major role is performed by the HMG-box domain. In the C-terminus and in the N-terminus of this domain there are nuclear localization signals (NLS/NES) that are recognized by importins to mediate the active transport of transcription factors from the

nucleus to the cytoplasm (Poulat et al. 1995). Alteration in this process of import-export cause severe defects during organogenesis (Poulat et al. 1995; Smith and Koopman 2004).

1.3.1 SOXF *group*

SOX18, together with SOX7 and SOX17, belongs to the SOXF group (Bowles et al. 2000). The structure of the *SoxF* genes is conserved throughout the animal kingdom and it is characterized by the presence of only one intron within the HMG-box coding region (Bowles et al. 2000).

SoxF proteins are characterized by high identity in the HMG-box domain, localized at the N-terminus. A trans-activation domain (TAD) is in the central part of Sox18 and Sox7, while in Sox17, the TAD domain is located at the C-terminus (Hosking et al., 1995). A beta-catenin interaction motif is present in the C-terminus of Sox7 and Sox18; in Sox17 this motif precedes the TAD domain (fig. 1.13) (Sinner et al., 2004; Sandholzer et al., 2007).

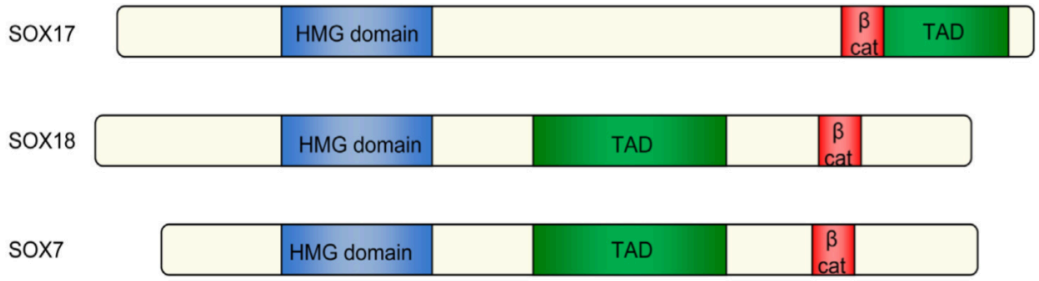

Fig.1.13 Schematic representation of SOXF structure in mammals. SOXF proteins have an HMG-box (blue) at the N-terminus, a transactivation domain (green) and a beta-catenin interaction motif (red) at the C-terminus (Lilly et al. 2016).

Like other Sox proteins, also SoxF proteins interact with different partners to regulate specific cellular processes. For example, biochemical analyses demonstrated that, during endothelial differentiation, SOX18 interacts with MEF2C (Hosking et al. 2001) and RBPJ (Fontaine et al., 2017; Overman et al., 2017) through the HMG-box domain. Not HMG-box domains are crucial to stabilize the interaction, indeed deletion of these domains disrupts the formation of SOX18 and MEF2C complex (Hosking et al. 2001).

SoxF proteins play key and redundant roles in endothelial cells differentiation during embryogenesis both in mammals and zebrafish (Francois et al. 2010). The three *SoxF* genes show overlapping expression patterns and, in mouse, *Sox17/Sox18* double mutants show more severe defects at the level of the endocardium if compared with single mutants

(Sakamoto et al. 2007). In addition, the combined deletion of *Sox7, Sox17*, and *Sox18*, but not the deletion of individual genes, at the onset of retinal angiogenesis leads to a dense capillary plexus with a nearly complete loss of radial arteries and veins (Zhou Y. et al. 2015).

In mouse, *SoxF* genes are transiently expressed in endothelial cells during vascular development (Francois et al. 2010). Sox18 is also expressed in the mesenchymal component of all hair types, where it regulates the normal differentiation of the dermal papillae (Villani et al., 2017). Sox17 is initially expressed in the endoderm (Downes and Koopman 2001; Lilly et al., 2016); its endothelial expression is established later and is limited to arteries (Corada et al. 2014; Lilly et al., 2016). Sox17 has been shown to be critical for hemogenic endothelium specification before endothelial-to-hematopoietic transition (EHT) (Bos et al., 2015; Clarke et al., 2013). The loss of Sox17 promotes hematopoietic fate over endothelial fate during EHT. Sox17 negatively regulates hematopoietic fate through repression of *Runx1* and *Gata2* (Lizama et al., 2015).

soxF genes share a similar, though not identical, expression pattern also in zebrafish. *sox17* is initially expressed in the endoderm (Alexander et al. 1999) and it is important for left-right asymmetry establishment (Aamar and Dawid 2010). Later, *sox17* is detectable also in a subset of cells of the DA possibly corresponding to the putative hemogenic endothelium (unpublished observations). As for *sox7* and *sox18*, their expression is largely overlapping in endothelial cells of all blood vascular beds during embryogenesis and they play redundant roles in arterio-venous differentiation (Cermenati et al. 2008; Herpers et al., 2008; Pendeville et al.,2008).

sox18 is detectable at 6-8 somites stage in bilateral stripes corresponding to the posterior lateral plate mesoderm (PLM; Fig. 1.14 D and F) and, at a lower level, in the anterior lateral plate mesoderm (ALM; Fig. 1.14 F) (Cermenati et al. 2008), where the presumptive common precursors of blood and endothelial cells reside (Gering et al., 1998; Brown et al., 2000). Moreover, *sox18* is expressed in the innermost PLM *fli1*-positive cells, corresponding to endothelial cell precursors, as revealed by double in situ hybridization analysis (ISH) (Fig. 1.14 F). Later in development, *sox18* marks the developing axial and intersomitic vessels (ISVs), the intermediate cell mass (ICM), where endothelial and blood cell precursors reside, and the developing head vasculature (Fig. 1.14 J-K-L-M) (Cermenati et al., 2008). At around 24 hpf, a *sox18* signal is also detectable in the eye region (Fig. 1.14 L) (Cermenati et al., 2008).

The *sox7* signal is detectable a little bit earlier than that of *sox18* in the LPM during somitogenesis (4 somites), but at the following stages, up to 29 hpf, *sox7* and *sox18* are

expressed in the same vascular districts (Cermenati et al., 2008). However, *sox7* expression in the PCV goes down earlier and at 36 hpf only *sox18* is detectable in this venous trunk vessel (Cermenati et al., 2013). Sox7 appears to be particularly important for the LDA (Lateral Dorsal Aortae) development and *sox7* mutants show abnormal shunts between the arteries and the veins of the head (Hermkens et al. 2015).

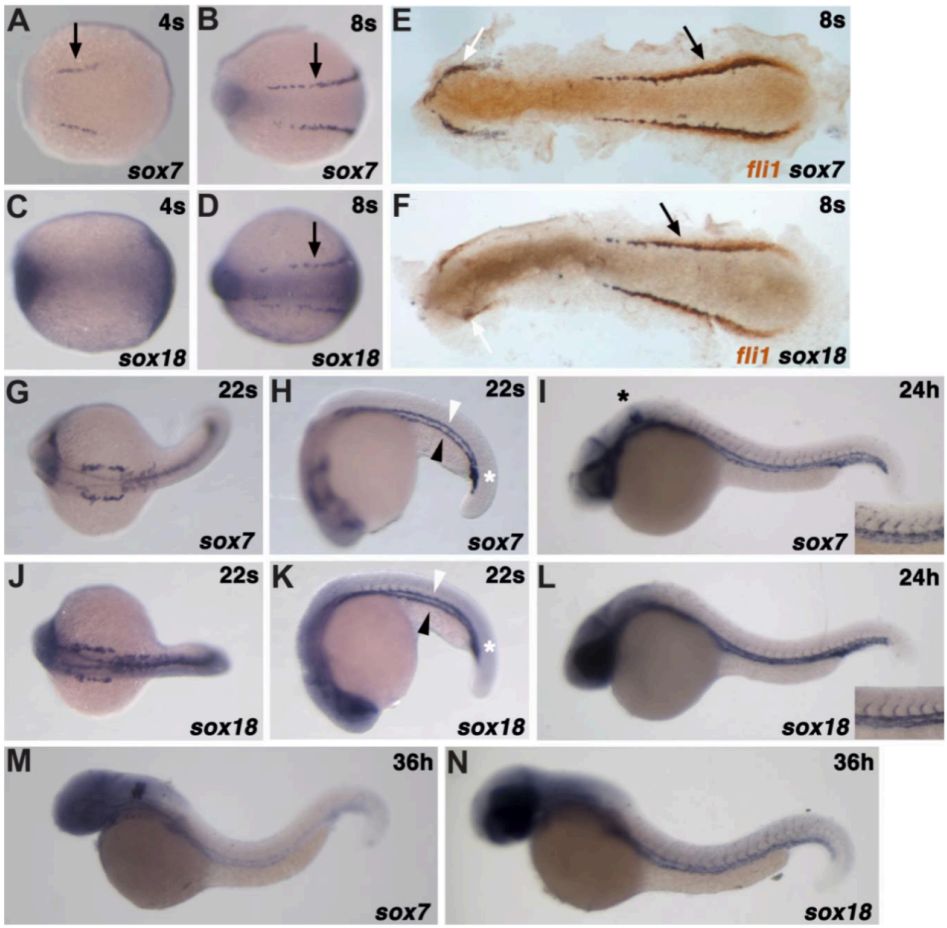

Fig. 1.14 *sox7 and sox18* expression pattern during zebrafish embryogenesis from 8 somites stage to 36 hpf by WISH. Double ISH with *fl1a* endothelial cell precursors marker (modified from Cermenati et al., 2008).

sox7 and *sox18* redundant role in vascular development is demonstrated by the fact that the knockdown of either gene, using moderate doses of specific morpholinos, has minimal effects on vessels, but *sox7/sox18* double partial morphants show multiple fusions between the major axial vessels. In these embryos, endothelial cells are specified but fail to acquire a full arterio-venous identity (Cermenati et all. 2008). It is important to underline that in *sox7/sox18* double partial morphants, venous markers are more affected than arterial ones and that the most downregulated gene is *vsg1* (*vessel specific gene 1*) (Cermenati et all.,

2008). This gene has initially a panendothelial expression, but later during development, it is restricted to the veins (Covassin et al. 2006; Quian et al. 2005).

Sox18 is involved in vascular and lymphatic development in different species (Irrthum et al., 2003; Francois et al., 2008). In humans, mutations in SOX18 are associated with the Hypotrichosis-Lymphedema-Telangiectasia (HLT) syndrome, characterized by defects in hair, blood vessels and lymphatic development (Irrthum et al., 2003); a renal failure associated with *SOX18* mutations has been recently reported (hence HLT has been renamed HLT-renal defect syndrome or HLTRS) (Moalem et al., 2014). Initially, it was supposed that at the basis of HLTS there were mutations in *VEGFC* and *FOXC2*, two genes already implicated in many pathologies affecting the lymphatic system. Then it was observed that the syndrome had many similarities to the phenotypes caused by spontaneous mutations in *Sox18* in mice. The murine counterpart of the disease is indeed represented by the *ragged* phenotype, first described in the 1950s, due to mutations in *Sox18* (Slee, 1957; Pennisi et al., 2000).

Human A104P and W95R mutations affect the HMG-box domain interfering with the binding to the DNA; they are inherited recessively (Irrthum et al. 2003). The dominant mutation C240X affects the transactivation domain and causes the production of a truncated protein (fig. 1.15). Four allelic variants of the *ragged* phenotype have been identified. The most severe mouse allele, *ragged-opossum* (*RaOp*), causes embryonic lethality before E11.0 in homozygous mutant mice (Green and Mann, 1961; Pennisi et al., 2000b; Downes and Koopman 2001). This mutation falls within the transactivation domain giving rise to a truncated SOX18 protein which acts in a dominant-negative manner and interferes with functionally redundant SOX transcription factors (Pennisi et al., 2000a; Downes and Koopman,2001).

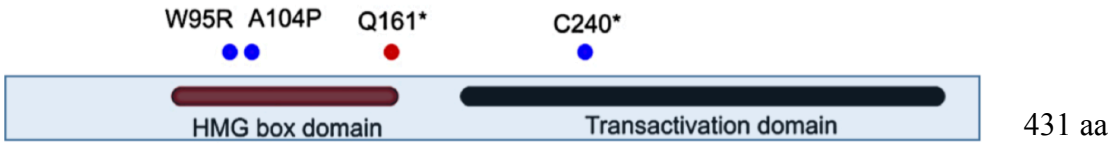

Fig. 1.15 Scheme of *SOX18* mutations. Mutations identified by Irrthum and colleagues are indicated with blue pools, while the red pool indicates de novo mutation described in a patient with aortic dilatation. W95R/A104P mutations are recessive and fall in the HMG-box domain; C240X falls within the transactivation domain; asterisks indicate X (modified from Wuennemann et al. 2016).

On the other hand, *Sox18*-null mice were originally described as viable and presented only a mild coat defect (Pennisi et al., 2000a). Some years later, in another study, *Sox18* null mice

showed gross subcutaneous edema at E13.5 and died after E14.5 (Fig. 1.16) (Francois et al., 2008).

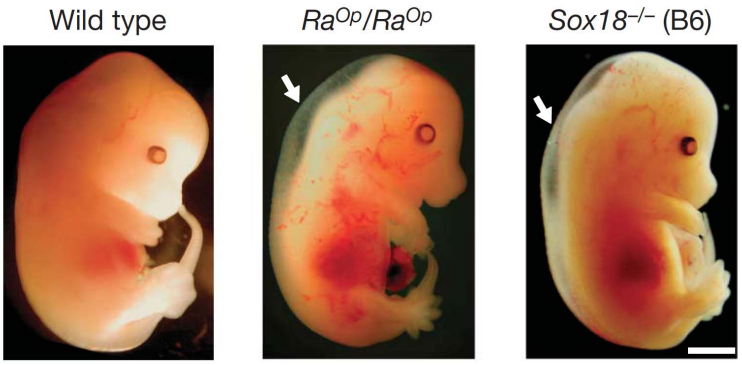

Fig. 1.16 *Sox18*$^{-/-}$ (B6) and *Ra*^{Op}/*Ra*^{Op} mutant embryos show edema at E13.5 (white arrows) (Francois et al., 2008)**.**

The difference between the two studies was the background in which experiments were carried out: mixed 129-CD1 background in the former study and pure B6 in the latter. In the absence of Sox18, in a mixed, but not in a pure background, Sox7 and Sox17 are ectopically upregulated during mouse lymphangiogenesis and they act as strain specific modifiers compensating lymphatic defects caused by *Sox18* dysfunction (Hosking et al., 2009).

In mice, Sox18 acts as a molecular switch to induce differentiation of lymphatic endothelial cells (LECs) (Francois et al., 2008). It has been demonstrated that *Sox18* is expressed in a subset of cardinal vein cells where it activates the expression of the transcription factor *prospero-related homeobox 1* (*Prox1)* by binding to its promoter. Coup-TFII probably cooperates with Sox18 in *Prox1* activation. Over-expression of Sox18 in blood vascular endothelial cells induces them to express Prox1 and other lymphatic endothelial markers, while Sox18-null embryos in the pure B6 background show a complete blockage of lymphatic endothelial cell differentiation from the cardinal vein (Francois et al., 2008). *Prox1* positive cells then migrate to form lymphatic vessels, under the control of a VegfC signal (Fig. 1.17).

My laboratory showed that *sox18* has a conserved role also in zebrafish lymphangiogenesis, indeed *sox18* morphants are not able to form a normal thoracic duct. Moreover, *sox18* genetically interacts with the central lymphatic growth factor *vegfc* in the early phases of lymphatic development, since the combined partial knockdown of *sox18* and *vegfc*, using subcritical doses of specific morpholinos, causes defects in both venous and lymphatic sprouting in zebrafish (Cermenati et al. 2013).

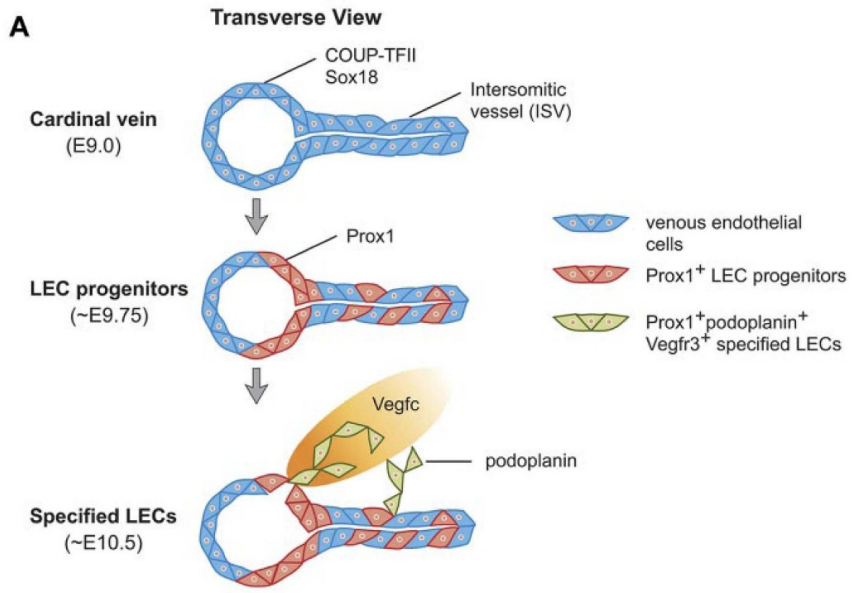

Fig. 1.17 Control of LEC specification via Sox18-CoupTFII-Prox1 axis. (Yang et al., 2012).

However, a recent article questioned Sox18 role in zebrafish lymphatic vessels development, showing that *sox18* mutants do not show a lymphatic phenotype (van Impel et al. 2014).
It is of crucial importance to clarify this issue to understand if the molecular pathway regulating lymphatic development is conserved in both mammals and zebrafish.

1.3.2 Sox13

SOX13 belongs to the SoxD group with its closely related SOX proteins, SOX5 and SOX6. Differently from the other SOX proteins, SoxD proteins have their HMG-box domain in the C-terminus and do not present a trans-activation nor a trans-repression domain.
This means that SOXD proteins regulate transcription by interacting with other proteins with functional domains (Lefebvre 2010). For example, Sox5 and Sox6 interact with Sox9, a member of the SoxE, to drive chondrocytes differentiation (Lefebvre et al. 1998; Han and Lefebvre 2008), while they seem to inhibit oligodendrocytes development (Stolt et al. 2006). In particular, it seems that SoxD proteins bind DNA as dimers, thereby preferential binding to pairs of DNA recognition sites (Lefebvre, 2010).

Other domains characteristic of SoxD group are a coiled-coil leucine zipper domain, in the N-terminus and a neighboring glutamine-rich sequence stretch, which was named Q box (Kido et al., 1998; Lefebvre, 2010). The leucine zipper is known to serve as a protein–protein interaction domain; the Q-box domain may reinforce the leucine zipper-mediated protein–

protein interaction or function to specify target proteins during the interaction (Kido et al., 1998).

In mice, the Sox13 expression pattern during embryogenesis was firstly analyzed by Roose and colleagues by *in situ* hybridization on histological sections (Roose et al., 1998). Sox13 signal was found in many structures such as the saccular and in the utricular components of the inner ear, the ampullae of the semicircular canals, the thymus and in developing central nervous system where it identifies a sub-population of post-mitotic differentiating neuronal cells (Wang et al., 2005; Wang et al., 2006).

SOX13 was also expressed in the condensing mesenchyme and cartilage progenitor cells during endochondral bone formation, in the limb as well as in the somite sclerotome and its derivatives (Wang et al., 2006). Finally, SOX13 was detected in the developing kidney, pancreas, and liver as well as in the visceral mesoderm of the extra-embryonic yolk sac and in the spongiotrophoblast layer of the placenta (Wang et al., 2006); Sox13 is also involved in differentiation of oligodendrocyte (Baroti et al., 2017).

As for vessels, Sox13 was first detected in the wall of the great arteries at E13.5 (Roose et al., 1998; Fig. 1.18 A), while the vein walls did not express *Sox13*. Just before birth (E18.5), staining in the arteries is strongly increased and it appears confined to the media and intima layers (Fig. 1.18 C). In addition to the great vessels, *Sox13* expression included other smaller vessels.

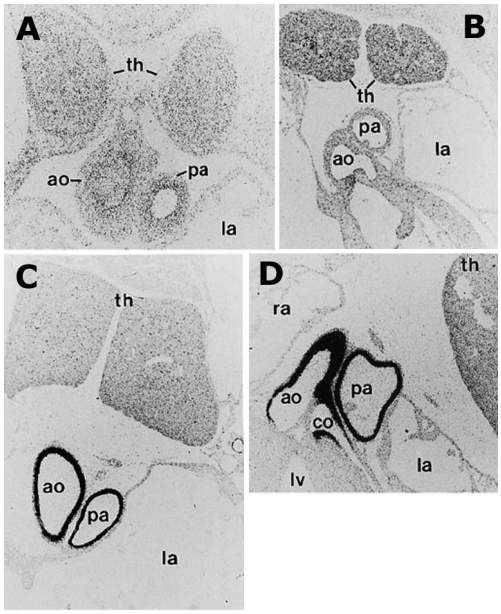

Fig. 1.18 *Sox13* expression in arterial walls during embryonic development in mice. *In situ* hybridization on histological sections at E13.5 (A), E16.5 (B), E18.5 (C) and P1 newborns (D). ao: aorta, pa: pulmonary artery. Positive signals have been detected also in thymus (th); (modified from Roose et al., 1998).

In humans, Northern blot analyses reveal that *SOX13* is expressed in multiple tissues, including heart, brain, placenta, lung, liver, kidney, and pancreas; this suggests that SOX13 may be involved in a variety of cellular processes (Kasimiotis et al., 2000).

One of these processes is T-cell differentiation during which Sox13 promotes gamma-delta T cell development (Gray et al. 2013) while opposing alpha-beta T cell differentiation (Melichar et al., 2007). One effect of *Sox13* deficiency on gamma-delta T cells is to diminish progenitor survival (Turchinovich and Hayday, 2011). In addition, Sox13 may enhance IL-7 responsiveness for the survival of such thymocytes.

During T cell differentiation SOX13 acts by directly binding and presumably sequestering TCF1 and/or modifying its activity (Melichar et al., 2007). TCF1 is one of the member of the canonical Wnt signaling pathway; TCF1 associates with the coactivator beta-catenin regulating the expression of target genes.

In T cell differentiation, SOX13 acts as an inhibitor of the Wnt signaling because it binds TCF1 preventing it from binding beta-catenin (Melichar et al., 2007). The ability of SOX13 to modulate Wnt activity has been further demonstrated (Marfil et al., 2010), indeed the binary interactions between Hhex, SOX13, and TCF to regulate Wnt activity has been shown both *in vitro* and *in vivo*. The addition of Hhex results in the formation of the Hhex-SOX13 complex that could restore the TCF1-beta catenin interaction and results in restoration/elevation of the Wnt levels (Marfil et al., 2010).

ISH analyses in *Xenopus laevis,* revealed that *sox13* was detectable in some vascular districts and that *sox13* knockdown, by morpholino injection, altered expression of a vascular marker (McGary et al. 2010). Furthermore, *SOX13* siRNA-mediated knockdown in HUVEC causes defects also in HUVECs, which fail to form vessels-like structures when cultured in 2D-matrigel (McGary et al. 2010). However, these data are very preliminary and just point to a possible angiogenic function: the 2D-matrigel is not the best assay to reproduce physiological conditions.

In zebrafish, RT-PCR analysis reveals that *sox13* transcripts are present from early developmental stages up to 5 dpf. In adult zebrafish, *sox13* is detected in ovary, kidney, gills, gut and, at a very low level, also in liver, heart and muscle (Omini, unpublished).
In particular, *sox13* expression is widely detectable in the developing Central Nervous System (CNS) (Fig. 1.19), as described in mice (Wang et al., 2005; Wang et al., 2006).
During somitogenesis, *sox13* is weakly expressed by angioblasts and later it is detectable in the forming axial vessels. At 22 hpf, as for vascular territories, *sox13* is expressed only in the

endothelium of the dorsal aorta and in the intermediate cell mass (ICM), where cells of the erythroid lineage develop (Fig. 1.18, Omini et al., unpublished).

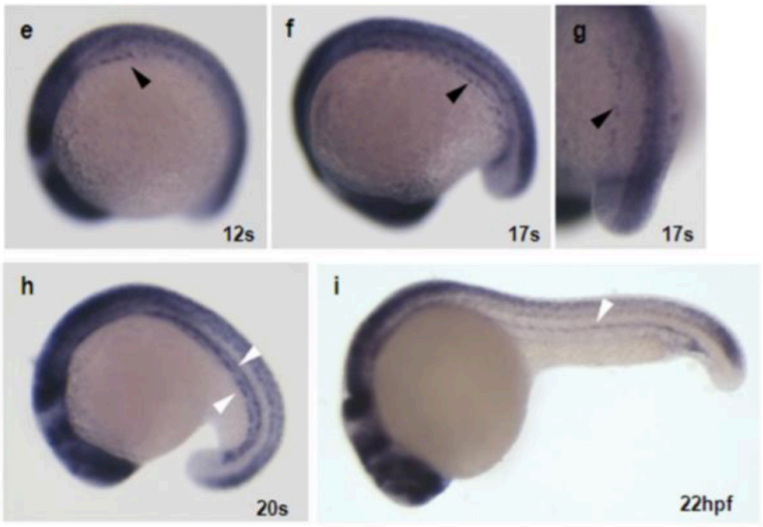

Fig. 1.19 Sox13 expression profile during embryonic development in zebrafish. (See the text). Black triangles indicate the lateral mesoderm from different points of view. The main axial vessels are indicated with white triangles. i: DA, s: somites. (Omini et all., unpublished).

Since *sox13* is transiently expressed in endothelial cells, my laboratory studied its role in vascular development. Morpholino-induced knockdown experiments reveal that *sox13* is involved in angiogenesis, since *sox13* morphants show a wide range of ISV defects that lead to partially formed or completely absent DLAVs. These defects are specific because they could be rescued by *sox13* RNA injection.

ISVs defects of *sox13* morphants are similar to those caused by Notch pathway hyper-activation. So, my laboratory investigated if there was a relationship between Sox13 and the Notch pathway. The expression of the Notch-controlled gene *efnB2* is slightly upregulated in *sox13* morphants and the Notch pathway inhibitor DAPT is able to rescue ISVs migration and DLAVs formation defects in *sox13* morphants. All these findings suggest an involvement of Sox13 in zebrafish angiogenesis as a modulator of the Notch signaling pathway (Omini et al., unpublished).

My laboratory also proposed for the first time an involvement for Sox13 in primitive erythropoieisis. Indeed, *sox13* is expressed in the ICM, where primitive erythrocyte progenitors accumulate before entering circulation. *sox13* morphants present defects both in T-cell and in erythrocyte differentiation, pointing to a role for Sox13 in these processes (Omini et al., unpublished).

1.4 AIM OF THE PROJECT

The interest of my laboratory is to study the role of *Sox* genes in vascular development, using zebrafish as model system. We focus our attention on *sox18* and *sox13*, both expressed in endothelial cells and involved in angiogenesis.

Our data on zebrafish morphants demonstrated that *sox7* and *sox18* have a redundant role in arterio-venous differentiation (Cermenati et al. 2008) and that *sox18* has a conserved role in zebrafish lymphangiogenesis (Cermenati et al. 2013). However, data published on mutants then questioned the evolutionary conservation of the entire Sox18/Prox1/Coup-TFII regulatory axis (van Impel et al. 2014).

We tried to clarify the role of *sox18* in zebrafish vascular and lymphatic development by characterizing a new, independent mutant allele: $sox18^{sa12315}$ that should behave as a null allele.

In this context, we tried also to elucidate the relationship existing between the SoxF and the Notch pathway. It is known from literature that artero-venous differentiation is driven by VEGFA and Notch pathways both in mammals and in zebrafish. VEGF pathway activates Notch signaling that is fundamental for arterial commitment (Lawson and Weinstein 2002a); in zebrafish, the main molecules involved in this process are the receptors Notch1 and Notch4 and the ligands Dll4 and Rbpj (Lawson and Weinstein 2002a).

However, alterations of the Notch pathway do not fully recapitulate the angiogenic defects caused by *vegfa* deletion (Lawson and Weinstein 2002c; Carmeliet et al. 1996), suggesting that other molecular pathways may be implicated in arterial differentiation.

One of the most promising candidates are SoxF transcription factors, indeed RNA sequencing unpublished data from my laboratory suggest a link between SoxF and Notch. In *sox7/sox18* double partial morphants *notch1b*, a *Notch1* orthologous gene, is strongly downregulated at 22hpf, a developmental stage close to the onset of primary angiogenesis. So, I was included in a collaborative research project that tried to elucidate the interplay of SoxF with Notch pathway. My aim was to investigate *notch1b* expression in *sox7/sox18* double partial morphants and in $sox18^{sa12315}$ mutants by In Situ Hybridization (ISH). This technique has the advantages to give spatial information about gene expression allowing me to understand if the downregulation seen in RNAseq data occurs only in the vascular district or not.

My laboratory has evidence that also *sox13* is involved in zebrafish vascular development, since it is transiently expressed in the DA and *sox13* morphants show defects in the ISVs (Omini et al., unpublished).

Furthermore, *sox13* expression in the DA is downregulated in *sox7/sox18* double partial morphants, suggesting that SoxF may regulate *sox13* expression (Boezio et al., unpublished). On one hand, I collaborated in setting up the experimental condition of long-term time-lapse analyses with SPIM (Bassi et al. 2015) to dynamically characterize the angiogenic phenotypes of *sox13* morphants *in vivo*.

On the other hand, I combined analysis on morphants and mutants to confirm that Sox18 and Sox7 positively regulate *sox13*.

The interplay between SoxF and Sox13 could be a mechanism in the fine-tuning of Notch signaling during vascular development, since the Notch pathway seems to be regulated in a positive way by SoxF and in a negative way by Sox13.

MATERIALS AND METHODS

2.1 ZEBRAFISH AS A MODEL SYSTEM

2.1.1 Zebrafish: breeding and reproduction

Zebrafish *(Danio rerio)* is a small freshwater teleost tropical fish. It belongs to the *Cyprinidae*. Sexual maturity is reached at about 3-4 months: from this moment, during each mating, females can lay up to 100-200 eggs, which are externally fertilized.

The laboratory housing system is composed of stand-alone systems with multiple shelves carrying several 1-10 l tanks. Water is continuously recirculated and filtered by a pump-system and it is maintained at 28°C. Water parameters such as pH and conductivity are daily monitored: their optimal values are respectively 7.2 and 400-600 μS. There are other parameters like nitrite and nitrate levels, which are periodically checked. Males and females are housed together in common tanks, and they are fed three times a day with brine shrimps and granular food. They follow an artificial light cycle of 14 hours of light and 10 hours of dark.

For breeding, the evening before mating, males and females are put in specific smaller tanks where they are separated by a net. In this way, mating is still prevented, but pheromones can be exchanged. The following morning, when light turns on, the net is removed: once fish are together, eggs can be laid and fertilized. Eggs are collected and eventually injected depending on experiments. Then, fertilized eggs are transferred into Petri dishes with *Fish Water* and grown at 28°C in a dedicated incubator. If experiments require the analysis of embryos at 24 or more hours post fertilization (hpf), they are kept in *PTU1X (1-Phenyl-2-Thiourea; Sigma)*, in order to inhibit pigmentation. To get new adult fish, zebrafish are grown in Petri dishes during their embryonic and early larval stages. Starting from 6 days post fertilization (dpf), larvae are grown in 3 l tanks until they reach a size sufficient to ascertain their sex.

Fish water

- 0.1g Instant Ocean Sea Salt
- 0.1 g NaHCO3
- 0.19 g CaSO4
- 500 μl methylene blue (0.4 mg/ml)
- deionized H_2O for a final volume of 1 l

System tanks water composition

- 150 ml di Instant Ocean Sea Salt solution in 30 l
- 2 g NaHCO3/250 l (added only when the pH is lower than 7.2)

Instant Ocean Sea Salt solution

- 34 g Instant Ocean Sea Salt
- deionized H_2O to a final volume of 1 l

PTU10X

- 0.3 g PTU (1-Phenyl-2-Thiourea; Sigma)
- 1 l Fish water

2.1.2 Zebrafish lines

We use six different lines for our experiments:

- AB wild-type line for reverse transcriptase analysis on *sox13* morphants.
- Transgenic line tg(*fli1a*:EGFP)^{y1}, for *sox13* knockdown experiments. This line is characterized by the presence of the EGFP (Enhanced Green Fluorescent Protein) coding sequence (cds) under the endothelial *fli1a* promoter region (*Lawson and Weinstein, 2002*). The line was obtained from the Didier Stainier laboratory (Max Planck Institute for Heart and Lung Research, Bad Nauheim).
- Transgenic line tg(*gata1*:dsRed)^{sd2};(*kdrl*:EGFP)^{s843} for *in vivo* time lapse analysis with the SPIM technology. This line is characterized by the presence of EGFP cds under the endothelial *kdrl* promoter region and the dsRed reporter cds under the hematopoietic *gata1* promoter region. The line was provided by Massimo Santoro lab, Università degli studi di Torino, Italy.
- *sox18*^{sa12315} mutant line generated by the zebrafish mutation project (ZMP) (A systematic genome-wide analysis of zebrafish protein-coding gene function) at Sanger Insitute (http://www.sanger.ac.uk). In this mutant the transition G>A occurs in the second exon of *sox18* gene, within the HMG-box domain coding sequence, leading to the formation of a premature stop codon (W132X). Identified carries are kept in heterozygosity and

the line is maintained by outcrossing with an AB wild-type line. The *sox18*^{sa12315} line is used for *in vivo* analysis and for several in situ hybridization (ISH) experiments.

- Mutant line *sox18*$^{sa12315/+}$*; tg(lyve1:*dsRed)^{nz101} for thoracic duct analysis. In this line, previously generated in our laboratory, the fluorescent dsRed protein (Discosoma sp Red fluorescent Protein) is under the control of the *lyve1* venous/lymphatic promoter region and combined with the *sox18* mutation.
- Mutant line *sox18*$^{sa12315/+}$*; tg(fli1a:*EGFP)^{y1} for lymphatic precursors and thoracic duct analyses. In this line, previously generated in our laboratory, the fluorescent protein EGFP is under the endothelial *fli1a* promoter region and combined with the *sox18* mutation.

2.2 MORPHOLINOS INJECTION AND MICROINJECTION CONTROLS

Morpholinos are synthetic molecules, usually 25 bases in length, that bind to complementary sequences of RNA or single-stranded DNA by standard nucleic acid base-pairing. In terms of structure, the difference between morpholinos and DNA is that, while morpholinos have standard nucleic acid bases, those bases are bound to morpholine rings, instead of 2-deoxyribose, linked through phosphorodiamidate groups instead of phosphates. Replacement of anionic phosphates with the uncharged phosphorodiamidate groups eliminates ionization in the usual physiological pH range, so that morpholinos are uncharged molecules in organisms or cells. Morpholino can act by blocking translation or by interfering with the splicing process. In the first case, the morpholino is designed to target the AUG codon region of the RNA of interest to interfere with the translation initiation complex. Splice blocking morpholinos, instead, are designed to target splicing sites and interfere with the normal splicing of the transcript of interest. In this case *intron retention* or *exon skipping* can occur with the formation of an aberrant mRNA codifying for a non-functional protein.

Morpholinos are resuspended in a saline solution with appropriate physiological parameters (*Danieau Buffer* 1X), and additioned with a fluorescent vital tracer, dextran labeled with tetramethylrhodamine (hereafter "rhodamine", Invitrogen), or alternatively, with phenol red (Sigma). These dyes allow checking the injection efficacy and the correct distribution of the morpholino in the embryos. Microinjection is performed through a micromanipulator (Micromanipulator 5171; Eppendorf), and a microinjector (Femtojet; Eppendorf.) A

borosilicate-glass needle containing the morpholino solution is assembled on this injection system. Morpholinos are injected at the proper concentration in the yolk of fertilized eggs at the stage of 1-2 cells, aligned in a Petri dish, on a cover slip with a thin layer of water.

To evaluate the specificity of the morpholino-induced phenotypes, some embryos are injected with a control morpholino, named standard control morpholino (*std*-MO). *std*-MO targets a human β-globin intron mutation that causes β-thalassemia and has no RNA targets in zebrafish. In this way, it is possible to understand whether the embryo phenotypes are due to the morpholino specific action or to the injection procedure.

Injected embryos are transferred into Petri dishes containing *Fish Water* and put in a 28°C incubator. They are let grow here until they reach the desired developmental stage. Only embryos positive to rhodamine or phenol red staining are selected, to be sure to analyze correctly injected embryos. In this way, false negatives are avoided.

Microinjection solution

- 1-1.25 µl morpholino stock or dilutions (MO stock and MO dilutions are in Danieau Buffer)
- 0.5 µl *rhodamine-dextran* 10 kDa
- *Danieau Buffer* 1X for a final volume of 5 µl

Morpholinos are resuspended in Sigma water and stored at -20°C at the concentration of 1mM. They are opportunely diluted in *Danieau Buffer* depending on the required dose for each embryo, which is injected with 4 nl of the injection solution.

Rhodamine-dextran (10kDa)

A 5% rhodamine solution in RNase-free water is prepared starting from the stock powder (D1816, Invitrogen). This solution is considered as 100X. Starting from it, 10X aliquots are prepared and stored in darkness at -20°C. The solution is injected in embryos at a concentration of 1X.

Danieau Buffer 1X

- 58 mM NaCl

- 0.7 mM KClO,
- 4 mM $MgSO_4$
- 0.6 mM $Ca(NO_3)_2$5 mM
- HEPES pH 7.2

Before injection, morpholinos and the *Danieau Buffer* are heated at 65°C for 5 minutes. Then, rhodamine is added to the solution and the needle is loaded and assembled on the micromanipulator.

2.2.1 Sequences of the morpholinos

Antisense morpholinos are purchased from Gene Tools (LLC, Philomath, OR).

For *in vivo* analysis of blood circulation in *sox18* mutants, *sox7*MO1 (Cermenati et al. 2008) is used, while for PLs and TD analyses, *vegfc*-MO2 is used (Yaniv et al., 2006). These two morpholinos are used at subcritical doses that is to say the dose of morpholino that does not cause a full phenotype but only a marginal or a null phenotype when injected in a non-mutant background.

For *sox7*MO1, we use the subcritical doses described in Cermenati et al., 2008, while to find the subcritical dose of *vegfc*MO2 we performed a dose response curve. A high dose of *vegfc*MO2 (0.5 pmol) is used as control of *vegfc*MO effectiveness; 0.045 pmol and 0.03 pmol are the two doses chosen for the transgenic background and for the kind of structure and or the developmental stage analyzed.

sox13-MO3 is used for SPIM analysis. This morpholino targets the region between the second intron and the third exon of the *sox13* gene (i2e3 splice site), interfering with the correct splicing of the transcript.

For ISVs analysis *sox13*MO4 is used. This morpholino targets the region between the ninth intron and the tenth exon (i9e10 splice site) of *sox13* gene.

std-MO 5'-CCTCTTACCTCAGTTACAATTTATA-3'

sox7- MO1 5'-ACGCACTTATCAGAGCCGCCATGTG-3'

vegfc-MO2 5'-AGACAGAAAATCCAAATAAGTGCAT-3'

sox13-MO3 5'-GAGAACGCTCCTATAAACAGAGATA-3'

*sox13*MO4 5' – CTCCCAAGAAGCCTGGAGAGTGAAA – 3'

2.3 PLASMID DNA: PREPARATION AND PURIFICATION

2.3.1 Bacterial Transformation with plasmids

The transformation reaction is based on a heat shock which causes formation of holes in the bacterial cell membrane of chemically competent cells. DNA molecules can enter the cell through these pores. *E. coli* "DH5α sub-cloning efficiency" (Invitrogen) competent cells are used for the transformation with plasmid vectors.

Procedure:

- Thaw 50 µl of competent cells on wet ice.
- Add to the cells 1-10 ng of plasmid DNA.
- Mix gently and keep on ice for 30 minutes.
- Heat shock at 42°C for 20 seconds.
- Incubate on ice for 2 minutes.
- Add to cells 950 µl of liquid *LB medium* (Luria-Bertani) and incubate at 37°C for 1hour in agitation.
- Plate 20-200 µl from each transformation on solid LB medium containing the specific antibiotic depending on the plasmid resistance.

Bacteria are let grow on the plates at 37°C o/n (overnight). Then, single colonies are inoculated in 100 ml of liquid LB medium containing the right antibiotic to select transformed bacteria. Again, bacteria are let grow in agitation, at 37°C o/n. In this way, it is possible to increase the quantity of bacterial cells, and therefore, the quantity of the desired plasmid.

Liquid LB medium

- NaCl 1%
- Yeast extract 0.5%
- Tryptone 1%

Solid LB medium

- LB medium

- Agar 15g/l

2.3.2 Plasmid DNA purification

To extract and purify plasmid DNA, "Hispeed Plasmid Midi Kit" (Qiagen) and/or "QIAprep Spin Plasmid Miniprep kit" (Qiagen) is used, following the procedures suggested by the associated protocols.

To quantify the DNA in each sample, absorbance at 260 nm is measured, considering that 1 O.D. at 260nm = 50 μg/ml for DNA.

Moreover, absorbance at 280 nm is measured. Sample quality and purity is estimated considering the O.D.260/O.D.280 ratio, whose optimal values for DNA range between 1.8 and 1.9.

2.4 AGAROSE GEL ELECTROPHORESIS

The electrophoresis technique allows separating molecules of nucleic acids according to their molecular weight. In this way, it is possible to check the dimension and the quality of DNA or RNA samples. The agarose gel is prepared starting from agarose powder (UltraPure Agarose; Invitrogen) which is dissolved in *TAE 1X* at high temperatures. Ethidium bromide (25 μl ethidium bromide stock 0.5 μg/ml every 100ml of gel; Sigma) is added to the molten agarose before it gets solid. It is an intercalating agent, which emits fluorescence when hit by UV light, therefore allowing visualization of DNA or RNA molecules. Once solid, the agarose gel is submerged in a specific electrophoretic apparatus containing *TAE 1X*. Samples are mixed with a coloured loading dye to facilitate loading on the gel and to visualize the electrophoretic run. A molecular weight marker containing DNA or RNA fragments of known molecular weights and concentrations is loaded on the gel as well. This allows to estimate the size of each DNA or RNA sample and to quantify them. The electrophoretic run is performed at a voltage of 2-3V/cm.

TAE 1X

- 40 mM Tris acetate pH 8.0
- 1 mM EDTA pH 8.0

2.4.1 DNA electrophoresis

DNA samples aliquots are diluted in *TE 1X* and mixed with *Loading-Dye Solution 6X*.
It is possible to choose among several molecular weight markers, which differ in the dimension of the DNA fragments:

- GeneRuler 1Kb DNA Ladder (Thermo scientific)
- GeneRuler 100 bp plus DNA Ladder (Thermo scientific)
- LMW DNA ladder, NEB

Loading-Dye Solution 6X

- 60% glycerol in TE
- 0.3% bromophenol blue
- 0.3% xylene cyanol
- 60 mM EDTA
- 10 mM Tris-HCl pH 7

2.4.2 RNA electrophoresis

For RNA samples, a specific electrophoretic apparatus with cooling liquid is used. Agarose gel and *TAE 1X* solution must be prepared fresh. Moreover, all the components of the apparatus must be cooled at 4°C for at least 1 hour before the electrophoretic run. This limits RNA damages caused by the heat generated by electric current. RNA samples are diluted in DEPC water and mixed with *2X RNA Loading-Dye (Thermo Scientific)*. A specific RNA molecular weight marker is used: *RiboRuler High Range RNA Ladder (Thermo Scientific)*. Before loading the agarose gel, samples and molecular weight markers are kept at 70°C for 10 minutes in order to get them completely denatured.

2X RNA Loading Dye

- 95% formamide
- 0.025% SDS
- 0.025% bromophenol blue
- 0.025% xylene cyanol
- 0.025% ethidium bromide
- 0.5 mM EDTA

2.5 REVERSE TRANSCRIPTASE PCR (RT-PCR)

Reverse transcription polymerase chain reaction (RT-PCR) is a variant of polymerase chain reaction (PCR) and it is commonly used to qualitatively detect gene expression through creation of complementary DNA (cDNA) transcripts from RNAs and their amplification.

2.5.1 Extraction of total RNA from embryos

Total RNA are extracted from embryos with Trizol using the protocol described below.

Homogenization

- Start from 20-30 embryos
- Add 500 µl of Trizol (Ambion)
- Incubate RT 5 minutes
- Centrifuge 12000 RPM 10 minutes at 4°C
- Transfer the supernatant in a new Epperdorf tube

RNA extraction

- Add 200 µl of chloroform (Sigma)
- Shake up and down for 15 seconds
- Centrifuge 12000 RPM 15 minutes at 4°C
- Transfer aqueous phase in a new Eppendorf

RNA precipitation and wash

- Add 250 µl of isopropanol (Carlo Erba) and 1µl of glycogen 20mg/ml (Roche)
- Vortex
- Centrifuge 12000 RPM 8 minutes at 4°C
- Discard the supernatant
- Add 500 µl of ethanol 75% (Carlo Erba)
- Centrifuge 7500 RPM 5 minutes at 4°C
- Discard the supernatant and dry the pellet
- Add 50 µl of RNAse free water (Sigma)

- Run RNA on a 1% gel and quantify it using spectrophotometer

2.5.2 Reverse Transcription

1 µg of RNA is reverse transcribed using the SuperScript II Reverse Transcriptase kit (Invitrogen). For each sample:

- Add 1 µl of random primers
- Add 1 µl of dNTPs 10 mM
- Put the sample 5 minutes at 70°C
- Put the sample 2 minutes at 4°C
- Add 4 µl of buffer 5X
- Add 1 µl dTT
- Add 1 µl of SuperScript II
- Leave the sample 1 hour at 50°C
- Put the sample 15 minutes at 70°C

2.5.3 PCR

actb1 PCR is performed to control the cDNA quality and to check whether samples have comparable concentrations. Then a PCR for the gene of interest is performed.

The following primers are used:

actb1-F: 5'- TGTTTTCCCCTCCATTGTTGG- 3'
actb1-R: 5'- TTCTCCTTGATGTCACGGAC- 3'
sox13-ex9-F: 5'- CCAACCTCTCAACCTCACCG- 3'
sox13-ex11/12-R: 5'- GCCATCTGCCCCTCAGAATC- 3'

The PCR reaction is made in a volume of 25μl of a mix, which is composed of:

- DNA template 2 μl
- dNTPs 2 mM 2.5 μl
- primer F 100 mM 0.2 μl

- primer R 100 mM 0.2 μl
- BufferI 5X 5 μl
- Go Taq G2 (Promega), 5 U/μl 0.125 μl
- mQ H_2O 15 μl

The PCR conditions for *actb1* are the following:

Phase	**Temperature (°C)**	**Duration**	**Number of cycles**
Initial denaturation	95	2 min	1
Denaturation	95	30 s	25
Annealing	58	30 s	
Elongation	72	30 s	
Final elongation	72	10 min	1

The PCR conditions for *sox13* are the following:

Phase	**Temperature (°C)**	**Duration**	**Number of cycles**
Initial denaturation	95	2 min	1
Denaturation	95	30 s	30
Annealing	56	30 s	
Elongation	72	30 s	
Final elongation	72	10 min	1

2.5 μl of PCR are run on a 2% gel.

2.6 MORPHANTS AND MUTANTS ANALYSES

sox18^{sa12315} mutants, uninjected or injected with subcritical doses of *sox7* morpholino, are analyzed by ISH to evaluate the expression of some interesting genes (*sox7*, *sox18*, *vsg1*, *cdh5*, *flt1*, *notch1b* and *sox13*) involved in vascular development. *In vivo* analyses are also performed in mutant embryos to detect vascular defects.

Analyses of ISV defects are performed in tg(*fli1al*:EGFP) embryos injected with *std*MO and *sox13*MO4.

The transgenic line tg(*kdrl*:EGFP; *gata1*:dsRed) is used for SPIM analysis, performed in collaboration with professor Andrea Bassi.

TD analyses are performed in the *sox18*$^{sa12315/+}$*; tg(lyve1:*dsRed) and *sox18*$^{sa12315/+}$*; tg(fli1a:*EGFP) lines. The second line is used also for PL analysis.

Before the analysis, the chorion is mechanically removed and embryos are anesthetized with *tricaine* 1X (ethyl 3-aminobenzoate methane sulfonate salt; Sigma) in *PTU* 1X (1-Phenyl-2-thiourea; Sigma). Only fluorescent transgenic embryos are selected for the analysis.

Tricaine 25X

- 0.08 g tricaine (Sigma)
- 20 ml deionized H_2O

2.6.1 Genotyping

The *sox18*^{sa12315} zebrafish mutant line is characterized by a G to A transition in the HMG box domain coding sequence of the *sox18* gene. This mutation causes the formation of a premature stop codon and the disruption of a restriction site for the BstNI/MvaI enzymes.

A standardized procedure is followed to determine the embryos genotype.

The genomic DNA is extracted and the *sox18* region is amplified via PCR. Then, the PCR product is digested with BstNI/MvaI restriction enzymes. It is possible to determine the embryo genotype analyzing the digestion pattern on a gel. This genotyping procedure can be used both for embryos analyzed *in vivo* and for fixed embryos after ISH.

Genomic DNA extraction

To obtain the genomic DNA from embryos, the following procedure must be followed:

- Anesthetize embryos in *tricaine 1X* (160 μg/ml)
- Digest single embryos in 25 μl of *Proteinase K working solution* for at least 4 hours at 55°C
- Inactivate Proteinase K keeping the solution for 10 minutes at 95°C
- Centrifuge for 30 s at 5000 RPM to pellet cellular debris
- Transfer the supernatant in a new Eppendorf tube.

Proteinase K working solution

Proteinase K 10 mg/ml diluted 1:10 in *TE Buffer* pH 8

Tricaine 25X

Dissolve 0.08 g of tricaine powder (Sigma) in 20 ml of deionized H_2O. Prepare aliquots and store at -20°C.

Polymerase chain reaction (PCR)

For genotyping, the PCR reaction is made in a volume of 25μl of a mixture which is composed of:

- DNA template	2 μl
- dNTPs 2 mM	2.5 μl
- *sox18-Bst*NI-F2/F1 100 mM	0.2 μl
- *sox18-Bst*NI-R2/R1 100 mM	0.2 μl
- BufferI 5X	5 μl
- Go Taq G2 (Promega), 5 U/μl	0.125 μl
- mQ H_2O	15 μl

The PCR conditions are the following:

Phase	Temperature (°C)	Duration	Number of cycles
Initial denaturation	95	10 min	1
Denaturation	95	30 s	35
Annealing	57	30 s	
Elongation	72	30 s	
Final elongation	72	10 min	1

For PCR reactions performed directly on genomic DNA, *sox18*-BstNI-F2/R2 primers is used. When the PCR products were not enough, a *nested-PCR* using the *sox18*-BstNI-R1/F1 internal primers is made to further amplify the PCR product. Primer sequences are reported here:

Primer	Melting temperature (°C)	Sequence (5'-3')
sox18-BstNI-F1	60.1	GATTGCATTTAGATGATGTTGTCCTG
sox18-BstNI-R1	61.3	CATCTTCTTGGGTTGTTTCTTCCTC
sox18-BstNI-F2	59.8	CAGTGCTCTGGCACTAGATTG
sox18-BstNI-R2	59.4	AAGCCTTGGAGAAGGAGACC

2.5 μl of the PCR products are loaded on a 2% agarose gel. The PCR product has a different size depending on the primers couple (F1/R1 or F2/R2):

- 305 bp (base pairs) for *Bst*NI F2/R2 primers
- 254 bp for *Bst*NI F1/R1 primers

Restriction enzyme digestion

BstNI restriction enzyme (10 U/μl, New England BioLab) or its isoschizomer Mv*a*I (10 U/μl Thermo Fisher) can be used for the digestion reaction. In both cases, a total volume of 15 μl is prepared for each sample.

For BstNI digestions, the reaction mix for each sample is composed as follows:

- Template 5 μl

- Buffer3.1 10X 1.5 μl
- BstNI 10 U/μl 0.9 μl
- H_2O mQ 7.4 μl

Samples are incubated at 60°C for 2 hours.

For Mv*a*I digestion, the reaction is performed at 37°C for 2 hours or overnight. Depending on the chosen incubation time, different volumes of the enzyme are mixed in the reaction solution:

	2 hours at 37°C	**Overnight at 37°C**
Template	5 μl	5 μl
Buffer3.1 10X	1.5 μl	1.5 μl
Mva1 10U/μl	0.9 μl	0.5 μl
H_2O mQ	7.4 μl	7.9 μl

After the enzymatic digestion, the entire reaction volume (15 μl) is loaded on a 3% agarose gel. Different genotypes generate different digestion patterns, characterized by DNA bands of different size, as reported in the following table:

	***sox18-Bst*NI-R1/F1**	***sox18-Bst*NI-R2/F2**
***sox18* +/+**	125 bp; 73 bp; 56 bp	141 bp; 91 bp; 73 bp
***sox18* +/-**	198 bp; 125 bp; 73 bp; 56 bp	214 bp; 141 bp; 91 bp; 73 bp
***sox18* -/-**	198 bp; 56 bp	214 bp; 91 bp

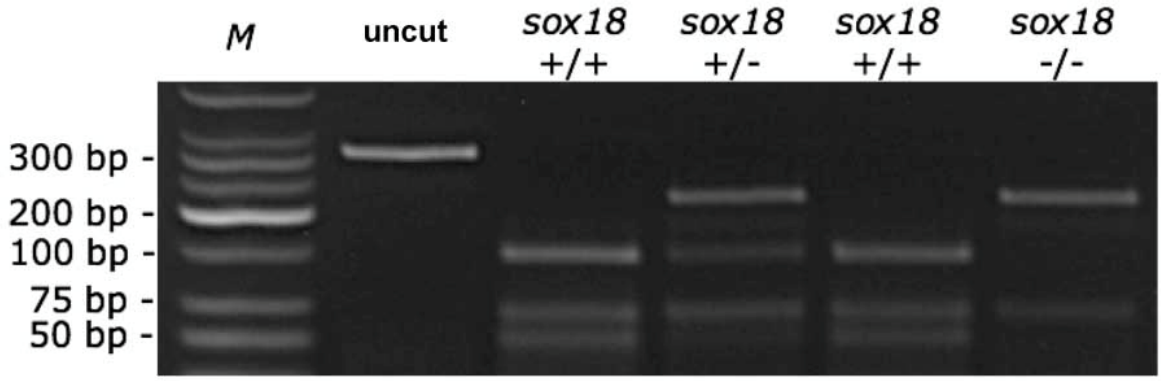

Figure 2.1. Digestion pattern of wild-type and mutant conditions for *sox18*-BstNI-F2/R2 PCR products. From left to right: Low Molecular Weight DNA ladder (M), uncut control, *sox18* wild type control (*sox18* $^{+/+}$), *sox18* heterozygous mutant (*sox18* $^{+/-}$), *sox18* wild type (*sox18*$^{+/+}$), *sox18* homozygous mutant (*sox18* $^{-/-}$).

2.6.2 Lymphatic precursors (PL) analysis

For lymphatic precursors (PL) analysis, the offspring of intercrosses of *sox18*$^{sa12315/+}$ mutants, in a tg(fli*1a*:EGFP) background, is analysed at 52 hpf. The analysis is performed using the Leica DFC 405C stereomicroscope; selected embryos are analyzed also at a confocal microscope to acquire images. Only circulating larvae are analyzed. They are anesthetized and positioned laterally in Petri dishes. Larvae analyzed at the confocal microscope are positioned in Petri dishes specific for confocal microscopy ("Glass Bottom Culture Dishes"; MatTek Corporation). Here, they are included in a solution of 1% low-melting agarose in *PTU* 1X and *Tricaine* 1X to keep them fixed in the right position. This solution is kept at 37°C in order to maintain the agarose melted. We analyze the PL in a region of ten trunk segments. The observed area starts with the first segment above the end of the yolk extension, in the anal region, and continues for ten segments toward the head.

The presence or absence of the PL in each of the ten segments is registered for all the larvae; representative images are acquired.

2.6.3 Thoracic Duct (TD) analysis

For thoracic duct (TD) analysis, the offspring of intercrosses of *sox18*$^{sa12315/+}$ mutants, in tg(l*yve1*:dsRed) and in tg(fli*1a*:EGFP) backgrounds, are analyzed at 5 dpf. The analysis is performed using a confocal microscope. Only circulating larvae are analysed; they are

anesthetized and positioned laterally in Petri dishes specific for confocal microscopy as described before.

The analyzed area of the trunk is the same as for PL analysis. The presence or absence of the TD in each of the ten segments is scored for all the larvae.

Then, larvae are divided in three different categories, depending on the number of TD-positive segments:

1. TD-positive segments: 10/10 → normal TD (100%)
2. TD-positive segments: 1-9/10 → 10-90% TD
3. TD-positive segments: 0/10 → absent TD (0%)

For each category, representative images are acquired.

2.6.4 Intersomitic vessels (ISVs) analysis

std control embryos and embryos injected with *sox13*MO4 are analyzed in the tg(*fli1a*:EGFP)^{y1} background at 2 dpf. All the embryos are analyzed on the same side, the left one. We analyze the intersomitic vessels (ISVs) in the same region described for PL analysis.

For each segment along the analyzed area we score the presence or absence of the corresponding ISV or its incomplete formation; the arterial or venous origin of each ISV is registered as well. Analyses are performed using the Leica DFC 405C stereomicroscope and pictures are taken with Leica Digital Camera DC200.

2.6.5 Statistical analysis

Statistical analyses are performed with Student's *t*-test or one-way ANOVA followed by Dunnett's Multiple Comparison post-test, when needed, using GraphPad PRISM version 5.0 (GraphPad, San Diego, CA). In the graphs, statistically highly significant data, with a p value <0.001, are marked by ***, p value<0.05 are marked by ** while p value <0.5 are marked with *.

2.7 *In situ* HYBRIDIZATION (ISH)

In-situ hybridization (ISH) is a technique used to visualize the spatial expression of a gene through a colorimetric reaction. A specific antisense RNA probe hybridizes with the transcript of the gene of interest. Some of the uridines in the probe are covalently linked to digoxygenin (DIG) molecules: they are recognized and bound by a specific antibody which is conjugated to alkaline phosphatase (AP). Once appropriate substrates are provided, AP catalyzes reactions which lead to a coloured precipitate. In this way, it is possible to directly visualize where and when a specific gene is expressed. ISH can be performed on tissue sections or on entire organisms (whole-mount ISH). In zebrafish, whole-mount ISH gives good results thanks to the transparency of the embryos.

2.7.1 Probes preparation for whole mount ISH

Plasmid DNA containing the cDNA of the genes of interest is used to transform *E.coli* bacterial cells. Then, DNA is extracted, purified, and linearized. For linearization, it is important to consider the orientation of the insert in the plasmid. In fact, appropriate phage polymerase and restriction enzymes must be chosen to generate an antisense probe. The following table summarizes the utilized probes and their characteristics.

PROBE	VECTOR	RESTRICTION ENZYME	RNA POLYMERASE
sox18	pBSKS	SmaI	T7
sox7	pExpress	BamHI	T7
cdh5	pCR$-TOPO	NotI	T3
vsg1	pGEMTeasy	NcoI	SP6
sox13	pBS-KS+	Sal1	T3

notch1b	pPCR-Script	BamHI	T3
flt1	pGEM-T	NcoI	Sp6

Restriction enzymes digestion

Specific restriction enzymes are used to linearize plasmid DNA prior to in vitro transcription. The digestion reaction occurs in a solution containing:

- 10 μg of plasmid DNA in 5-10 μl di TE1X
- Digestion Buffer (specific for each restriction enzyme; dilute 1:10, stock 10X)
- BSA (if necessary and not yet contained in the digestion buffer)
- 1 U of restriction enzyme/μg of DNA to digest
- deionized H_2O to reach the final volume

Samples are incubated at the optimal enzyme activity temperature until all DNA is digested.

Phenol/chloroform/isoamyl alcohol purification and DNA precipitation

After the enzymatic digestion, the linearized DNA must be purified from the proteins, which are still present in the solution and it must be precipitated and concentrated.

Purification :

- Add to the digestion mix *TE Buffer* 1X to reach a final volume of 200 μl.
- Add 1 V (volume) of phenol/chloroform/isoamyl alcohol 25:24:1 (Ambion).
- Mix vigorously
- Centrifuge at RT for 3 min at 11000 RPM
- Take the upper aqueous phase and transfer it into a new tube

Precipitation:

- Add 1 μl glycogen 20 mg/ml
- Add 1/9 V NaAc 3M
- Mix and add 2.5 V EtOH 100%

- Incubate on ice for at least 10 min
- Centrifuge at 4°C, for 30 min, at 11000 RPM
- Remove the supernatant
- Add 1 V EtOH 80%
- Centrifuge at 4°C, for 5 min, at 11000 RPM
- Remove the supernatant and dry the pellet at RT
- Resuspend the pellet in 10 μl H_2O DEPC

DEPC H_2O

DEPC (diethylpyrocarbonate: Sigma) diluted 1:1000 in deionized H_2O. Let in agitation at RT for few hours, then autoclave.

TE 1X

- 10 mM Tris-HCl pH 7.5
- 1 mM EDTA pH 8.0

In vitro transcription

During transcription, the RNA polymerase incorporates digoxygenin-conjugated uridine triphosphate nucleotides (DIG-UTP) in the nascent RNA. The transcription mix is composed as follows:

- x μl of DNA to have 1μg
- 2 μl DIG RNA labelling mix 10X (ATP, CTP, GTP 10 mM; UTP 6.5 mM; DIG-UTP 3.5 mM; Roche)
- 2 μl Transcription Buffer 10X (Roche)
- 2 μl RNA polymerase 2 U/μl
- 0.5 μl RNase inhibitor 40 U/μl (Promega)
- H_2O DEPC to a final volume of 20 μl

The transcription mixture is incubated at 37°C for 2 hours. After this incubation, 2 μl DNase I RNase-free (Roche) are added to remove DNA and the mixture is incubated at 37°C for 15 minutes.

To precipitate RNA the following reagents are added, in order:

- 1 µl EDTA 0.5 M pH 8
- 1/10 V NaAc 3M
- 1 µl glycogen (1 mg/ml)
- 2.5 V cool 100% EtOH

RNA is precipitated o/n at -20°C (or for 1 hour at -80°C). Then the following steps are required:

- centrifuge at 11000 RPM for 30 min at 4°C
- wash with ethanol 80%
- centrifuge at 11000 RPM for 5 min at 4°C
- remove the supernatant and dry the pellet at RT
- resuspend the pellet in 20 µL H_2O DEPC.

To test the concentration and the quality of the probe, an aliquot is run on a 1% agarose gel and, finally, its absorbance is measured at the spectrophotometer. For RNA absorbance, the following relation is considered: 1 O.D. at 260nm = 40 µg/ml for RNA
For RNA, the optimal values of O.D.260/O.D.280 ratio range between 1.9 and 2.0.

2.7.2 Embryos fixation

Once embryos have reached the desired developmental stage, they must be fixed to preserve the integrity of their tissues. Fixation is made in paraformaldehyde 4 % (PFA) in *PBS* (Phosphate Buffered Saline) 1X, o/n at 4°C or for 2 hours at RT. PFA causes the formation of cross-links between proteins in the tissues preserving them. Before fixation of embryos at 24 hpf or more, the chorion must be mechanically removed with needles. If embryos must be fixed at earlier developmental stages, the chorion can be removed after fixation. Then, fixed embryos are treated as follows:

- wash twice with PBS1X
- dehydrate embryos through incubation for 5 min in solutions with increasing methanol concentration:
    - 25%-MeOH/75%-PBS1X

- 50%-MeOH/50%-PBS1X
- 75%-MeOH/25%-PBS1X
- 100% MeOH

Embryos are stored in 100%MeOH at -20°C for at least one night.

PBS 4X

- Dissolve 2 "Phosphate Buffered Saline" tablets (Sigma # P4417) in 100 ml di deionized H_2O
- Add DEPC (final dilution 1:1000)
- Let in agitation for at least 2 hours and then autoclave

PFA 4%

Dissolve at 60°C 2 g of PFA (Sigma) in 50 ml PBS 1X. Aliquot and store at -20°C.

2.7.3 Protocol used for whole mount ISH

The ISH experiments follow four main steps in four different days:

1. Hybridization with digoxigenin-labelled RNA probes
2. Incubation with anti-dig antibody conjugated with alkaline phosphatase (AP)
3. PBT washings
4. Colorimetric reaction to visualize the precipitate

The protocol is an adaptation of the C. Thisse e B. Thisse protocol, 2008.

***First day**:*

Embryo rehydration:

- rehydration through incubations of 5 min in solutions with decreasing methanol concentration in PBS 1X (100%, 75%, 50%, 25%)
- 4 washes in PBT, each of 5 min

Embryos permeabilization:

Embryos are incubated in Proteinase K (10 µl/ml from a stock of 10 mg/ml) for different times depending on their developmental stage:

• 1 cell – tailbud	no PK
• early somitogenesis	1 min
• advanced somitogenesis	3 min
• 24 hpf (hours post fertilization)	5 min
• 29 hpf	10 min
• 32 hpf	12 min
• 36 hpf	15 min
• 2 dpf (days post fertilization)	30 min
• 3 dpf	40 min
• 4 dpf	50 min
• 5 dpf	1 h

Post-proteinase fixation and washing in PBT:

- remove PK/PBT solution
- incubate in PFA 4% in agitation, 20 min at RT
- wash embryos 5 times in PBT, 5 min each washing at RT

Prehybridization and hybridization of the embryos:

- Prehybridize embryos in 800 µl of prehybridization mix (pre-HM) at 65°C for 2-5 h
- Remove the prehybridization mix
- add 400 µl of new hybridization mix (HM) containing 200-400 ng of RNA antisense probe, previously heated at 65 °C
- Hybridize embryos o/n at 65 °C. The hybridization temperature varies depending on the stringency required by each probe.

Second day:

Washes at the hybridization temperature (65°C):

- wash briefly in 100% HM
- incubation in solutions of increasing concentration of SSC 2X in HM (each of 15 min)
    - 75% HM-/25% SSC2X
    - 50% HM-/50% SSC 2X

  - 25% HM-/75% SSC 2X
  - SSC 2X
- 2 washes of 30 min in SSC 0.1X

Washes at RT:

- Incubation in solutions of increasing concentration of PBT in SSC 0.1X (each of 10 min, in agitation):
  - 25% PBT/75% SSC 0.1X
  - 50% PBT/50% SSC 0.1X
  - 75% PBT/25% SSC 0.1X
  - 100% PBT

Incubation with anti-DIG antibody:

- Incubate embryos for 2 hours at RT in agitation in 1 ml of preincubation solution (PBT/2% sheep serum/2 mg/ml BSA) to saturate and avoid subsequent binding of the antibody to non-specific sites
- Substitute the incubation solution with a new one containing the anti-DIG antibody (Roche; final dilution 1:5000)
- Incubate o/n in the dark

Third day:

After seven washes in PBT at RT (each of 15 min), embryos are kept in PBT o/n at 4°C. This additional step allows getting a clearer and cleaner staining of the embryos.

Fourth day:

Staining:

To develop the coloration, the chromogenic substrates must be added to the staining buffer. Embryos must be constantly monitored during the staining step, which is performed as follows

- 3 washes of 5 min at RT in the staining buffer
- Removal of the staining buffer and addition of the staining solution

Stop of the coloration:

- Removal of the staining solution
- Post-fixation in PFA 4% for 2 hours at RT
- Removal of the fixation solution

Embryos are stored in PBS at 4°C.

PBT

- PBS 1X
- 1% Tween 20 (Sigma)

SSC 20X

- 3 M NaCl
- 0.3 M NaCitrate

Proteinase K (10 mg/ml)

Dissolve 10 mg of powder (Sigma) in 1 ml of sterile water (aliquot and store at -20°C).

Heparin (15 mg/ml)

Dissolve 15 mg of powder in 1 ml SSC 4X. Filter the solution, aliquot and store at -20°C.

tRNA (500 mg/ml)

Dissolve in water bath 25 g yeast tRNA in 50 ml of DEPC water until the suspension becomes translucent. Aliquot and store at -20°C.

Pre-hybridization Mix (pre-HM)

- 60% Formamide (Roche)
- SSC 5X

- 0.1% Tween20
- Citric acid 4.6 mM pH 6.0
- tRNA 500 μg/ml
- heparin 50 μg/ml
- deionized H_2O

Hybridization Mix (HM)

Add 200-400 ng of the probe to the pre-hybridization mix.

HM wash

- 60% Formamide (Roche)
- SSC 5X
- 0.1% Tween20
- Citric acid 4.6 mM pH 6.0
- deionized H_2O

Pre-incubation solution

- 2% sheep serum (Sigma)
- 2 mg/ml BSA (Sigma)
- PBT

Incubation solution with antibody

Add the anti-DIG antibody (Roche) diluted 1:5000 to the pre-incubation solution.

Staining buffer

- 100 mM Tris HCl pH 9,5
- 50 mM $MgCl_2$
- 100 mM NaCl
- 0.1% Tween 20

Staining solution

- 2.3 μl NBT (Nitro Blu Tetrazolium, Roche; stock 100 mg/ml)
- 3.5 μl BCIP (5-bromo-4-chloro-3-indolyl phosphate, Roche; stock 50 mg/ml)
- 1 ml of staining buffer

Embryos have been analyzed with stereomicroscope Leica MZFLIII and pictures have been taken with Leica Digital Camera DC200.

2.8 SPIM

SPIM (*single plane illumination mycroscopy*) technique allows a long term time-lapse acquisition of fluorescent samples (Bassi et al. 2015).

2.8.1 Cleaning of FEP tubes

For SPIM analysis embryos are included in FEP (fluorinated ethylene propylene) tubes with a diameter of 0.8x1.6 mm. Tubes must be washed with the following specific protocol before being used.

Cleaning tubes protocol:

- flush with NaOH 1M
- place in NaOH 0.5 M
- Sonicate 10 min RT in water
- flush with double-distilled water
- flush with EtOH 70%
- place in EtOH 70%
- Sonicate 10 min RT in water
- flush and store in double-distilled water
- cut tubes in segments of 2.5 cm in length
- stock in deionized and distilled water.

All solutions are degassed and filtered using a syringe filter (Millex-HV PVDF 0.45 μm).

Before embryos inclusion, tubes must be lubricated with methylcellulose 3% and wash with deionized and distilled water.

2.8.2 Mounting of the embryos

The mounting medium is composed of 0.1% agarose LMP (low melting point; Sigma) and tricaine 160 µg/ml. Embryos are placed in the mounting medium and drawn into the tube with a needle and syringe. Once the position of the embryos has been controlled, the tube is plugged with solid 1.5% agarose. After that, tubes are cut away from the syringe and positioned in an Eppendorf tube containing E3-1X, PTU1X and tricaine 160 µg/ml. The so mounted embryos are positioned in the SPIM machinery, ready for the acquisition. The SPIM machinery is equipped of a thermostat to maintain temperature at 28°C that is the optimal temperature for zebrafish embryo development.

PTU10X in E3-1X

- 0.3 g PTU (1-Phenyl-2-Thiourea; Sigma)
- 1 l E3-1X *E3-60X*
- 34.8 g NaCl
- 1.6 g KCl
- 5.8 g $CaCl_2 \cdot 2H_2O$
- 9.78 g $MgCl_2 \cdot 6H_2O$
- add double-distilled water until 2l volume is reached.

Adjust the pH to 7.2 and autoclave. The medium is conserved at RT.

Tricaine 160 µg/ml in PTU1X in E3-1X

Dilute Tricaine 25X (1:25) in E3-1X with PTU1X.

0.1% agarose LMP

Dissolve 0.1 g of LMP agarose (Sigma) in 100 ml of PTU1X in E3-1X with tricaine. Dissolve at high temperature and let the medium solidify at RT.

1.5% agarosio LMP

Dissolve 1.5 g of LMP agarose (Sigma) in 100 ml of PTU1X in E3-1X with tricaine. Dissolve at high temperature and let the medium solidify at RT.

2.8.3 Acquisition of the embryos

The embryo of interest is mounted in a little cell of the SPIM machinery containing E3-1X with PTU1X and tricaine 1X. The cell is equipped of a thermostat to maintain temperature at 28°C that is the optimal temperature for zebrafish embryo development. Every 5 minutes, a "*z-spacing*" of 5 μm between two consecutive frames is acquired. The acquisitions are converted in photograms and mounted in videos. The software saves a stack every 50 acquisitions in order to allow 3D reconstruction of the image.

2.8.4 Data analysis

Acquisitions are analyzed with the ImageJ software adjusting brightness and contrast parameters. With ImageJ is also possible to mount single acquisition in a video.

2.9 ANALYSES OF ENDOTHELIAL CELLS OVEREXPRESSING Sox13

2.9.1 Overexpression of Sox13 in immortalized endothelial cells

We use the pCMV5-Sox13 plasmid published in Stolt C., 2005.

Endothelial cells, immortalized with polyomavirus T, are seeded in Petri dishes of 60 mm of diameter in order to be $3.2*10^4$ cells/cm^2 in MCDB 131 (Gibco) supplemented with glutamine, 20% FBS NA, heparin and ECGS. The second day, cells are washed 2 times with OPTIMEM (Life Technologies) and finally 4 ml of OPTIMEM are added; these passages must be done in the dark because OPTIMEM is photosensitive. Then the transfection solution, containing lipofectamine 2000 (Life Technologies) and Sox13 plasmid, is prepared as described by the following protocol.

- Mix A: 0.5 ml of OPTIMEM+ 8 μg of DNA
- Mix B: 0.5 ml of OPTIMEM+ 17 μl of lipofectamine

Mix A and mix B are mixed within 30 minutes and incubated for 20 minutes in the dark and at RT. Eventually cells are incubated for 5.5 hors at 37°C with 1 ml of transfection medium. At the end of the incubation the medium is changed and ampicillin is added to the medium. The day after, medium is changed and only transfected cells manage to survive because they have acquired ampicillin resistance.

2.9.2 Transwell 3D migration assay

Endothelial cells are seeded 50.000 ECs/well in 6 well plate. The day after, they are transfected with 15 ug of Sox13 plasmid using lipofectamine 2000. The third day medium is changed and, at day 4, cells are seeded for transwell migration. After 8 hours, cells are extracted for WB analysis and/or fixed with 4% PAF and stained for DAPI to acquire images. Cell count is performed with ImageJ.

2.9.3 Western blot

Total proteins are extracted by lysing cells in boiling sample buffer 2X. Lysates are incubated at 100°C for 10 minutes, to allow protein denaturation, then they are centrifuged 5 minutes at 1500 RPM to eliminate cellular residues. Protein concentration of the samples is measured with the bicinchoninic acid assay (BCA assay, Thermo Fisher Scientific).

Buffer 4X is added to protein samples before loading them on 8% SDS-polyacrylamide gel (Biorad mini-protean 3 kit) to the electrophoresis. Protein are then transferred on a nitrocellulose filter for 3 hours at 240 mA in transfer buffer additioned with 20% of MeOH. The filter is incubated 1 hour with the blocking solution at RT in PBST with 5% milk and then with the opportune primary antibody (Vinculin antibody, Sigma; for Sox13 antibody see Baroti et al., 2016) for 4 hours at RT in PBST with 5% milk.

Finally the filter is washed with PBST and incubated with the opportune secondary antibodies for 45 minutes at RT. Secondary antibodies are coniugated with peroxidase and can be revealed using a chemiluminescence kit (ECL kit; GE Healtcare). The intensity of the so obtained bands is quantified using ImageJ software.

RESULTS

3.1 CHARACTERIZATION OF A NEW *sox18* MUTANT: the *sa12315* ALLELE

Our data on zebrafish morphants demonstrated that *sox7* and *sox18* have a redundant role in arterio-venous differentiation (Cermenati et al. 2008) and that Sox18 has a conserved role in zebrafish lymphangiogenesis (Cermenati et al. 2013). However, data published on mutants then questioned the evolutionary conservation of the entire Sox18/Prox1/Coup-TFII regulatory axis (van Impel et al. 2014).

In this context, we re-evaluated the role of Sox18 in zebrafish by making use of a new, independent mutant allele: *sox18*^{sa12315}, that should behave as a null allele.

The new *sox18* ^{sa12315} mutant line, coming from the Sanger Institute, carries a non-sense mutation within the HMG-box coding region that leads to a putative null allele encoding a truncated protein (fig.3.1A).

In *sox18*^{sa12315}, the mutation was kept in heterozygosity and the line was manteined by outcrossing with an AB wild-type line. For this reason we performed genotyping to identify heterozygotes. Genotyping could be done directly on adult fish, by fin clip, or through the analysis of the progeny, by extracting DNA from single embryos.

We designed primers to amplify by PCR the region of *sox18* gene carrying the mutation, then we could proceed by following two strategies. The former is to sequence the PCR product and to look at the pherograms to understand the genotype (fig.3.1B); the latter is the digestion of the PCR product. In this case, we took advantage of the fact that the mutation destroys a BstNI/MvaI restriction site, so the genotype of the embryos can be deduced from the digestion pattern. Genotyping can be performed on both non-fixed embryos and on embryos after ISH or *in vivo* analysis.

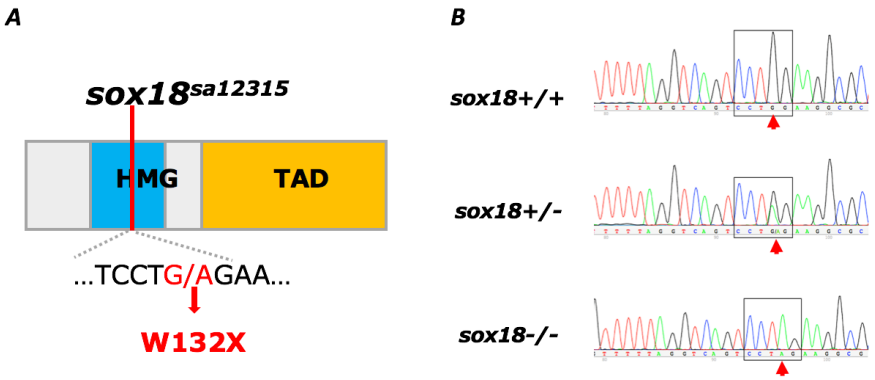

Fig.3.1 The *sox18*^{sa12315} allele. A) Scheme of the *sox18*^{sa12315} allele that carries a non-sense mutation within the HMG-box coding region. The mutation converts the tryptophan in position 132 in a stop codon. B) Pherograms of a *sox18*$^{+/+}$, *sox18*$^{+/-}$ and a *sox18*$^{-/-}$ mutant; the box indicates BstNI/MvaI restriction site in wild type and the corresponding region in heterozygotes and homozygotes. Red arrows indicate the mutated base.

3.1.1 Analysis of soxF expression in sox18^{sa12315} mutants

sox7

It is known from literature that, in mouse, *Sox7* and *Sox17* are ectopically expressed to compensate *Sox18* mutation and restore a correct lymphatic development in a mixed background (Hosking et al., 2009). It is also known that the zebrafish *sox18*^{hu10320} mutant described by van Impel does not show lymphatic defects, but the authors of the article did not investigate about *sox7* and *sox17* expression pattern (van Impel et al., 2014). For this reason, we decided to evaluate *sox7* expression in *sox18*^{sa12315} mutant by ISH analysis on the offspring of heterozygous mutants at 30 hpf. At this stage, *sox7* is mainly expressed in the DA and in the caudal vein (CV), together with *sox18*, but its expression is detectable also in rhombomers in correspondence to the optic vesicle (fig.3.2). Genotyping, performed after ISH analysis, reveals that there are not significant differences in *sox7* expression among wild-type, heterozygous and homozygous embryos at 30 hpf in the AB background. To confirm that *sox7* is not ectopically expressed in *sox18*^{sa12315} mutant line, my colleagues expanded ISH analysis to other developmental stages and other backgrounds since it is known from literature that, in mouse, the fine regulation of *soxF* depends on the genetic background (Hosking et al., 2009). *sox7* ISH signal is upregulated in homozygous mutant embryos in the tg(*lyve1*:dsRed) background (see discussion).

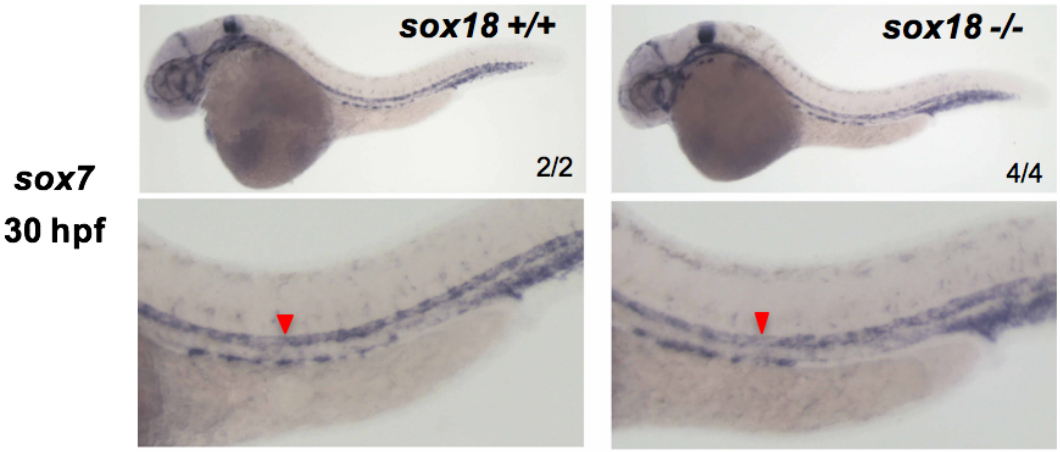

Fig. 3.2 *sox7* expression is not grossly altered in *sox18*^{sa12315} mutants. ISH analysis followed by genotyping shows that *sox7* expression is not grossly altered in the trunk region of *sox18*^{sa12315} in a AB background at 30 hpf. Red arrowheads indicate the DA.

sox18

We decided to evaluate if *sox18*^{sa12315} mutation causes variation in *sox18* expression profile. To understand if *sox18* RNA was eventually destabilized, we performed ISH analysis on the offspring of heterozygous mutants at 30 hpf in the AB background (fig.3.3). At this stage *sox18* is mainly expressed in the posterior cardinal vein (PCV) and in the dorsal aorta (DA) but also in the eye. All the embryos show a comparable *sox18* staining in non-vascular territories while in 15/18 embryos the vascular signal seems to be slightly reduced. We genotyped a pool of embryos with high and low signal and we found that there is not a correspondence between the genotype and the slight reduction of *sox18* staining. Only 2/5 *sox18*$^{-/-}$ embryos show a slight reduced *sox18* expression while in 3/5 the expression is comparable to that of *sox18*$^{+/+}$ embryos. So, we can conclude that, in the AB background, *sox18*^{sa12315} mutation does not cause variation in *sox18* expression profile.

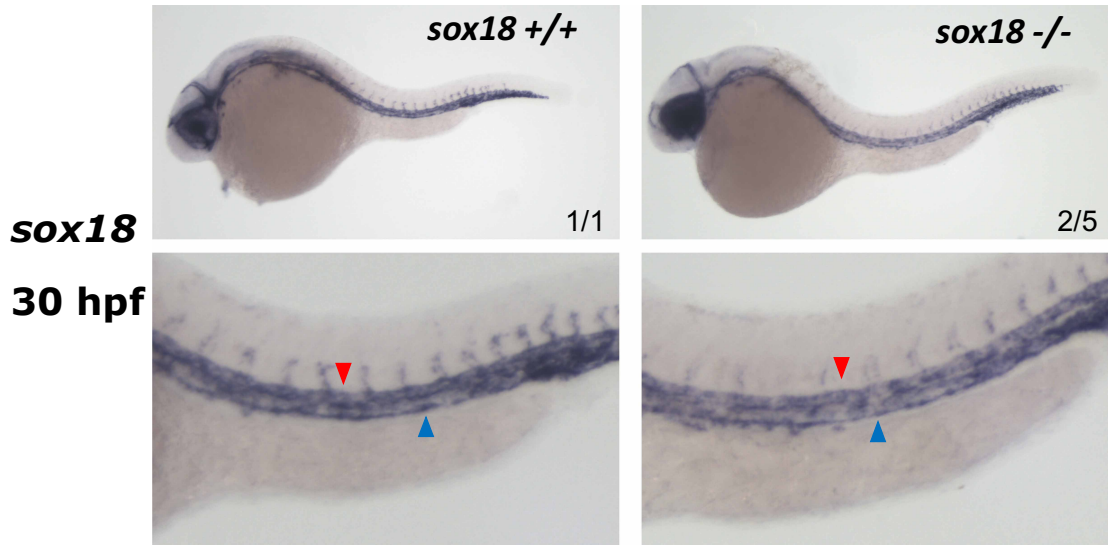

Fig. 3.3 *sox18* ISH signal is still detectable in *sox18*^{sa12315} mutants at 30 hpf. ISH analyses followed by genotyping show that *sox18* signal is not grossly reduced in *sox18*^{sa12315} in a AB background at 30 hpf. Red and blue arrowheads: DA and PCV respectively.

3.1.2 sox18^{sa12315} behaves as expected for a null mutant

In vivo analysis of blood circulation

To understand if *sox18^{sa12315}* behaves as expected for a null mutant, we decided to analyze the circulatory phenotype of the offspring of heterozygous mutants.

We analyzed three groups of embryos:

- uninjected mutant embryos, to evaluate the effect of *sox18* mutation;
- *sox18* mutant embryos injected with subcritical doses of *sox7* morpholino to compare the phenotype caused by *sox7* knockdown in a *sox18* mutant background with the circulatory phenotype observed in *sox7/sox18* double partial morphants (fig 3.4A). The doses of *sox7*MO were selected as they were shown to be subcritical in previous studies (Cermenati et al., 2008);
- embryos injected with a control morpholino (*std*-MO) to exclude that the circulatory phenotype was caused by the microinjection itself.

Embryos were followed from 1 dpf to 3 dpf and, in general, they do not show severe morphological alterations or developmental delays. We analyzed the circulation of the trunk-tail region because this is the region in which *sox7/sox18* double partial morphants show circulatory defects (Cermenati et al., 2008). We defined three different phenotypic classes: normal, reduced or absent trunk-tail circulation.

At 2 dpf, most of uninjected and *std*-MO embryos show a normal trunk-tail circulation, while only a small number of embryos have absent trunk-tail circulation. Most of the embryos having absent trunk-tail circulation show a "short circulatory loop" involving the heart region and the Cuvier duct. The number of embryos showing circulatory defects becomes higher after the injection of low doses of *sox7* morpholino; the circulatory phenotype is dose-dependent since it is more evident when the higher dose of *sox7*MO (0.25 pmol) is used (fig. 3.4B and 3.4C). Since it is known from literature that *sox7/sox18* double partial morphants (Cermenati et al. 2008) and *sox7*/*sox18* double mutants have circulatory defects (Hermkens et al. 2015), it is interesting to notice that a significant number of *sox18* mutant embryos show a "short circulatory loop" after *sox7* perturbation.

At 3dpf, we have a similar situation (fig.3.4D); most of uninjected and *std* control embryos show normal trunk-tail circulation, while injection of subcritical doses of *sox7*MO causes the absence of trunk tail circulation and the presence of the "short circulatory loop".

We focused our interest on embryos showing absent trunk-tail circulation to understand if this phenotypic class was enriched in heterozygous and homozygous embryos. Genotyping analyses, performed at 3 dpf, of 9 uninjected embryos with absent circulation reveal that this phenotype is typical of *sox18* heterozygotes (7/9) and regards only few wild type embryos (2/9). Among the 20 genotyped embryos with absent circulation and injected with 0.25 pmol of *sox7*MO, 15/20 are $sox18^{+/-}$ and 1/20 is $sox18^{-/-}$. Those numbers become more interesting in embryos injected with 0.125 pmol of *sox7*MO and showing absent circulation; in this case, we found 4/14 heterozygotes and 10/14 homozygotes. So, genotyping reveals that perturbation of *sox7* expression exacerbates the circulatory defects in heterozygous and homozygous embryos.

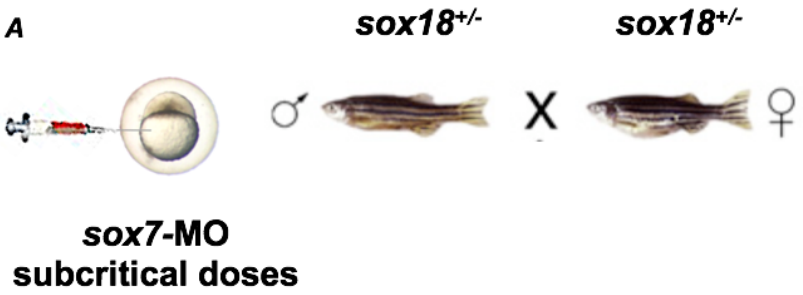

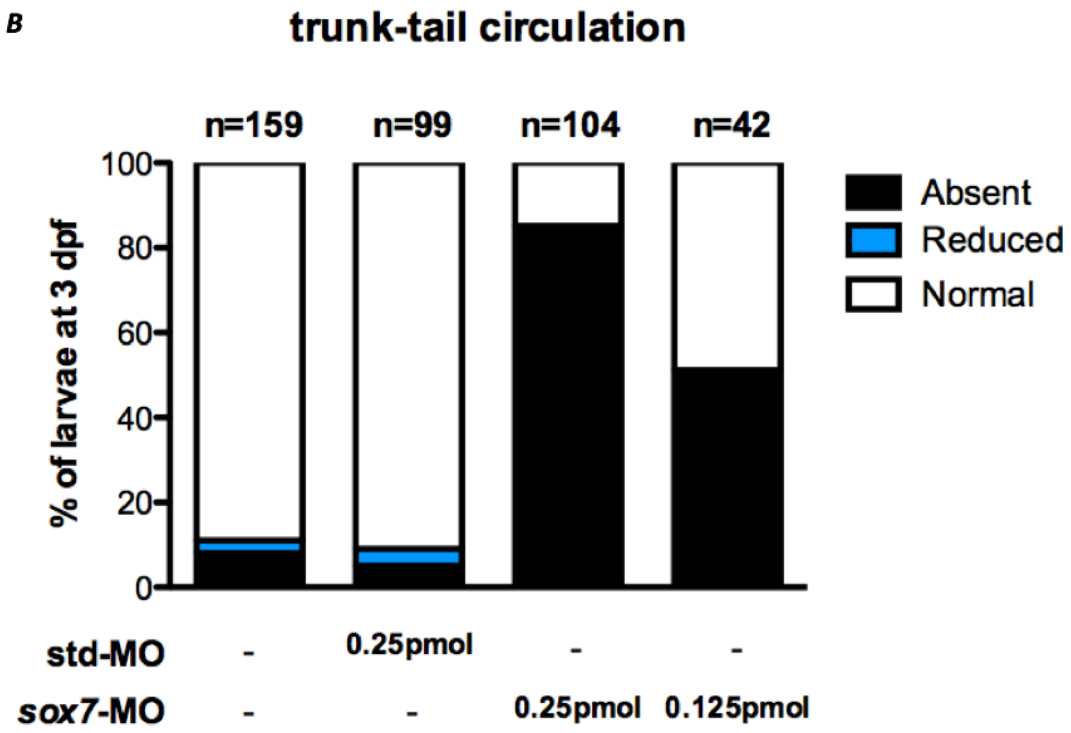

C

Day2: trunk-tail circulation	Uninjected	stdMO 0.25pmol-e	*sox7*MO1 0,25pmol/e	sox7MO1 0,125pmol/e
Normal	128	70	19	20
Reduced	16	24	7	2
Absent	15	5	78	20
Total number of embryos	159	99	104	42

D

Day3: trunk-tail circulation	Uninjected	stdMO 0.25pmol-e	*sox7*MO1 0,25pmol/e	sox7MO1 0,125pmol/e
Normal	136	90	15	20
Reduced	4	4		
Absent	12	5	88	21
Total number of embryos	152	99	103	41

Fig. 3.4 In vivo analysis of trunk-tail circulation in the offspring of *sox18* heterozygous adult fish. A) Experimental scheme: two subcritical doses of *sox7*-MO (0.25 pmol and 0.125 pmol) are injected in the offspring of *sox18* heterozygous adult fish. B) The new allele *sox18*^{sa12315} behaves as expected for a null mutant: genotyping analysis indicates that *sox18*^{sa12315} homozygous mutants are enriched in the "absent circulation" category of embryos when *sox7* expression is perturbed. C) and D) Tables showing the number of embryos analyzed for each experimental condition at 2 dpf and 3 dpf, respectively.

Molecular analysis of *sox18*^{sa12315} mutants

We decided to analyze the structure of the vascular tree by performing ISH analysis for some interesting markers on the offspring of *sox18*^{sa12315} heterozygotes in order to understand the effect of *sox18* mutation at a molecular level and to identify possible targets of Sox18.

In each experiment, fertilized eggs have been divided stochastically in 3 experimental groups: uninjected, injected with subcritical doses of *sox7*MO and injected with a control morpholino (*std*-MO). For each embryo, the ISH signal of the marker of interest has been analyzed and genotyping analyses were performed after ISH to score for any correlation between the intensity of the ISH staining of the marker and the genotype of the embryo.

- ***vsg1***

Zebrafish *vsg1* (*vessel specific gene1*) is the homologue of human *PLVAP (plasmalemma vescicle associated protein)* gene and, in zebrafish, it has a panendothelial expression around 30 hpf when it becomes to be expressed preferentially in the PCV. We focused our attention on *vsg1* because it is the most downregulated marker in *sox7*/*sox18* double partial morphants both in ISH analysis (fig. 3.5A, Cermenati et al. 2008) and in RNA sequencing data (unpublished results in collaboration with Giulio Pavesi from the University of Milan).

To understand if *sox18*^{sa12315} mutants behave as *sox18* morphants, we analyzed *vsg1* expression at 30 hpf by ISH in mutants and siblings either uninjected or injected with a subcritical dose of *sox7*MO and a *std*-MO (fig. 3.5C). According to the intensity of *vsg1* signal in the PCV, we divided embryos in three phenotypic classes: strong, intermediate and very faint/absent *vsg1* signal.

In mutants and siblings either uninjected or injected with a *std*-MO, there are only the first two phenotypic classes, while embryos injected with a subcritical dose of *sox7*MO show also a faint/absent *vsg1* signal (fig. 3.5B and C).

All the embryos have been genotyped to look for a correlation between the genotype and *vsg1* expression level. Genotyping reveals that *vsg1* expression in the PCV is not altered in most wild-type embryos in all the three experimental conditions.

As for *sox18*^{sa12315} homozygous mutants, there is a close correlation between the phenotype and the genotype. Indeed, uninjected and *std*MO homozygotes show a slight reduction of *vsg1* signal in the PVC and this reduction becomes stronger when we perturbed *sox7* expression by injecting a subcritical dose of morpholino (fig. 3.5B and C).

Heterozygotes, instead, show a more variable phenotype in all the experimental conditions analyzed: most of them have a slightly reduced *vsg1* signal in the PCV, while in a small number of embryos, *vsg1* signal is comparable to that of wild type.

In conclusion, *vsg1* signal is strong in wild-type embryos, slightly reduced in heterozygotes and extremely faint or completely absent in homozygous embryos when *sox7* is perturbed, as expected from redundancy of *soxF* genes (fig. 3.5B and C).

To demonstrate that the absence of *vsg1* signal was not due to alterations in the structure of the vascular tree, we performed ISH for the panendothelial marker *cdh5 (vascular endothelial cadherin)*. Genotyping analyses show that *cdh5* expression does not change in wild-type, heterozygous and homozygous mutant embryos at 30 hpf (fig. 3.5D).

A

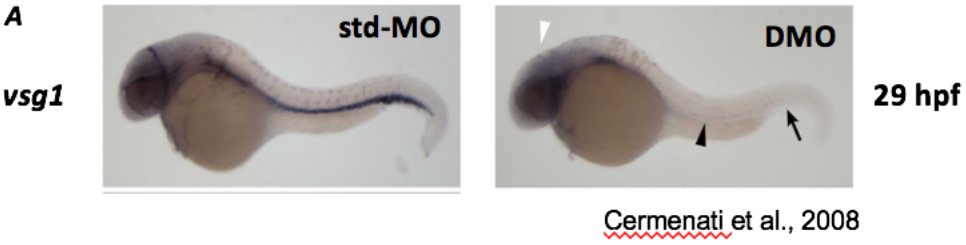

B

***vsg1* ISH signal**	**Uninjected** (n=48)			***std*-MO 0.25 pmol/e** (n=28)			***sox7*-MO1 0.25 pmol/e** (n=50)		
	sox18			***sox18***			***sox18***		
	+/+	**+/-**	**-/-**	**+/+**	**+/-**	**-/-**	**+/+**	**+/-**	**-/-**
strong	10/13	10/28	-	6/8	2/11	2/9	12/14	4/16	-
intermediate	3/13	18/28	7/7	2/8	9/11	7/9	2/14	12/16	1/20
Faint/absent	-	-	-	-	-	-	-	-	19/20

C

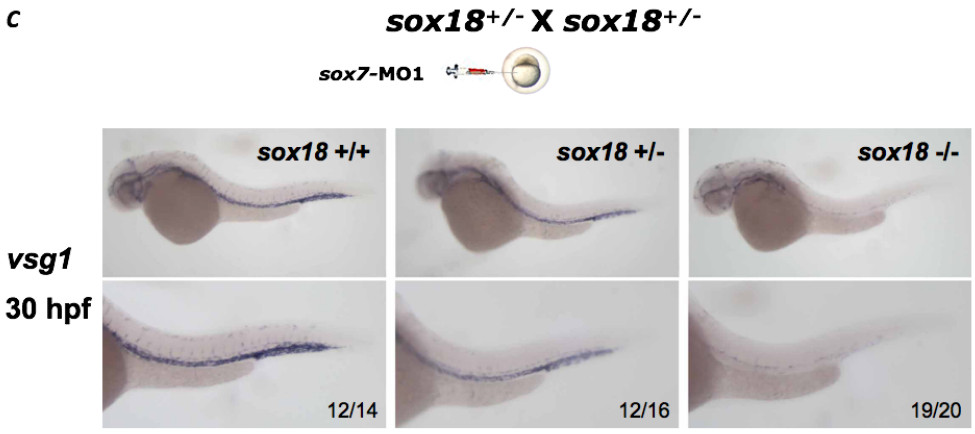

D

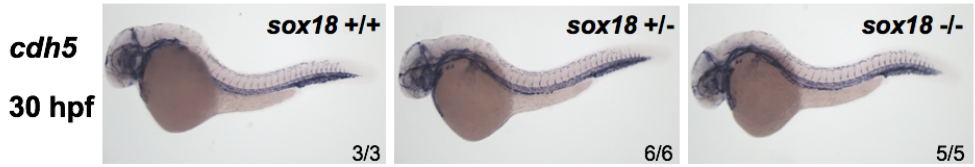

Fig. 3.5 *vsg1* expression is strongly downregulated both in *sox7*/*sox18* double partial morphants and in *sox18*^{sa12315} embryos injected with subcritical doses of *sox7*-MO. A) *vsg1* is the most downregulated gene in *sox7*/*sox18* double partial morphants as shown by ISH analysis at 29 hpf (Cermenati et al., 2008). B) Table showing the results of genotyping analysis; prevalent categories are highlighted in yellow. C) At 30 hpf, *vsg1* expression is slightly downregulated in *sox18* heterozygotes mutants, while it is strongly downregulated in homozygotes after *sox7* perturbation. D) *vsg1* downregulation is not caused by gross alteration in axial vessels that are normally formed as shown by *cdh5* staining at 30 hpf.

- ***notch1b***

notch1b is one of the two paralogues of mammalian *Notch1* (the other is *notch1a*). I focused my interest on Notch1 because Notch signaling is involved in arterio-venous differentiation of endothelial cells, and it is important for intersomitic sprouts.

Moreover, *notch1b* has been linked to lymphangiogenesis, indeed, a recent work shows that lymphatic vessels arise from specialized angioblasts of the ventral wall of cardinal vein that express *notch1b* together with *nr2f2* and *fzd7a* (Nicenboim J. et al. 2015). The analysis of RNA sequencing data performed during my first PhD year pointed to a statistically significant downregulation of *notch1b* in *sox7/sox18* double partial morphants at 22 somites stage (unpublished results, in collaboration with Giulio Pavesi from the University of Milan).

My first aim was to validate the results obtained in RNA sequencing by in situ hybridization. I chose this technique because, differently from others such as Real-Time PCR, it gives spatial information about gene expression. In situ of *sox7/sox18* double partial morphants at 22 somites stage did not give informative results (data not shown) because at this stage *notch1b* signal in the somites masks the signal in the axial vessels.
However, I expanded the analysis of *notch1b* expression in *std* control embryos and in *sox7/sox18* double partial morphants at 24hpf (fig.3.6A).
At this stage, in control embryos, *notch1b* is expressed not only in the DA and in the intersomitic vessels (ISVs) but also in the central nervous system. *sox7/sox18* double partial morphants show a very strong vessel-specific *notch1b* downregulation. *notch1b* downregulation is not due to alteration of the vascular system because the signal of the panendothelial marker *cdh5* and of the arterial one *flt1* is comparable among control embryos and *sox7/sox18* double partial morphants. In RNA sequencing probably we do not see the strong vascular reduction of *notch1b* at 24 hpf because the strong signal in the nervous system masks the downregulation in the vascular one.

To understand if the *sox18*^{sa12315} mutant behaves as a null mutant, I analyzed *notch1b* expression pattern at 24 hpf in mutants and siblings either uninjected or injected with a subcritical dose of *sox7*MO and a *std*MO (fig.3.6B). ISH analyses, followed by genotyping, show that *notch1b* expression is comparable in wild type, heterozygotes and homozygotes uninjected or injected with *std*MO. The perturbation of *sox7* expression causes a strong specific vascular *notch1b* downregulation in the vascular district of most homozygotes (6/7), while wild-type and heterozygous embryos show a comparable and vastly unchanged

notch1b signal. So, *sox18*^{sa12315} mutant behaves as *sox7/sox18* double partial morphants when *sox7* is perturbed.

All this data about *notch1b* are part of an article published this year and stating that, in zebrafish, SoxF proteins positively regulate *notch1b*. Indeed, *notch1b* mRNA expression is strongly downregulated both in *sox7/sox18* double partial morphants and in *sox7/sox18* double knockout. This work identifies SoxF responsive enhancers in *Notch1* and *notch1b* loci in mouse and in zebrafish, respectively, demonstrating for the first time that Sox7 and Sox18 physically interact with *Notch1/notch1b* enhancers (Chiang et al. 2017).

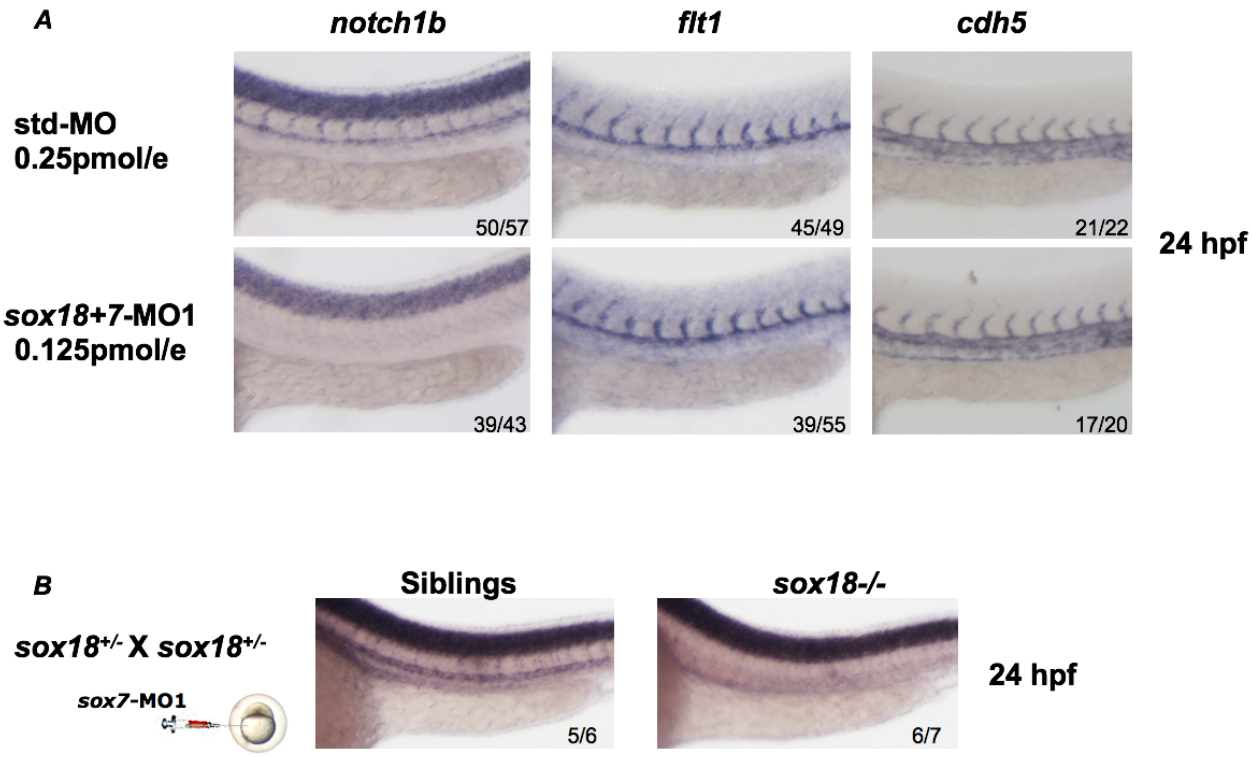

Fig. 3.6 SoxF TFs regulate *notch1b* endothelial expression. A) At 24 hpf, *notch1b* ISH signal is downregulated in *sox7/18* double partial morphants. This downregulation is not caused by alteration in axial vessels that are normally formed as shown by *flt1* and *cdh5* staining. B) At 24hpf, *nocth1b* is strongly downregulated in the vascular district of *sox18*$^{-/-}$ mutants when *sox7* is partially knocked down.

3.1.3 sox18^{sa12315} mutants show subtle lymphatic defects, highly enhanced under perturbed Vegf-C *signaling*

In mammals, Sox18, with Prox1 and Coup-TFII, is at the top of the molecular hierarchy that drives lymphatic development. *Sox18*-null mice develop lymphedema only in certain genetic backgrounds (Hosking et al., 2009) and only a subset of patients carrying *SOX18* mutations show signs of lymphatic dysfunction (Slee, 1957; Irrthum et al., 2003).
My laboratory demonstrated that *sox7/sox18* double partial morphants show defects in arterio-venous differentiation (Cermenati et al. 2008) and that *sox18* morphants have impaired lymphangiogenesis (Cermenati et al. 2013). However, the entire Sox18/Prox1/Coup-TFII regulatory axis has been questioned by data published on mutants (van Impel et al. 2014).

In this context, we tried to clarify the role of Sox18 in zebrafish lymphangiogenesis by analyzing lymphatic development in *sox18^{sa12315}* mutants.
There are two critical phases during lymphatic system development. In the former, lymphatic precursors (PLs) migrate along the arterial intersomitic vessels to reach the horizontal myoseptum following Vegf-C signaling; PLs reside at the horizontal myoseptum at 2.5 dpf. The latter phase is the formation of the thoracic duct (TD) which starts around 3.5 dpf and is complete by 5 dpf.
In order to follow lymphatic system development *in vivo*, we crossed *sox18* heterozygous mutants with two endothelial-specific transgenic lines: *lyve1*:dsRed and *fli1a*:EGFP .
In the *lyve1*:dsRed line, reporter gene expression is driven by a venous/lymphatic regulatory region; this line is useful to analyze TD formation. In *fli1a*:EGFP transgenic line, the expression of the reporter gene is detectable in the whole vasculature and it is interesting to study PL migration at the horizontal myoseptum.

sox18^{sa12315} mutants show a subtle decrease in lymphatic precursors (PLs)

We started to analyze PL migration in uninjected *sox18* mutant embryos at 52 hpf in the transgenic background *fli1a*:EGFP. The number of PL^{+} segments on one side of each embryo was counted and plotted after genotyping (Fig.3.7 A and B).
As shown by confocal images (fig.3.7A), in *sox18* mutants there is a wide range of phenotypes. At 52 hpf, the mean value of PLs that manage to reach the horizontal myoseptum is lower in heterozygotes and homozygotes if compared to wild-type embryos.

The partial decrease in PL^+ segments at the horizontal myoseptum in heterozygous and homozygous mutant embryos is subtle but statistically significant (fig. 3.7B).
Taken together these data confirmed the phenotype observed in *sox18* morphants and reinforce the notion of an involvement of *sox18* in zebrafish lymphatic development.

Since data gathered in my laboratory pointed to a genetic interaction between *sox18* and *vegfc* in lymphatic development (Cermenati et al., 2013), we tried to clarify this point by performing PL analysis also in *sox18* mutant embryos injected with *vegfc* morpholino, using doses which were shown to be subcritical in other genetic backgrounds (Cermenati et al., 2013). Unfortunately, we had some problems in defining the dose of *vegfc*MO because the dose we used (0.045 pmol) affected PL migration independently from the genotype of the embryos (fig. 3.7C). Preliminary data, using a lower dose of *vegfc*MO (0.03 pmol), suggest that this dose affects PL migration in a genotype-dependent manner (data not shown).

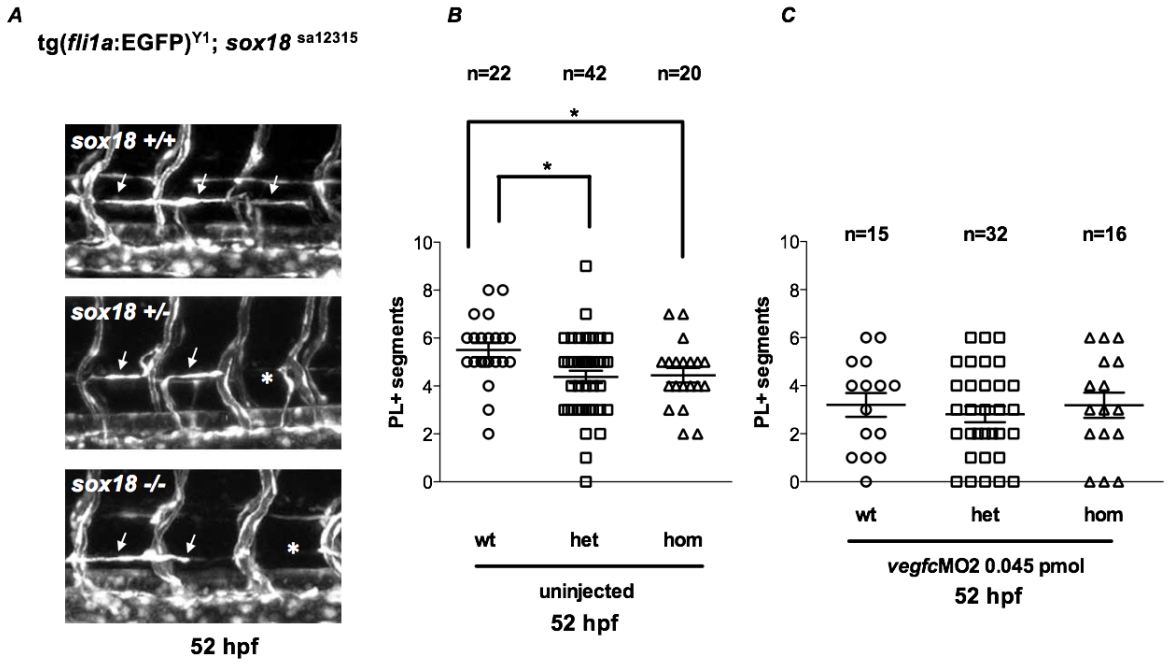

Fig. 3.7 *sox18* mutants show PL defects at 52hpf in a *fli1a:*EGFP transgenic background. A) Confocal images of PL defects in uninjected *sox18* mutants at 52 hpf. Arrows indicate the presence of PLs, while asterisks indicate PL^- segments. B) and C) The number of PL^+ segments from one side of each embryo was counted and plotted after genotyping. B) At 52hpf, heterozygous and homozygous mutants have a slight but statistically significant reduced number of PLs if compared to wild-type embryos. C) 0.045 pmol of *vegfc*MO affected PL migration independently from the genotype of the embryos, so it is not a subcritical dose in this genetic background. n=number of analyzed embryos.

sox18^{sa12315} mutants show subtle defects in TD formation, exacerbated when Vegf-C signaling is perturbed

To better characterize the role of Sox18 in zebrafish lymphangiogenesis and to clarify if Sox18 genetically interacts with Vegf-C during this process, we analyzed TD formation at 5 dpf in mutant and sibling larvae either uninjected or injected with a subcritical dose of *vegfc* morpholino. We performed the analysis in both *lyve1*:dsRed and *fli1a*:EGFP transgenic backgrounds. The number of TD^{+} segments on one side of each embryo was counted and plotted after genotyping.

Data obtained in uninjected tg(*lyve1*:dsRed);*sox18*^{sa12315} line reveal that the mutation does not cause strong alterations of lymphatic system development, but larvae show a very heterogeneous range of phenotypes. In general, most of wild-type larvae show a completely formed TD (fig. 3.8A) but some of them can have defects in TD formation. The number of larvae with TD defects becomes significantly higher in homozygotes, while heterozygotes show an intermediate phenotype (fig. 3.8B).

Perturbation of *vegfc* signaling, injecting a subcritical dose of *vegfc*MO, exacerbates TD defects in a genotype-dependent manner (fig. 3.8B). TD analysis performed in the tg(*fli1a*:EGFP);*sox18*^{sa12315} line confirmed the phenotype observed in the previous line (fig. 3.8C). Even in this case, wild-type larvae show a heterogeneous TD phenotype, with most larvae showing a completely formed TD and some others showing TD defects. TD alterations are more common in homozygotes, while heterozygotes have a phenotype comparable to that of wild-type larvae in this line.

Also in tg(*fli1a*:EGFP);*sox18*^{sa12315} , injection of a low dose of *vegfc*MO is crucial in highlighting TD defects in *sox18*^{sa12315} mutants. This is true even if the dose of *vegfc*MO used is not a truly subcritical dose because it exacerbates TD defects also in injected wild-type larvae (fig. 3.8C). However, TD defects caused by this dose of *vegfc*MO are not comparable to the strong phenotype observed after injection of high doses of *vegfc*MO.

Taken together, these data confirmed the phenotype observed in *sox18/vegfc* compound double morphants and reinforce the notion of a *sox18-vegfc* genetic interaction that had been suggested by previous knockdown studies (Cermenati et al, ATVB 2013).

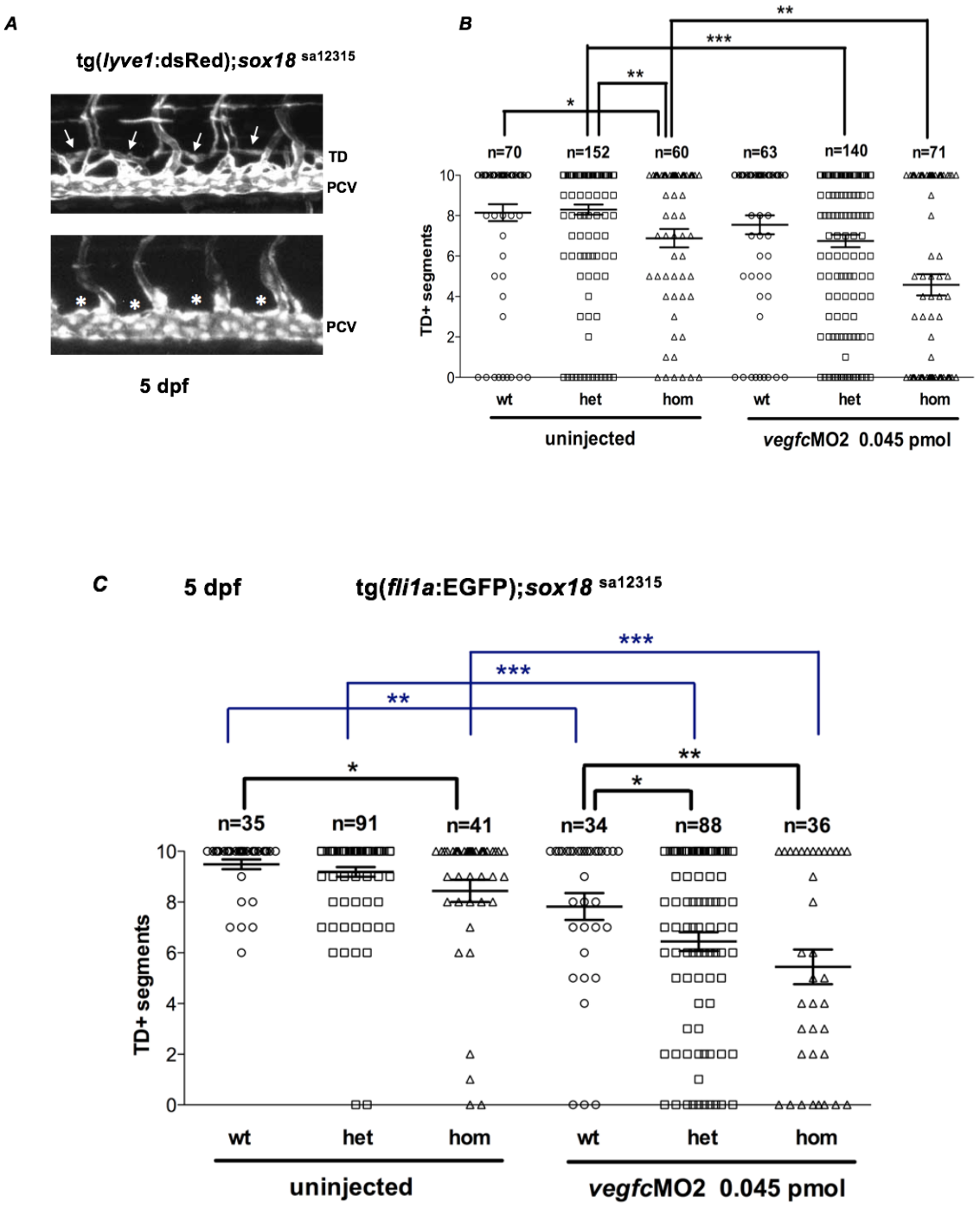

Fig. 3.8 *sox18* homozygous mutants show statistically significant TD defects at 5 dpf in two different transgenic backgrounds. A) Confocal images of TD defects in uninjected *sox18* mutants in the transgenic background *lyve1*:dsRed. Arrows indicate TD^+ segments, while asterisks indicate TD^- segments. B) and C) The number of TD^+ segments from one side of each embryos was counted and plotted after genotyping. Analyses were performed respectively in a *lyve1*:dsRed and in a *fli1a*:EGFP transgenic background. TD defects are exacerbated in *sox18* heterozygous and homozygous mutants under slightly perturbed VegfC signaling. n=number of analyzed embryos.

3.1.4 Hierarchy of SoxF *and* SoxD *transcription factors*

I decided to evaluate *sox13* expression in *sox18*^{sa12315} mutants because my laboratory had recently shown that *sox13* is transiently expressed in the endothelial cells of the dorsal aorta (DA) and that, in *sox7/sox18* double partial morphants, *sox13* vascular expression is strongly downregulated while its expression in the central nervous system is unchanged (fig. 3.9A) (Boezio et al., unpublished).

Since *sox13* expression in the DA is detectable until 24 hpf, we chose the stage of 22 hpf to perform ISH analysis on the offspring of *sox18*^{sa12315} heterozygotes injected with a subcritical dose of *sox7*MO. Embryos injected with a *std*MO were used as a control of the microinjection and uninjected embryos were analysed to understand the effect of the *sox18* mutation only on the expression of *sox13*. Genotyping was performed after ISH analysis.

All the embryos show a comparable level of *sox13* expression in the central nervous system, while some of them show a slightly reduced *sox13* signal in the DA (fig. 3.9B). We classified embryos in three phenotypic classes according to *sox13* signal in the DA: strong, reduced and faint/ absent signal and we genotyped some embryos for each phenotypic class and for each experimental condition.

Genotyping reveals that in mutants and siblings either uninjected or injected with a *std*MO, the vast majority of wild-type embryos and most heterozygotes show a strong level of *sox13* in the DA. Homozygotes show a slight reduction of *sox13* signal in the DA; this reduction becomes stronger when *sox7* is perturbed in heterozygotes and homozygotes (fig. 3.9D). *sox13* reduction in the DA it is not caused by alteration of the vascular system because *cdh5* staining at 22 hpf is comparable among the three experimental conditions (fig. 3.9C), we therefore decided to not genotype embryos hybridized with the *cdh5* probe.

Fig. 3.9 Endothelial expression of *sox13* is strongly downregulated both in *sox7*/*sox18* double partial morphants and in *sox18*^{sa12315} embryos injected with subcritical doses of *sox7*-MO. A) At 22 hpf, *sox13* ISH signal is downregulated in *sox7*/*18* double partial morphants (Boezio et al., unpublished). B) At 22 hpf, in mutants and siblings, either uninjected or injected with a *std*MO, the vast majority of wild-type embryos and most heterozygotes show a strong level of *sox13* in the DA. Homozygotes show a slight reduction of *sox13* signal in the DA. After *sox7* perturbation, most of the heterozygotes show an intermediate or a low *sox13* signal in the DA, while all the homozygotes show a faint or absent *sox13* staining in the DA. Red arrowheads indicate the DA C) *sox13* downregulation is not caused by alteration in the DA that is normally formed as shown by *cdh5* staining at 22 hpf. D) Table showing the results of genotyping analysis; prevalent categories are highlighted in yellow.

A

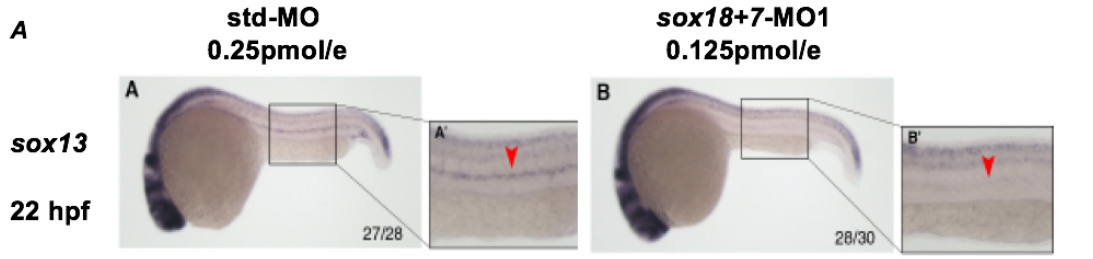

Boezio et al., unpublished

B

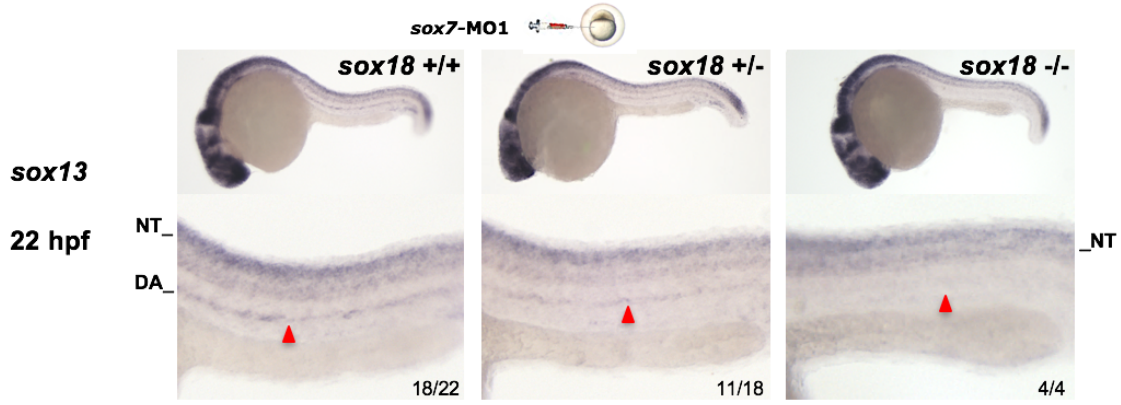

C

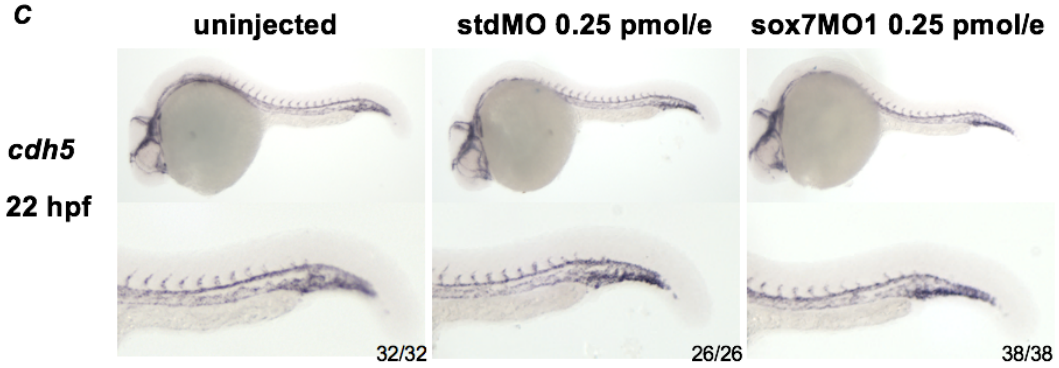

D

sox13 **ISH signal**	**Uninjected** (n=27)			***std*-MO 0.25 pmol/e** (n=23)			***sox7*-MO1 0.25 pmol/e** (n=44)		
	sox18			***sox18***			***sox18***		
	+/+	+/-	-/-	+/+	+/-	-/-	+/+	+/-	-/-
strong	8/8	4/7	5/12	4/5	7/10		18/22	4/18	
intermediate		3/7	2/12	1/5	1/10	2/8	2/22	11/18	
Faint/ absent			5/12		2/10	6/8	2/22	3/18	4/4

3.2 CHARACTERIZATION OF SOX13 ROLE IN ANGIOGENESIS

3.2.1 A dynamic characterization of ISV defects in sox13 morphants using SPIM technique

In my laboratory, there is the evidence that also *sox13* is involved in zebrafish vascular development, indeed it is transiently expressed in the DA and *sox13* morphants show defects in the ISVs (Omini et al., unpublished; Boezio et al., unpublished).

However, the analyses performed on *sox13* morphants have been limited to a static observation of ISVs defects at different time points. *sox13* morphants show a compromised primary angiogenesis, with a wide range of ISV defects. Some ISVs are blocked at the horizontal myoseptum while some others are completely absent. Moreover, some possible defects in ISVs maturation during secondary angiogenesis have been hypothesized (Boezio et al., unpublished).

To dynamically characterize the angiogenic phenotypes of *sox13* morphants *in* vivo, we collaborated with Professor Andrea Bassi, from the "Politecnico di Milano", to perform long-term time-lapse analysis of *sox13* morphants with SPIM.

SPIM (*single plane illumination microscopy*) technique had never been used in my laboratory and my colleagues set up the experimental conditions on the base of the information available in literature (Kaufmann et al. 2012).

After setting up the best experimental conditions (well described in the material and methods section), we started the *in vivo* analysis of *sox13* morphants in the *kdrl*:EGFP;*gata1*:dsRed transgenic background. This transgenic line allows the visualization of the whole vascular tree since the EGFP is under the control of the endothelial regulatory region of *kdrl*.

sox13 morphants and uninjected control embryos were acquired from 26 hpf to 3 dpf. Our initial aim was to acquire embryos at 22 hpf in order to characterize the events occurring during both primary and secondary angiogenesis. However, some technical problems prevented us from doing this: *sox13* morphants are too fragile to be included at 22 hpf. The advantage of including *sox13* morphants at 26 hpf is that we can select and include only the embryos with the most interesting phenotype.

The acquisitions are converted in photograms, mounted in videos and analyzed. Data analysis confirmed developmental delay of *sox13* morphants and allowed a better characterization of the ISV defects.

Control embryos develop a completely normal vascular tree in which all the ISVs manage to reach the dorsal portion of the embryo and form complete dorsal longitudinal anastomotic

vessels (DLAVs). On the contrary, *sox13* morphants show a wide range of ISV defects: some ISVs are blocked at the myoseptum, others migrate slowly and some others merged together (fig. 3.10B). We also saw a new type of event that can be seen only in a dynamical *in vivo* analysis: some ISVs first migrate up to the DLAV and then regress in a ventral to dorsal direction after detaching from the axial vessel (fig. 3.10A).

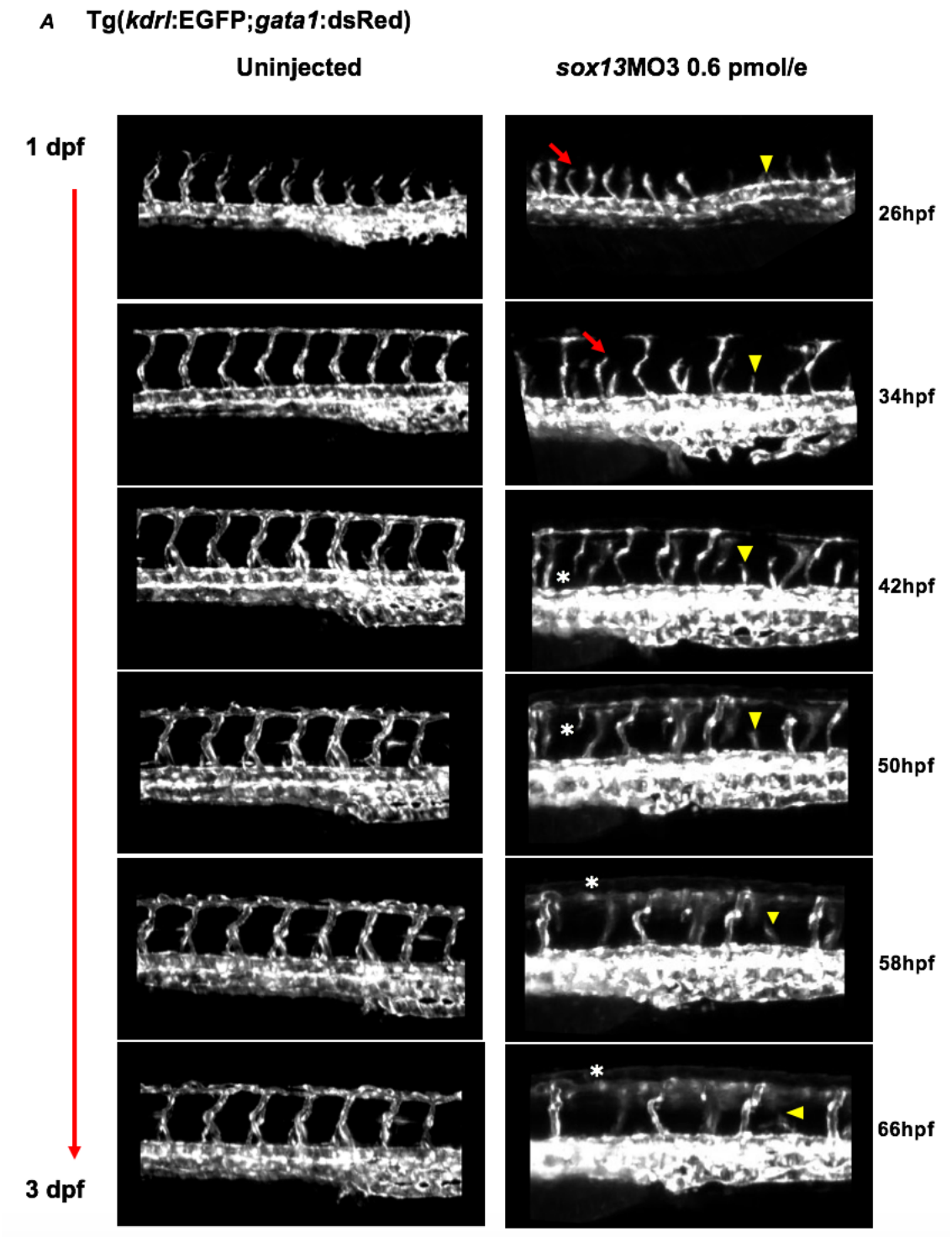

B

ISV defects in *sox13*MO3 0.6pmol/e	ISVs blocked at the horizontal myoseptum	Slowly migrating ISVs	Anomalous fusion between ISVs	Regression from axial vessels
	6/30	5/30	1/30	5/30

Fig. 3.10 *In vivo* dynamic characterization of the angiogenic phenotypes of *sox13* morphants in tg(*kdrl*:EGFP;*gata1*:dsRed) line. A) In *sox13* morphants, there are a wide range of ISV defects. Yellow arrowheads indicate an ISV blocked at the horizontal myoseptum. Red arrows and asterisks indicate an ISV that first migrates up to the DLAV (red arrows) and then regresses in a ventral to dorsal direction after detaching from the axial vessel (asterisks). Control embryos do not show ISV defects. B) Table showing the type of ISV defects found in three *sox13* morphants analyzed along ten consecutive segments rostral to the anus. Uninjected control embryos show a perfectly formed vascular tree. n= number of analyzed ISVs.

3.2.2 Knockdown experiments using an independent sox13 morpholino confirmed Sox13 *involvement in ISV angiogenesis*

In my laboratory, it had been demonstrated that, in *sox13* morphants, primary and secondary angiogenesis are compromised. In particular, *sox13* morphants show a lower number of venous ISVs at 2.5 dpf (Omini et al., unpublished; Boezio et al., unpublished).

To reinforce these data, we performed *in vivo* analysis of ISV defects in embryos injected with an independent *sox13* morpholino (see the material and methods section for details).

First, we tested morpholino efficacy using reverse transcriptase (RT) PCR to measure *sox13* expression levels at 22 hpf in embryos of the AB line injected with *sox13*MO and in control embryos. As expected, *sox13* RNA expression level is lower in *sox13* morphants than in *std*MO embryos. This is not due a lower concentration of the RNA extracted by *sox13* morphants as the *actb1* RT-PCR points out (fig. 3.11A).

Then we started *in vivo* analysis of ISV defects at 2.5 dpf to confirm the phenotype observed in previously analyzed *sox13* morphants. *sox13* morpholino and *std*MO control embryos were analyzed in a tg(*fli1a*:EGFP) background.

ISVs on one side of each embryo were counted and classified as arterial (aISVs) or venous (vISVs) ISVs, depending on their sprouting from the DA or from the PCV.

At this stage, in *std* control embryos there is a comparable number of arterial and venous ISVs, as expected. *sox13* morphants show the absence of some ISVs. The number of arterial and venous ISVs are reduced, in a highly significant way (fig. 3.11B). So, this independent *sox13* morpholino causes the reduction of both arterial and venous ISVs, thus affecting both

primary and secondary angiogenesis, as previously hypothesized (Boezio et al., unpublished). Taken together, these data support the involvement of *sox13* in angiogenesis.

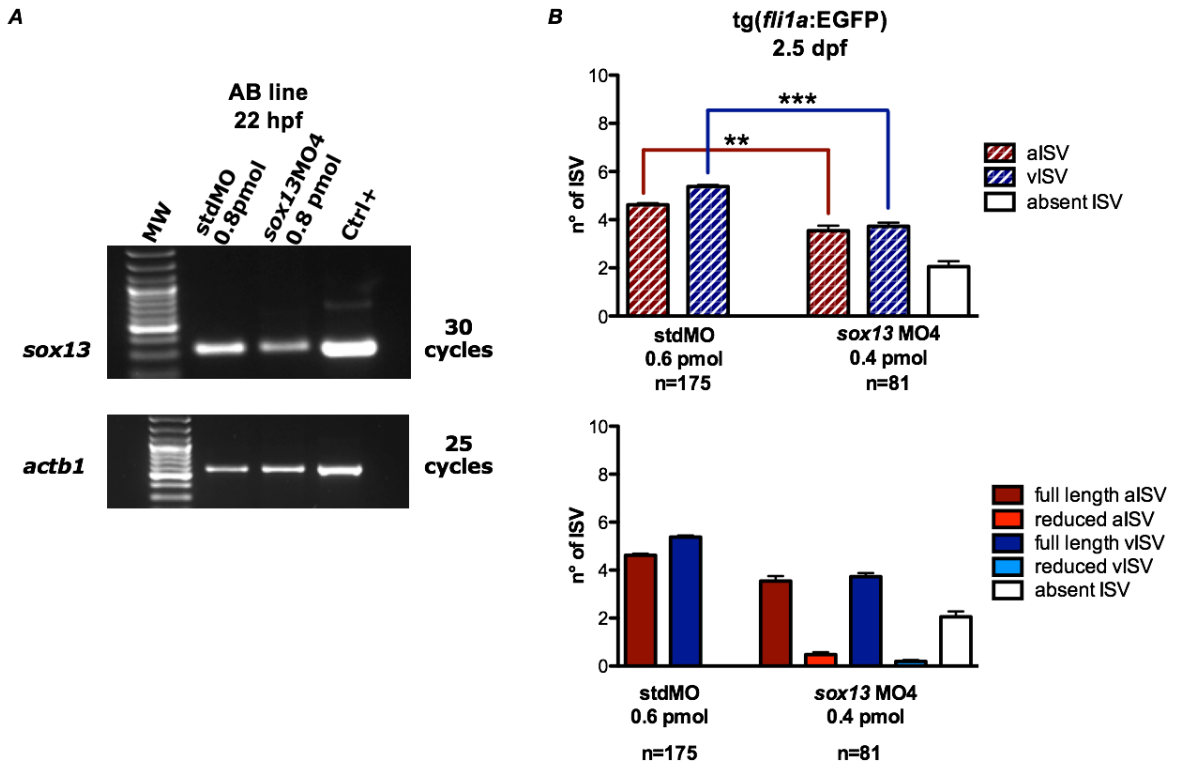

Fig. 3.11 Characterization of *sox13*MO4 morphants phenotype. A) RT-PCR on total RNA extracted from *sox13* morphants injected with *sox13*MO4 and control embryos. The size *sox13* PCR fragments is 454 bp in both *sox13* morphants and controls. *actb1* PCR fragment is 560 bp. *sox13*MO4 causes the decrease of *sox13* RNA, as expected. Embryos of the AB line were injected with 0.8 pmol of *sox13*MO4 and 0.8 pmol of *std*MO. B) *sox13*-MO4 injection in tg(*fli1a*:EGFP) line causes a statistically significant reduction of both arterial ISVs and venous ISVs. In the upper graph, absent (white bars), arterial (red patterned bars) and venous (blue patterned bars) ISVs are plotted. In the bottom graph, full length aISVs (red bars) and full length vISVs (blue bars) are separated from ISVs blocked at the myoseptum to better describe the range of ISV defects detectable in *sox13* morphants. White bars indicate absent ISVs, light red bars reduced in length aISVs, light blue bars reduced in length vISVs. n= number of analyzed embryos.

3.2.3 Sox13 overexpression increases endothelial cell migration

To understand if ISV defects found in *sox13* morphants was due to a problem in endothelial cells migration, our collaborator Costanza Giampietro, a former member of our Department, currently at ETH of Zurich, performed some in *vitro* experiments. We transfected Sox13 plasmid in immortalized mouse lung endothelial cells and performed an *in vitro* migration assay; non-transfected cells were used as control. Western blot analysis confirmed that Sox13 protein level was higher in endothelial cells in which Sox13 had been overexpressed

compared to controls (fig. 3.12A). So, we started the transwell migration assay for 8 hours and then we fixed cells and counted them with ImageJ (fig. 3.12B). Statistical analysis revealed that Sox13 overexpressed cells migrate more than control cells (fig. 3.12C). These data suggest an involvement of Sox13 in endothelial cell migration. In particular, we can speculate that, if Sox13 overexpression increases endothelial cells migration, Sox13 absence could cause migration problems. Therefore, ISV defects found in *sox13* zebrafish morphants could be caused by the fact that *sox13* absence in endothelial cells affects their migration.

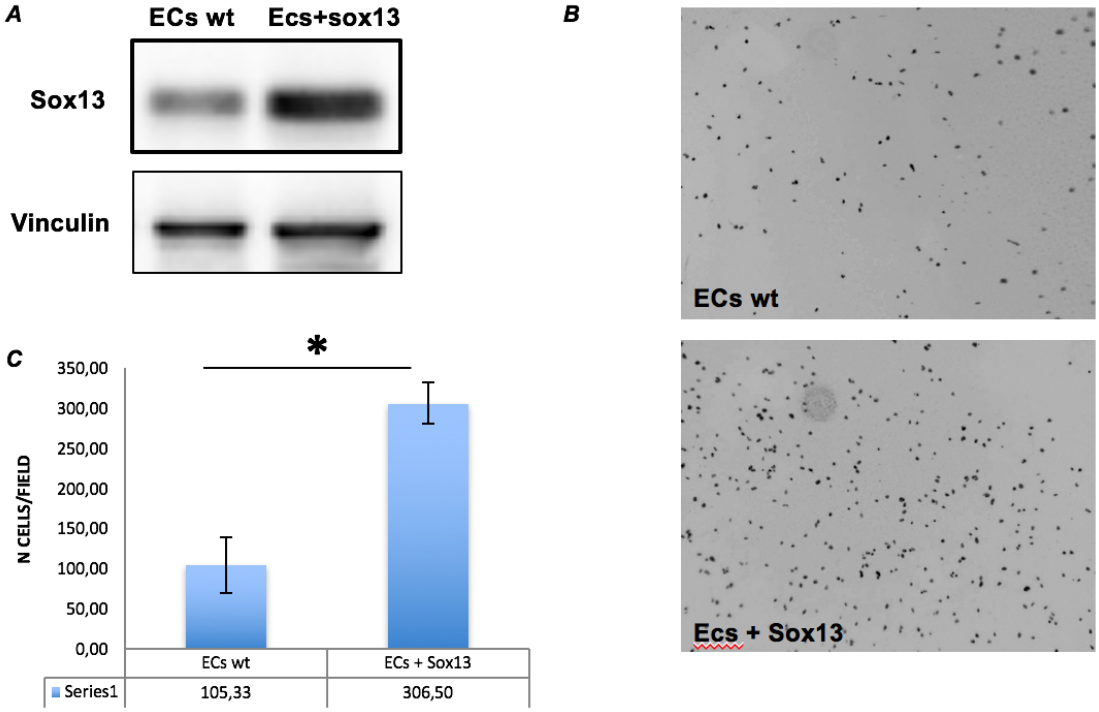

Fig. 3.12 *sox13* overexpression increases endothelial cell migration. A) Western blot analysis confirmed that Sox13 protein level was higher in endothelial cells in which Sox13 had been overexpressed compared to control cells. B and C) *In vitro* transwell migration assay of Sox13 overexpressed endothelial cells and control cells. B) DAPI staining; C) Statistical analysis of the number of cells/field. 6 experiments have been performed, each in duplicate. ImageJ software has been used for automated count of cell nuclei in 1 field/sample.

DISCUSSION

An accurate knowledge of the players, the signaling pathways and the mechanisms that regulate the correct patterning of the cardiovascular system is very relevant, especially because the molecular mechanisms involved in pathological processes could be sometimes similar or identical to those used during embryogenesis (Folkman, 1995).

SOXF transcription factors are crucial for vascular and lymphatic system development (François et al. 2010; Lilly et al. 2016). Several laboratories, including ours, have shown with knockdown approaches that *sox7* and *sox18* play redundant roles in arterio-venous differentiation of endothelial cells (Cermenati et al. 2008; Herpers et al. 2008; Pendeville et al. 2008). In *sox7/sox18* double partial morphants endothelial cells fail to acquire a full arterio-venous identity. This causes the formation of anomalous shunts between arteries and veins leading to the block of circulation in the trunk- tail region of the embryo. The same phenotype has been recently observed in *sox7/sox18* double mutants (Hermkens et al. 2015). The correspondence between the mutants and the morphants phenotype is of crucial importance since morpholino reliability has been recently questioned.

Morpholino (MO) based knockdown approach has revolutionized the study of gene function and a lot of work has been done by using this technique. However, the recent development of new genome engineering techniques has allowed the easy generation of a lot of mutants. The problem is that not all the zebrafish mutants show the same phenotype of the corresponding morphants, so the use of MOs has been debated. Moreover, MO injection can induce *p53*-dependent apoptosis and off-target cell-type-specific changes in gene expression that confound phenotypic analysis (Ekker and Larson 2001). The mechanism of *p53* activation after MO injection has not been fully understood, but it is demonstrated that off-target phenotypes can be avoided by coinjecting the MO of interest with *p53*MO (Robu et al. 2007). Since several hypotheses can explain the phenotypic differences among mutants and morphants, morpholino reliability is still recognized but there are some recommendations to take into account when using MO, as described in the introduction.

In humans, mutations in SOX18 are associated with the Hypotrichosis-Lymphedema-Telangiectasia (HLT) syndrome, characterized by defects in hair, blood vessels and lymphatic development (Irrthum et al., 2003); a renal failure associated with *SOX18* mutation (HLT-renal defect syndrome or HLTRS) has also been reported (Moalem et al., 2014).

The murine counterpart of the disease is represented by the *ragged* phenotype (Slee, 1957) due to the spontaneous mutations in *Sox18* (Pennisi et al., 2000). The most severe allele, *ragged-opossum* (*RaOp*), causes the production of a truncated SOX18 protein which acts in

a dominant-negative manner (Pennisi et al., 2000a; Downes and Koopman, 2001). This allele causes embryonic lethality before E11.0 in homozygous mutant mice (Green and Mann, 1961; Pennisi et al., 2000b; Downes and Koopman 2001). On the other hand, *Sox18*-null mice were originally described as viable and presented only a mild coat defect (Pennisi et al., 2000a). This happens because, Sox7 and Sox17 are ectopically upregulated during mouse lymphangiogenesis and they act as strain specific modifiers compensating lymphatic defects caused by *Sox18* dysfunction in a mixed 129-CD1 background (Hosking et al., 2009). Indeed, *Sox18* null mice show gross subcutaneous edema at E13.5 and died after E14.5 in a pure B6 background (Francois et al., 2008).

In zebrafish, the role of *sox18* in lymphangiogenesis is now debated. Indeed, *sox18*^{hu10320} mutants (van Impel et al. 2014) do not show the lymphatic phenotype observed in *sox18* morphants (Cermenati et al., 2013). However, van Impel and colleagues did not check if the absence of lymphatic phenotype was due to *sox7* or *sox17* ectopic expression.

To clarify Sox18 role in zebrafish lymphangiogenesis, we made use of a new, independent mutant allele: *sox18*^{sa12315}, that should behave as a null allele. In *sox18*^{hu10320} mutant, a 1-bp insertion preceding the HMG-box causes a frame-shift leading to a premature stop codon after additional 50 amino acids. The new *sox18* ^{sa12315} mutant line, generated at the Sanger Institute, carries a non-sense mutation within the HMG-box coding region that leads to a putative null allele encoding a truncated protein.
We started the characterization of this *sox18* mutant to understand if it behaves as a null.

As first step, we decided to evaluate *sox18* and *sox7* expression profile at 30 hpf in the mutant background. We chose this developmental stage because it is the moment in which *sox7* expression starts to be restricted to the dorsal aorta (DA), while *sox18* continues to be expressed both in the DA and in the posterior cardinal vein (PCV). The offspring of heterozygous mutants in the AB background was analyzed by ISH. Genotyping reveals that, in this background, *sox18*^{sa12315} mutation does not cause gross variation in *sox18* expression profile and that *sox7* is not overexpressed in *sox18*^{sa12315} mutant line. However, in the laboratory, my colleagues expanded ISH analysis to other developmental stages and other backgrounds, finding that *sox7* signal is higher in the caudal vein (CV) of homozygous embryos in a tg(*lyve1*:dsRed)^{nz101} background, at 24 hpf. They checked also for *sox17* expression profile, showing that it is not upregulated at this stage and in this background. Taken together, these data confirm that, also in zebrafish as in mouse, the fine regulation of *soxF* genes expression depends on the genetic background.

In vivo analyses of *sox18*^{sa12315} mutants show that they behave as expected for a null mutant and they recapitulate the circulatory phenotype observed in *sox7*/*sox18* double partial morphants, after perturbation of *sox7* expression with subcritical doses of *sox7*MO.
We analyzed, at 2 dpf and 3 dpf, mutants and siblings either uninjected or injected with subcritical doses of *sox7* morpholino and *std*MO, as a control for unspecific effects. Genotyping reveals that most of wild-type and heterozygous uninjected and *std* control embryos show a normal circulation; only a small number of heterozygotes show absent circulation. This means that the *sox18* mutation only is not sufficient to cause circulatory defects, because Sox7 can compensate Sox18 absence as shown in literature through knockdown studies (Cermenati et al. 2008; Herpers et al. 2008; Pendeville et al. 2008).
In embryos injected with subcritical doses of *sox7*MO, circulatory defects are exacerbated, indeed most of heterozygotes and homozygotes show absent circulation. These data are in agreement with literature, where it has been shown that both *sox7*/*sox18* mutants and *sox7*/*sox18* double partial morphants show defects in trunk-tail circulation (Cermenati et al. 2008; Herpers et al. 2008; Pendeville et al. 2008; Hermkens et al. 2015).

My laboratory performed a molecular analysis of *sox7*/*sox18* double partial morphants by ISH (Cermanati et al. 2008) and by RNA sequencing (unpublished data, in collaboration with Giulio Pavesi from the University of Milan) with the aim to identify possible Sox18 direct or indirect targets. The most promising gene is *vsg1* because it is the most downregulated marker in *sox7*/*sox18* double partial morphants both in ISH and in RNA sequencing data.

vsg1 (*vessel specific gene1*) is the homologue of human *PLVAP (plasmalemma vescicle associated protein)* gene that codifies for PV1, a transmembrane glycoprotein associated to the fenestrated endothelium (Hnasko et al. 2002; Strickland et al., 2005). In mammals, PLVAP is crucial for the development of diaphragms in fenestrated blood vessels (Guo et al., 2016), indeed homozygous *Plvap*-deficient mice lack diaphragms (Herrnberger et al., 2012; Stan et al., 2012; Herrnberger et al., 2014) and, in a pure background, die before birth because of subcutaneous edema, hemorrhages, and defects in the vascular wall of subcutaneous capillaries. Plvap$^{-/-}$ mice, in a mixed genetic background, are born and survive at the most for 4 weeks (Herrnberger et al., 2012; Herrnberger et al., 2014).

Furthermore, Plvap interacts with chemoattractants and adhesion molecules and regulates the extravasation of macrophage and leucocyte from fenestrated endothelium. Rankatari and colleagues showed that Plvap selectively controls the exit of macrophage precursors from the

fetal liver (Rankatari et al., 2016) and that it facilitates lymphocyte migration, presumably by sustaining the selective entry of lymphocytes into the parenchyma, in addition to offering the path of least resistance through cell bodies (Rankatari et al., 2015).

Different studies have also suggested that, in humans, PLVAP is upregulated in various pathophysiological processes associated with angiogenesis, including tumorigenesis (Carson-Walter et al., 2005). In a recent study, PLVAP was shown to be a preferable therapeutic target for cancer therapy, since administration of PLVAP antibodies effectively suppressed tumor growth and had minimal systemic toxicity (Wang et al., 2014).

In zebrafish, a very recent study shows that *vsg1/plvap* behaves as mammalian *Plvap*: it is initially expressed in brain endothelial cells, subsides during development, and is absent from adult brain vasculature (Umans et al., 2017).

As for other vascular districts, *vsg1* has a panendothelial expression around 30 hpf when it becomes to be expressed preferentially in the venous vessels (Qian et al. 2005; Covassin et al. 2006). *vsg1* is strongly downregulated in *sox7/sox18* double partial morphants, as mentioned before, but it is slightly downregulated also in *sox18* morphants and this suggest that *vsg1* can be a direct or indirect target of Sox18 (unpublished data). For all these reasons, we analyzed *vsg1* expression at 30 hpf by ISH in mutants and siblings either uninjected or injected with a subcritical dose of *sox7*MO and a *std*-MO. Genotyping reveals that there is a perfect correlation between *vsg1* signal intensity and the genotype of the embryos: *vsg1* signal is strong in wild-type embryos, slightly reduced in heterozygotes and faint or completely absent in homozygous embryos after *sox7* partial knockdown. These data are in agreement with those obtained in *sox7/sox18* double partial morphants (Cermenati et al. 2008) and *sox18* morphants (unpublished data) and confirm *vsg1* as a possible target of Sox18.

PLVAP has been recently linked to lymphatic structures: PLVAP forms a physical sieve that regulates the parenchymal entry of lymphocytes and soluble antigens (Rankatari et al., 2015). Considering *vsg1* expression pattern and the fact that it seems to be a promising direct target of Sox18, in future, it will be very interesting to investigate the role of *vsg1* in zebrafish lymphatic development.

RNA sequencing data pointed our attention also on another possible interesting marker of Sox18: *notch1b,* one of the two paralogues of *Notch1* (the other is *notch1a*).

It is very interesting to understand if Sox18 could modulate in some way the Notch pathway because Notch signaling is involved in arterio-venous differentiation of endothelial cells, and

it is important for intersomitic sprouts. Moreover, *notch1b* has been linked to lymphangiogenesis, indeed, a recent work shows that lymphatic vessels arise from specialized angioblasts of the ventral wall of the cardinal vein that express *notch1b* together with *nr2f2*/*couptfII* and *fzd7a* (Nicenboim et al., 2015).

RNA sequencing analysis pointed to a statistically significant downregulation of *notch1b* in *sox7*/*sox18* double partial morphants at 22 somites stage. Even if ISH analysis at this stage did not give informative results (data not shown), I expanded the analysis of *notch1b* expression in *std* control embryos and in *sox7*/*sox18* double partial morphants at 24 hpf.

At this stage, *notch1b* is expressed not only in the DA and in the intersomitic vessels (ISVs) but also in the central nervous system. *sox7*/*sox18* double partial morphants show a very strong vessel-specific *notch1b* downregulation if compared to *std* control embryos. *notch1b* downregulation is not due to alteration of the vascular system because the signal of the panendothelial marker *cdh5* and of the arterial one *flt1* are comparable among control embryos and *sox7*/*sox18* double partial morphants. To understand if *sox18*^{sa12315} mutant behaves as a null mutant, we analyzed *notch1b* expression pattern at 24 hpf in mutants and siblings either uninjected or injected with a subcritical dose of *sox7*MO and with *std*MO.

ISH analysis, followed by genotyping, reveals that *notch1b* vascular signal is strongly downregulated in *sox18* homozygous embryos after perturbation of *sox7*, while wild-type and heterozygous embryos show a comparable and unchanged *notch1b* vascular signal. So, when *sox7* is perturbed, *sox18*^{sa12315} mutants behave as *sox7*/*sox18* double partial morphants.

All this data about *notch1b* are part of an article published this year and stating that SoxF proteins positively regulate *notch1b* in zebrafish. Indeed, *notch1b* mRNA expression is strongly downregulated both in *sox7*/*sox18* double partial morphants and in *sox7*/*sox18* double knockout. This work identifies SoxF responsive enhancers in *Notch1* and *notch1b* loci in mouse and in zebrafish, respectively, demonstrating for the first time that Sox7 and Sox18 physically interact with *Notch1*/*notch1b* enhancers both in zebrafish and in mammals (Chiang et al. 2017). In zebrafish, mutations in SoxF responsive enhancer *(notch1b-15)* affect *notch1b* endogenous expression in both the DA and in ISVs, but not in the neural tube of the mutants. RT-PCR analyses confirmed *notch1b* downregulation in purified *flt1*-positive arterial endothelial cell populations from F_3 generation of homozygous fish. No vascular defects were observed in homozygotes, suggesting partial enhancer redundancy. However vascular defects in homozygous and heterozygous mutants were evident, when Notch signaling was perturbed using subcritical doses of *notch1b* morpholino or by treating mutant

embryos with sub-optimal concentration of DAPT, a well characterized inhibitor of the Notch signaling.

In future, it could be of great interest understanding if SoxF factors could regulate other members of the Notch pathway. We have some preliminary RNA sequencing and ISH data showing that *notch3* is downregulated in *sox7*/*sox18* double partial morphants (unpublished data), so *notch3* could be a candidate gene from which to start the analysis.

Our data on zebrafish morphants pointed to a conserved role for Sox18 in zebrafish lymphangiogenesis and let us to hypothesize that *sox18* interacts with *vegfc* in driving lymphangiogenesis (Cermenati et al. 2013). *sox18* morphants have a lower number of lymphatic precursors (PLs) at 2.5 dpf and they are not able to form a normal thoracic duct at 5 dpf. Moreover, the combined partial knockdown of *sox18* and *vegfc*, using subcritical doses of specific morpholinos, which do not exert a strong effect when injected in the embryos, exacerbates defects in both venous and lymphatic sprouting in zebrafish (Cermenati et al. 2013). However, a recent article questioned the role of Sox18 in zebrafish lymphatic vessels development, showing that *sox18* mutants do not show a lymphatic phenotype (van Impel et al. 2014).

Since zebrafish is a powerful model to study lymphangiogenesis and for the screening of small molecules with potential therapeutic effects, it is of crucial importance to clarify if molecular pathways regulating vascular and lymphatic development are conserved in both mammals and zebrafish. With this purpose, we analyzed the lymphatic system of *sox18*^{sa12315} mutants. The lymphatic development could not be followed in *sox18*^{sa12315} line in the AB background, due to the lack of a reporter highlighting lymphatic structures. So we crossed *sox18* heterozygous mutants with two endothelial-specific transgenic lines: *lyve1*:dsRed and *fli1a*:EGFP that allow, respectively, the analysis of venous /lymphatic vessels and of the whole vasculature.

Analysis in the tg(*fli1a:*EGFP);*sox18*^{sa12315} line revealed that, at 52 hpf, in most wild-type embryos PLs manage to reach the horizontal myoseptum, in homozygotes there is subtle but statistically significant reduction in PL number, while heterozygotes show an intermediate phenotype. TD analysis, at 5 dpf, pointed out that the mutation does not cause strong alterations of lymphatic system development, indeed, in both tg(*lyve1*:dsRed);*sox18*^{sa12315} and in tg(*fli1a:*EGFP);*sox18*^{sa12315} line, larvae show a very heterogeneous range of phenotype. Most of wild-type larvae show a completely formed TD, but some of them can have defects in TD formation. However, TD formation defects are statistically significant in homozygotes,

when compared to wild-type larvae. Perturbation of *vegfc* signaling, injecting a subcritical dose of *vegfc*MO, exacerbates TD defects in a genotype-dependent manner in tg(*lyve1*:dsRed);*sox18*^{sa12315}. Not only TD defects are more evident in homozygotes, but they become more marked and statistically significant also in heterozygotes after *vegfc* perturbation.

Taken together, analyses of the lymphatic system of *sox18*^{sa12315} mutant transgenic lines demonstrate that Sox18 has a conserved role in zebrafish lymphangiogenesis, with an interplay with VegfC in the formation of the TD.

These data are in contrast with the work mentioned before, questioning the evolutionary conservation of the entire Sox18/Prox1/Coup-TFII regulatory axis, because single *prox1a, coup-TFII* and *sox18* mutants did not show lymphatic defects (van Impel et al. 2014). However, a recent work showed that *prox1a* maternal-zygotic mutants show a strong lymphatic phenotype demonstrating that Prox1 role in zebrafish lymphangiogenesis is conserved (Koltowska et al. 2015).

There are two hypotheses to explain why the lymphatic defects seen in *sox18*^{sa12315} mutants are so subtle (and not so easy to see). The first is that *sox7* could compensate the absence of *sox18*. It is important to remember that *sox7* is upregulated in the tg(*lyve1*:dsRed) background used for TD analysis. The second hypothesis is that mRNA maternal deposition could compensate the absence of a functional zygotic Sox18 protein. For this reason, in future, it will be of crucial importance to generate a *sox18* maternal-zygotic mutant in which the lymphatic defect should be more evident.

Another important point is to try to understand if the Sox18/Prox1 axis is conserved also in zebrafish. In this case, we will evaluate *prox1a* expression levels by ISH and RT-PCR in *sox18*^{sa12315} mutants. Then, we will perform the same analysis in *sox18* mutants after perturbation of *sox7* or *vegfc* levels to understand if Sox7 and/or Vegfc may cooperate with Sox18 in regulating *prox1a*.

It is known that Sox TFs belonging to different subgroups are often involved in complex regulatory networks driving developmental processes and that they can modulate each other's function when coexpressed in the same territories (Kamachi and Kondoh, 2013). For example, Sox5 and Sox6, of the subgroup D, interact with Sox9, a member of the SoxE, to drive chondrocytes differentiation (Lefebvre et al. 1998; Han and Lefebvre 2008). Moreover, Sox18 (subgroup F) and Sox2 (subgroup B) are essential for derma papillae maturation (Kamachi and Kondoh, 2013; Villani et al., 2017).

The expression of *Sox* genes themselves is frequently subjected to auto-regulation or controlled by other Sox proteins (Kamachi and Kondoh, 2013).
My laboratory has the evidence that Sox7 and Sox18 regulate the vascular expression of *sox13*, a member of the SoxD subgroup (Boezio et al., unpublished).

In mice, *Sox13* expression pattern during embryogenesis was firstly analyzed by Roose and colleagues by *in situ* hybridization on histological sections. *Sox13* is mainly expressed in the central nervous system, but it is also detectable in arteries (Roose et al., 1998).

ISH analysis in *Xenopus laevis*, revealed that *sox13* was detectable in some vascular districts and that *sox13* knockdown by morpholino injection causes defects in vascular vessels (McGary et al. 2010). Furthermore, *SOX13* siRNA-mediated knockdown in HUVEC causes defects also in HUVECs, which fail to form vessels-like structures when cultured in 2D-matrigel (McGary et al. 2010).

In our laboratory, *sox13* expression pattern was analyzed by RT-PCR and ISH experiments on zebrafish embryos from early somitogenesis to 5 dpf. *sox13* expression is widely detectable in the developing central nervous system (CNS) at all the analysed developmental stages. It is also detectable in the DA until 24 hpf, even if the vascular staining is weak if compared to the signal in the CNS (Omini et al., unpublished).

sox13 expression is strongly reduced in the DA of *sox7/sox18* double partial morphants, suggesting that *sox13* vascular expression could be regulated by SoxF (Boezio et al., unpublished). To confirm this possible interaction, we analysed *sox13* expression in *sox18* mutants and siblings either uninjected or injected with a subcritical dose of *sox7*MO and a *std*MO. Since *sox13* expression in the DA is detectable until 24 hpf, I performed ISH analyses at 22 hpf.
ISH analyses, followed by genotyping, reveal that the vast majority of wild-type embryos and most heterozygotes show a strong level of *sox13* staining in the DA. *sox18* mutation causes a slight reduction of *sox13* signal in the DA and this reduction becomes stronger when *sox7* is perturbed in heterozygotes and homozygotes. Thus, we can speculate that Sox7 and Sox18 positively regulate *sox13* expression in the DA.

To investigate the role of *sox13* in angiogenesis, knockdown experiments were performed in my laboratory. *sox13* morphants were analysed from 22 hpf to 2 dpf, in order to cover the events occurring during both primary and secondary angiogenesis (Omini et al., unpublished; Boezio et al., unpublished). *sox13* morphants show defects in primary angiogenesis, indeed, at 30 hpf, some ISVs are blocked to the horizontal myoseptum and

some others are completely absent (Omini et al., unpublished). Moreover, at 2 dpf, *sox13* morphants show a lower number of venous ISVs if compared to control embryos, thus, also secondary angiogenesis is affected by *sox13* knockdown. Preliminary data show that ISVs defects are observed at 2 dpf also by using an independent *sox13* morpholino; in this case, *sox13* morphants show a lower number of both arterial and venous ISVs. However, a deeper analysis is required to better characterize ISVs defects observed using this independent morpholino. We must expand the analysis at 30 hpf to understand how primary angiogenesis is affected and at 1.5 dpf to understand if *sox13* morphants has defects in secondary sprouts. We hypothesize that defects in secondary angiogenesis are a consequence of defects in primary angiogenesis. Indeed, it is known from literature that venous ISVs originate from the fusion of a venous sprout with an arterial ISV (Ellertsdottir et al. 2010); if arterial ISVs are not formed correctly, venous sprouts could have problems in giving rise to venous ISVs.

Trans-migration assay in immortalized mouse lung endothelial cells performed in collaboration with Costanza Giampietro, a former member of our Department, currently at ETH of Zurich, points to an involvement of Sox13 in endothelial cell migration. Indeed, Sox13 overexpression improves the migratory behavior of endothelial cells in an assay that is very similar to physiological conditions. We can speculate that, if Sox13 overexpression increases endothelial cell migration, its absence could cause migration problems.

To dynamically characterize the angiogenic phenotypes of *sox13* morphants, we collaborated with Professor Andrea Bassi, from the "Politecnico di Milano", to perform *in* vivo long-term time-lapse analysis of *sox13* morphants with SPIM technique. The *in vivo* analysis was performed from 26 hpf to 3 dpf and confirmed the ISV defects seen in *sox13* morphants. While control embryos develop a completely normal vascular tree, in *sox13* morphants some ISVs are blocked at the myoseptum, others migrate slowly and some others reach the myoseptum, develop normal but later regress in a ventral to dorsal direction after detaching from the axial vessel. These events seem to indicate that not only the formation but also the stability of ISVs is compromised in *sox13* morphants.

ISVs regression is the most interesting phenotype observed in *sox13* morphants, because regression events occur both in physiological and pathological conditions. For example, ISV regression is crucial during secondary angiogenesis when half of venous sprouts connect to the preexisting arterial sprouts converting them into venous ISVs. When secondary sprouts contact the primary ISVs, blood flow changes its dynamics and the ventral portion of the sprout, in proximity to the DA, regresses until disappearing (Isogai et al. 2003).

Going into details, blood flow is interrupted in the portion of the ISV connecting the sprout to the DA and the thinning of the vessel starts until it regresses and disappears (Franco et al. 2015). The regression of ISVs observed in *sox13* morphants has a similar mechanism, but it is anomalous because it happens without the contact of the regressing vessel with other vessels. A similar phenotype has been observed in *hif-1α* mutants (Gerri et al., 2017) where ISV regression from the DA is caused by impaired interactions between macrophages and endothelial cells during developmental angiogenesis; in these mutants, macrophages are not able to repair vessels after hypoxic conditions leading to ISV regression from the DA (Gerri et al., 2017).

Since sox13 has a role also in hematopoiesis (Omini et al., unpublished), in future it will be of great interest to investigate if *sox13* morphants show defects in macrophages differentiation. It will be also very interesting to generate and characterize a *sox13* mutant in order to better understanding the role of Sox13 in zebrafish angiogenesis.

ISV regression is observed also after the perturbation of Notch and Wnt signaling in zebrafish, mouse retina and in HUVEC using respectively MO-induced knockdown and knockout approaches (Phng et al. 2009; Franco et al. 2015).

My laboratory collected data suggesting that Sox13 could modulate both Wnt and Notch pathway. Sox13 seems to negatively regulate Wnt pathway, because in *sox13* morphants the ISH staining of *ccdn1* (cyclin D1), a target of the Wnt canonical pathway, is upregulated if compared to control embryos (Boezio et al., unpublished).

As for the Notch pathway, *sox13* morphants show elevated *notch1b* staining and their angiogenic defects can be rescued by treatment with the Notch signaling inhibitor DAPT (Omini et al., unpublished). So, ISV defects of *sox13* morphants could be due to alteration of the Notch signaling that, together with Vegf signaling, plays a key role in ISV sprouting.

Taken together these data suggest that Sox13 is a negative regulator of the Notch pathway. This is very interesting if we think that *sox13* vascular expression seems to be regulated by SoxF TFs that are positive regulators of Notch signalling (Chiang et al., 2017).

Our data suggest that SoxF TFs and Sox13 form a complex regulatory network to fine-tune Notch signaling during vascular development. In future, further analyses will be necessary to better characterize the network involving SoxF TFs and Sox13; for example, one could check for the presence of a Sox18 responsive enhancer in *sox13* locus to understand if *sox13* is a direct or indirect target of Sox18.

REFERENCES

Aamar and Dawid. 2010. "Sox17 and Chordin are required for formation of Kupffer's vesicle and Left-Right asymmetry determination in zebrafish". Dev Dyn. 239(11): 2980–2988.

Alders, M., B. M. Hogan, E. Gjini, F. Salehi, L. Al-Gazali, E. A. Hennekam, E. E. Holmberg, M. M. Mannens, M. F. Mulder, G. J. Offerhaus, T. E. Prescott, E. J. Schroor, J. B. Verheij, M. Witte, P. J. Zwijnenburg, M. Vikkula, S. Schulte-Merker and R. C. Hennekam. 2009. "Mutations in CCBE1 cause generalized lymph vessel dysplasia in humans." Nat Genet 41(12): 1272-1274.

Alexander, J. and D. Y. Stainier. 1999. "A molecular pathway leading to endoderm formation in zebrafish." Curr Biol 9(20): 1147-1157.

Alitalo K. 2011. The lymphatic vasculature in disease. Nat Med 17:1371-1380.

Aranguren, X. L., M. Beerens, G. Coppiello, C. Wiese, I. Vandersmissen, A. Lo Nigro, C. M. Verfaillie, M. Gessler and A. Luttun. 2013. "COUP-TFII orchestrates venous and lymphatic endothelial identity by homo- or hetero-dimerisation with PROX1." J Cell Sci 126(Pt 5): 1164-1175.

Baroti et al. 2017. "Sox13 functionally complements the related Sox5 and Sox6 as important developmental modulators in mouse spinal cord oligodendrocytes". JOURNAL OF NEUROCHEMISTRY 136 | 316–328.

Bassi, A., B. Schmid and J. Huisken. 2015. "Optical tomography complements light sheet microscopy for in toto imaging of zebrafish development." Development 142(5): 1016-1020.

Boezio G. "Sox13 nell'angiogenesi: fenotipo e meccanismi molecolari in condizioni di sottodosaggio genico in zebrafish". Relatore: Monica Beltrame. Tesi di Laurea Magistrale in Biologia Molecolare della Cellula. 2014-2015.

Bos et al. 2015. "Single-cell resolution of morphological changes in hemogenic endothelium". Development 142, 2719-2724.

Bowles J, Schepers G, Koopman P. 2000. Phylogeny of the SOX family of developmental transcription factors based on sequence and structural indicators. Dev Biol 227:239-255.

Brown LA, Rodaway AR, Schilling TF, Jowett T, Ingham PW, Patient RK, Sharrocks AD. 2000. Insights into early vasculogenesis revealed by expression of the ETS-domain transcription factor Fli-1 in wild-type and mutant zebrafish embryos. Mech Dev 90:237-252.

Bussmann J, Bos FL, Urasaki A, Kawakami K, Duckers HJ, Schulte-Merker S. 2010. Arteries provide essential guidance cues for lymphatic endothelial cells in the zebrafish trunk. Development 137:2653-2657.

Carmeliet, P., V. Ferreira, G. Breier, S. Pollefeyt, L. Kieckens, M. Gertsenstein, M. Fahrig, A. Vandenhoeck, K. Harpal, C. Eberhardt, C. Declercq, J. Pawling, L. Moons, D. Collen, W. Risau and A. Nagy. 1996. "Abnormal blood vessel development and lethality in embryos lacking a single VEGF allele." Nature 380(6573): 435-439.

Carmeliet P. 2005. "Angiogenesis in life, disease and medicine". Nature 438:932-936.

Carson-Walter et al., 2005."Plasmalemmal Vesicle Associated Protein-1 Is a Novel Marker Implicated in Brain Tumor Angiogenesis". Clinical Cancer Research.

Cermenati S, Moleri S, Cimbro S, Corti P, Del Giacco L, Amodeo R, Dejana E, Koopman P, Cotelli F, Beltrame M. 2008. Sox18 and Sox7 play redundant roles in vascular development. Blood 111:2657-2666.

Cermenati S, Moleri S, Neyt C, Bresciani E, Carra S, Grassini DR, Omini A, Goi M, Cotelli F, Francois M, Hogan BM, Beltrame M. 2013. Sox18 genetically interacts with VegfC to regulate lymphangiogenesis in zebrafish. Arterioscler Thromb Vasc Biol 33:1238-1247.

Chiang IK, Fritzsche M, Pichol-Thievend C, Neal A, Holmes K, Lagendijk A, Overman J, D'Angelo D, Omini A, Hermkens D, Lesieur E, Fossat N, Radziewic T, Liu K, Ratnayaka I, Corada M, Bou-Gharios G, Tam PPL, Carroll J, Dejana E, Schulte-Merker S, Hogan BM, Beltrame M, De Val S, Francois M. 2017.SoxF factors induce Notch1 expression via direct transcriptional regulation during early arterial development. Development doi: 10.1242/dev.146241

Cirone, P., S. Lin, H. L. Griesbach, Y. Zhang, D. C. Slusarski and C. M. Crews. 2008. "A role for planar cell polarity signaling in angiogenesis." Angiogenesis 11(4): 347- 360.

Clarke et al. 2013. "Sox17 and Chordin are required for formation of Kupffer's vesicle and Left-Right asymmetry determination in zebrafish". Dev Dyn. 239(11): 2980–2988

Connell, F., K. Kalidas, P. Ostergaard, G. Brice, T. Homfray, L. Roberts, D. J. Bunyan, S. Mitton, S. Mansour, P. Mortimer, S. Jeffery and C. Lymphoedema. 2010. "Linkage and sequence analysis indicate that CCBE1 is mutated in recessively inherited generalised lymphatic dysplasia." Hum Genet 127(2): 231-241.

Corada, M., M. F. Morini and E. Dejana. 2014. "Signaling pathways in the specification of arteries and veins." Arterioscler Thromb Vasc Biol 34(11): 2372-2377.

Corada, M., D. Nyqvist, F. Orsenigo, A. Caprini, C. Giampietro, M. M. Taketo, M. L. Iruela-Arispe, R. H. Adams and E. Dejana. 2010. "The Wnt/beta-catenin pathway modulates vascular remodeling and specification by upregulating Dll4/Notch signaling." Dev Cell 18(6): 938-949.

Costa et al. 2017. "Endothelial cells divide unequally to sprout fairly". Cell Cycle.

Covassin, L., J. D. Amigo, K. Suzuki, V. Teplyuk, J. Straubhaar and N. D. Lawson. 2006. "Global analysis of hematopoietic and vascular endothelial gene expression by tissue specific microarray profiling in zebrafish." Dev Biol 299(2): 551-562.

Davidson AJ, Zon LI. 2004. The 'definitive' (and 'primitive') guide to zebrafish hematopoiesis. Oncogene 23:7233-7246.

Downes M, Koopman P. 2001. SOX18 and the transcriptional regulation of blood vessel development. Trends Cardiovasc Med 11:318-324.

Ekker, S. C. and J. D. Larson. 2001. Morphant technology in model developmental systems. Genesis 30(3): 89-93.

Ellertsdottir, E., A. Lenard, Y. Blum, A. Krudewig, L. Herwig, M. Affolter and H. G. Belting. 2010. Vascular morphogenesis in the zebrafish embryo. Dev Biol 341(1): 56- 65.

Fatma O. Kok. 2015. Reverse Genetic Screening Reveals Poor Correlation between Morpholino-Induced and Mutant Phenotypes in Zebrafish. Developmental Cell *32*, 97–108

Folkman J. 1995. Angiogenesis in cancer, vascular, rheumatoid and other disease. Nat Med 1:27-31.

Fouquet B, Weinstein BM, Serluca FC, Fishman MC. 1997. Vessel patterning in the embryo of the zebrafish: guidance by notochord. Dev Biol 183:37-48.

Franco, C. A., M. L. Jones, M. O. Bernabeu, I. Geudens, T. Mathivet, A. Rosa, F. M. Lopes, A. P. Lima, A. Ragab, R. T. Collins, L. K. Phng, P. V. Coveney and H. Gerhardt. 2015. Dynamic endothelial cell rearrangements drive developmental vessel regression. PLoS Biol 13(4): e1002125.

Francois M, Caprini A, Hosking B, Orsenigo F, Wilhelm D, Browne C, Paavonen K, Karnezis T, Shayan R, Downes M, Davidson T, Tutt D, Cheah KS, Stacker SA, Muscat GE, Achen MG, Dejana E, Koopman P. 2008. Sox18 induces development of the lymphatic vasculature in mice. Nature 456:643-647.

Francois, M., P. Koopman and M. Beltrame. 2010. "SoxF genes: Key players in the development of the cardio-vascular system." Int J Biochem Cell Biol 42(3): 445- 448.

Francois M, Short K, Secker GA, Combes A, Schwarz Q, Davidson TL, Smyth I, Hong YK, Harvey NL, Koopman P. 2012. Segmental territories along the cardinal veins generate lymph sacs via a ballooning mechanism during embryonic lymphangiogenesis in mice. Dev Biol 364:89-98.

Gerhardt H, Golding M, Fruttiger M, Ruhrberg C, Lundkvist A, Abramsson A, Jeltsch M, Mitchell C, Alitalo K, Shima D, Betsholtz C. 2003. VEGF guides angiogenic sprouting utilizing endothelial tip cell filopodia. J Cell Biol 161:1163-1177.

Gering M, Rodaway AR, Gottgens B, Patient RK, Green AR. 1998. The SCL gene specifies haemangioblast development from early mesoderm. EMBO J 17:4029-4045.

Gerri C., Rube´n Mar´ın-Juez, Michele Marass, Alora Marks, Hans-Martin Maischein & Didier Y.R. Stainier. 2017. Hif-1a regulates macrophage-endothelial interactions during blood vessel development in zebrafish. NATURE COMMUNICATIONS | 8:15492

Geudens, I., Herpers, R., Hermans, K., Segura, I., Ruiz de Almodovar, C., Bussmann, J., De Smet, F., Vandevelde, W., Hogan, B. M., Siekmann, A., et al. 2010. Role of delta-like-4/Notch in the formation and wiring of the lymphatic network in zebrafish. *Arterioscler Thromb Vasc Biol* 30, 1695–1702.

Gore, A. V., M. R. Swift, Y. R. Cha, B. Lo, M. C. McKinney, W. Li, D. Castranova, A. Davis, Y. S. Mukouyama and B. M. Weinstein. 2011. "Rspo1/Wnt signaling promotes angiogenesis via Vegfc/Vegfr3." Development 138(22): 4875-4886.

Gray EE, Ramirez-Valle F, Xu Y, Wu S, Wu Z, Karjalainen KE, Cyster JG. 2013. Deficiency in IL-17-committed Vgamma4(+) gammadelta T cells in a spontaneous Sox13-mutant CD45.1(+) congenic mouse substrain provides protection from dermatitis. Nat Immunol 14:584-592.

Green E, Mann S. 1961. Opossum, a semi-dominant lethal mutation affecting hair and other characteristics of mice. J Hered 52:223-227.

Gubbay J, Collignon J, Koopman P, Capel B, Economou A, Munsterberg A, Vivian N, Goodfellow P, Lovell-Badge R. 1990. A gene mapping to the sex-determining region of the mouse Y chromosome is a member of a novel family of embryonically expressed genes. Nature 346:245-250.

Guo et al. 2016. " Plasmalemma vesicle-associated protein: A crucial component of vascular homeostasis". EXPERIMENTAL AND THERAPEUTIC MEDICINE 12: 1639-1644,

Hagerling R, Pollmann C, Andreas M, Schmidt C, Nurmi H, Adams RH, Alitalo K, Andresen V, Schulte-Merker S, Kiefer F. 2013. A novel multistep mechanism for initial lymphangiogenesis in mouse embryos based on ultramicroscopy. EMBO J 32:629-644.

Han, Y. and V. Lefebvre. 2008. "L-Sox5 and Sox6 drive expression of the aggrecan gene in cartilage by securing binding of Sox9 to a far-upstream enhancer." Mol Cell Biol 28(16): 4999-5013.

Harvey, S. A., Sealy, I., Kettleborough, R., Fényes, F., White, R., Stemple, D. and Smith, J. C.. 2013. Identification of the zebrafish maternal and paternal transcriptomes. *Development* 140, 2703–2710

Hellstrom, M., L. K. Phng, J. J. Hofmann, E. Wallgard, L. Coultas, P. Lindblom, J. Alva, A. K. Nilsson, L. Karlsson, N. Gaiano, K. Yoon, J. Rossant, M. L. Iruela-Arispe, M. Kalen, H. Gerhardt and C. Betsholtz. 2007. "Dll4 signalling through Notch1 regulates formation of tip cells during angiogenesis." Nature 445(7129): 776-780.

Hen et al. 2015. " Venous-derived angioblasts generate organ-specific vessels during zebrafish embryonic development". Development 142, 4266-4278.

Herbert SP, Huisken J, Kim TN, Feldman ME, Houseman BT, Wang RA, Shokat KM, Stainier DY. 2009. Arterial-venous segregation by selective cell sprouting: an alternative mode of blood vessel formation. Science 326:294-298.

Hermkens, D. M., A. van Impel, A. Urasaki, J. Bussmann, H. J. Duckers and S. Schulte-Merker. 2015. "Sox7 controls arterial specification in conjunction with hey2 and efnb2 function." Development 142(9): 1695-1704.

Herpers, R., E. van de Kamp, H. J. Duckers and S. Schulte-Merker. 2008. Redundant roles for sox7 and sox18 in arteriovenous specification in zebrafish. Circ Res 102(1): 12-15.

Herrnberger et al. 2012. "Lack of endothelial diaphragms in fenestrae and caveolae of mutant Plvap-deficient mice". Histochem Cell Biol.

Herrnberger et al. 2014. " Formation of Fenestrae in Murine Liver Sinusoids Depends on Plasmalemma Vesicle-Associated Protein and Is Required for Lipoprotein Passage". PLoS ONE 9(12): e115005

Hnasko, R., M. McFarland and N. Ben-Jonathan. 2002. Distribution and characterization of plasmalemma vesicle protein-1 in rat endocrine glands. J Endocrinol 175(3): 649-661.

Hogan BM, Herpers R, Witte M, Helotera H, Alitalo K, Duckers HJ, Schulte-Merker S. 2009. Vegfc/Flt4 signalling is suppressed by Dll4 in developing zebrafish intersegmental arteries. Development 136:4001-4009.

Hogan, B. M., F. L. Bos, J. Bussmann, M. Witte, N. C. Chi, H. J. Duckers and S. Schulte-Merker. 2009b. "Ccbe1 is required for embryonic lymphangiogenesis and venous sprouting." Nat Genet 41(4): 396-398.

Hosking, B. M., S. C. Wang, S. L. Chen, S. Penning, P. Koopman and G. E. Muscat. 2001. "SOX18 directly interacts with MEF2C in endothelial cells." Biochem Biophys Res Commun 287(2): 493-500.

Hosking B, Francois M, Wilhelm D, Orsenigo F, Caprini A, Svingen T, Tutt D, Davidson T, Browne C, Dejana E, Koopman P. 2009. Sox7 and Sox17 are strain-specific modifiers of the lymphangiogenic defects caused by Sox18 dysfunction in mice. Development 136:2385-2391.

Hosking BM, Muscat GE, Koopman PA, Dowhan DH, Dunn TL. 1995. Trans-activation and DNA-binding properties of the transcription factor, Sox-18. Nucleic Acids Res 23:2626-2628.

Hou L., Srivastava Y., Jauch R. 2017. Molecular basis for the genome engagement by Sox proteins. Seminars in Cell & Developmental Biology 63: 2–12

Irrthum A, Devriendt K, Chitayat D, Matthijs G, Glade C, Steijlen PM, Fryns JP, Van Steensel MA, Vikkula M. 2003. Mutations in the transcription factor gene SOX18 underlie recessive and dominant forms of hypotrichosis-lymphedema-telangiectasia. Am J Hum Genet 72:1470-1478.

Isogai S, Horiguchi M, Weinstein BM. 2001. The vascular anatomy of the developing zebrafish: an atlas of embryonic and early larval development. Dev Biol 230:278-301.

Isogai S, Lawson ND, Torrealday S, Horiguchi M, Weinstein BM. 2003. Angiogenic network formation in the developing vertebrate trunk. Development 130:5281-5290.

Jakobsson L, Franco CA, Bentley K, Collins RT, Ponsioen B, Aspalter IM, Rosewell I, Busse M, Thurston G, Medvinsky A, Schulte-Merker S, Gerhardt H. 2010. Endothelial cells dynamically compete for the tip cell position during angiogenic sprouting. Nat Cell Biol 12:943-953.

Jeltsch M, Kaipainen A, Joukov V, Meng X, Lakso M, Rauvala H, Swartz M, Fukumura D, Jain RK, Alitalo K. 1997. Hyperplasia of lymphatic vessels in VEGF-C transgenic mice. Science 276:1423-1425.

Jung et al. 2017. "Development of the larval lymphatic system in zebrafish". Development 144, 2070-2081.

Kabrun N, Buhring HJ, Choi K, Ullrich A, Risau W, Keller G. 1997. Flk-1 expression defines a population of early embryonic hematopoietic precursors. Development 124:2039-2048.

Kallianpur AR, Jordan JE, Brandt SJ. 1994. The SCL/TAL-1 gene is expressed in progenitors of both the hematopoietic and vascular systems during embryogenesis. Blood 83:1200-1208.

Kamachi, Y. and H. Kondoh. 2013. "Sox proteins: regulators of cell fate specification and differentiation." Development 140(20): 4129-4144.

Karkkainen, M. J., P. Haiko, K. Sainio, J. Partanen, J. Taipale, T. V. Petrova, M. Jeltsch, D. G. Jackson, M. Talikka, H. Rauvala, C. Betsholtz and K. Alitalo. 2004. "Vascular endothelial growth factor C is required for sprouting of the first lymphatic vessels from embryonic veins." Nat Immunol 5(1): 74-80.

Kasimiotis H, Myers MA, Argentaro A, Mertin S, Fida S, Ferraro T, Olsson J, Rowley MJ, Harley VR. 2000. Sex-determining region Y-related protein SOX13 is a diabetes autoantigen expressed in pancreatic islets. Diabetes 49:555-561.

Kaufmann, A., M. Mickoleit, M. Weber and J. Huisken. 2012. Multilayer mounting enables long-term imaging of zebrafish development in a light sheet microscope. Development 139(17): 3242-3247.

Kido S, Hiraoka Y, Ogawa M, Sakai Y, Yoshimura Y, Aiso S. 1998. Cloning and characterization of mouse mSox13 cDNA. Gene 208:201-206.

Kohli V, Schumacher JA, Desai SP, Rehn K, Sumanas S. 2013. Arterial and venous progenitors of the major axial vessels originate at distinct locations. Dev Cell 25:196-206.

Koltowska K, Betterman KL, Harvey NL, Hogan BM. 2013. Getting out and about: the emergence and morphogenesis of the vertebrate lymphatic vasculature. Development 140:1857-1870.

Koltowska, K., A. K. Lagendijk, C. Pichol-Thievend, J. C. Fischer, M. Francois, E. A. Ober, A. S. Yap and B. M. Hogan. 2015. "Vegfc Regulates Bipotential Precursor Division and Prox1 Expression to Promote Lymphatic Identity in Zebrafish." Cell Rep 13(9): 1828-1841.

Kondoh H, Kamachi Y. 2010. SOX-partner code for cell specification: Regulatory target selection and underlying molecular mechanisms. Int J Biochem Cell Biol 42:391-399.

Kuchler AM, Gjini E, Peterson-Maduro J, Cancilla B, Wolburg H, Schulte-Merker S. 2006. Development of the zebrafish lymphatic system requires VEGFC signaling. Curr Biol 16:1244-1248.

Lawson ND, Scheer N, Pham VN, Kim CH, Chitnis AB, Campos-Ortega JA, Weinstein BM. 2001. Notch signaling is required for arterial-venous differentiation during embryonic vascular development. Development 128:3675-3683.

Lawson ND, Weinstein BM. 2002. Arteries and veins: making a difference with zebrafish. Nat Rev Genet 3:674-682.

Lawson, N. D., A. M. Vogel and B. M. Weinstein. 2002b. "sonic hedgehog and vascular endothelial growth factor act upstream of the Notch pathway during arterial endothelial differentiation." Dev Cell 3(1): 127-136.

Lefebvre, V., P. Li and B. de Crombrugghe. 1998. "A new long form of Sox5 (L-Sox5), Sox6 and Sox9 are coexpressed in chondrogenesis and cooperatively activate the type II collagen gene." EMBO J 17(19): 5718-5733.

Lefebvre, V., B. Dumitriu, A. Penzo-Mendez, Y. Han and B. Pallavi. 2007. "Control of cell fate and differentiation by Sry-related high-mobility-group box (Sox) transcription factors." Int J Biochem Cell Biol 39(12): 2195-2214.

Lefebvre V. 2010. The SoxD transcription factors--Sox5, Sox6, and Sox13--are key cell fate modulators. Int J Biochem Cell Biol 42:429-432.

Lelievre E, Lionneton F, Soncin F, Vandenbunder B. 2001. The Ets family contains transcriptional activators and repressors involved in angiogenesis. Int J Biochem Cell Biol 33:391-407.

Leslie JD, Ariza-McNaughton L, Bermange AL, McAdow R, Johnson SL, Lewis J. 2007. Endothelial signalling by the Notch ligand Delta-like 4 restricts angiogenesis. Development 134:839-844.

Liao EC, Paw BH, Oates AC, Pratt SJ, Postlethwait JH, Zon LI. 1998. SCL/Tal-1 transcription factor acts downstream of cloche to specify hematopoietic and vascular progenitors in zebrafish. Genes Dev 12:621-626.

Lilly, A. J., G. Lacaud and V. Kouskoff . 2016. SOXF transcription factors in cardiovascular development. Semin Cell Dev Biol.

Lizama et al. 2015. " Repression of arterial genes in hemogenic endothelium is sufficient for haematopoietic fate acquisition". NATURE COMMUNICATIONS | 6:7739.

Marfil V, Moya M, Pierreux CE, Castell JV, Lemaigre FP, Real FX, Bort R. 2010. Interaction between Hhex and SOX13 modulates Wnt/TCF activity. J Biol Chem 285:5726-5737.

McGary, K. L., T. J. Park, J. O. Woods, H. J. Cha, J. B. Wallingford and E. M. Marcotte. 2010. Systematic discovery of nonobvious human disease models through orthologous phenotypes. Proc Natl Acad Sci U S A 107(14): 6544-6549.

Melichar HJ, Narayan K, Der SD, Hiraoka Y, Gardiol N, Jeannet G, Held W, Chambers CA, Kang J. 2007. Regulation of gammadelta versus alphabeta T lymphocyte differentiation by the transcription factor SOX13. Science 315:230-233.

Moalem S, Brouillard P, Kuypers D, Legius E, Harvey E, Taylor G, Francois M, Vikkula M, Chitayat D. 2014. Hypotrichosis-lymphedema-telangiectasia-renal defect associated with a truncating mutation in the SOX18 gene. Clin Genet.

Mohamed A. et al., 2017. Genetic compensation: A phenomenon in search of mechanisms. PLOS Genetics.

Nicenboim J, Malkinson G, Lupo T, Asaf L, Sela Y, Mayseless O, Gibbs-Bar L, Senderovich N, Hashimshony T, Shin M, Jerafi-Vider A, Avraham-Davidi I, Krupalnik V, Hofi R, Almog G, Astin JW, Golani O, Ben-Dor S, Crosier PS, Herzog W, Lawson ND, Hanna JH, Yanai I, Yaniv K. 2015. Lymphatic vessels arise from specialized angioblasts within a venous niche. Nature 522(7554):56-61

Nicoli S, Presta M. 2007. The zebrafish/tumor xenograft angiogenesis assay. Nat Protoc 2:2918-2923.

Oliver G, Srinivasan RS. 2010. Endothelial cell plasticity: how to become and remain a lymphatic endothelial cell. Development 137:363-372.

Omini.A "SoxD and SoxF genes in hematopoietic and vascular development". PhD Thesis; Scientific tutor: Monica Beltrame. 2013-2014.

Ouyang K, Leandro Gomez-Amaro R, Stachura DL, Tang H, Peng X, Fang X, Traver D, Evans SM, Chen J. 2014. Loss of IP3R-dependent Ca(2+) signalling in thymocytes leads to aberrant development and acute lymphoblastic leukemia. Nat Commun 5:4814.

Overman et al. 2017. " Pharmacological targeting of the transcription factor SOX18 delays breast cancer in mice". eLife 6:e21221.

Pendeville, H., M. Winandy, I. Manfroid, O. Nivelles, P. Motte, V. Pasque, B. Peers, I. Struman, J. A. Martial and M. L. Voz. 2008. Zebrafish Sox7 and Sox18 function together to control arterial-venous identity. Dev Biol 317(2): 405-416.

Pennisi D, Bowles J, Nagy A, Muscat G, Koopman P. 2000a. Mice null for sox18 are viable and display a mild coat defect. Mol Cell Biol 20:9331-9336.

Pennisi D, Gardner J, Chambers D, Hosking B, Peters J, Muscat G, Abbott C, Koopman P. 2000b. Mutations in Sox18 underlie cardiovascular and hair follicle defects in ragged mice. Nat Genet 24:434-437.

Pevny LH, Lovell-Badge R. 1997. Sox genes find their feet. Curr Opin Genet Dev 7:338-344.

Pham VN, Lawson ND, Mugford JW, Dye L, Castranova D, Lo B, Weinstein BM. 2007. Combinatorial function of ETS transcription factors in the developing vasculature. Dev Biol 303:772-783.

Poulat, F., F. Girard, M. P. Chevron, C. Goze, X. Rebillard, B. Calas, N. Lamb and P. Berta. 1995. "Nuclear localization of the testis determining gene product SRY." J Cell Biol 128(5): 737-748.

Qian, F., F. Zhen, C. Ong, S. W. Jin, H. Meng Soo, D. Y. Stainier, S. Lin, J. Peng and Z. Wen. 2005. "Microarray analysis of zebrafish cloche mutant using amplified cDNA and identification of potential downstream target genes." Dev Dyn 233(3): 1163-1172.

Quillien, A., Moore, J. C., Shin, M., Siekmann, A. F., Smith, T., Pan, L., Moens, C. B., Parsons, M. J. and Lawson, N. D.. 2014. Distinct Notch signaling outputs pattern the developing arterial system. *Development*.

Rankatari et al. 2015. "The endothelial protein PLVAP in lymphatics controls the entry of lymphocytes and antigens into lymph nodes". nature immunology VOLUME 16 NUMBER 4.

Rankatari et al. 2016. " Fetal liver endothelium regulates the seeding of tissue-resident macrophages". NATURE VOL000l00.

Risau W. 1997. Mechanisms of angiogenesis. Nature 386:671-674.

Risau W, Flamme I. 1995. Vasculogenesis. Annu Rev Cell Dev Biol 11:73-91.

Rissone A, Foglia E, Sangiorgio L, Cermenati S, Nicoli S, Cimbro S, Beltrame M, Bussolino F, Cotelli F, Arese M. 2012. The synaptic proteins beta-neurexin and neuroligin synergize with extracellular matrix-binding vascular endothelial growth factor a during zebrafish vascular development. Arterioscler Thromb Vasc Biol 32:1563-1572.

Robu, M. E., J. D. Larson, A. Nasevicius, S. Beiraghi, C. Brenner, S. A. Farber and S. C. Ekker 2007. p53 activation by knockdown technologies. PLoS Genet 3(5): e78.

Roose J, Korver W, Oving E, Wilson A, Wagenaar G, Markman M, Lamers W, Clevers H. 1998. High expression of the HMG box factor sox-13 in arterial walls during embryonic development. Nucleic Acids Res 26:469-476.

Rossi a. et al., 2015. Genetic compensation induced by deleterious mutations but not gene knockdowns. Nature, VOL 524.

Saaristo A, Veikkola T, Tammela T, Enholm B, Karkkainen MJ, Pajusola K, Bueler H, Yla-Herttuala S, Alitalo K. 2002. Lymphangiogenic gene therapy with minimal blood vascular side effects. J Exp Med 196:719-730.

Sabin FR. 1902. On the origin of the lymphatic system from the veins and the development of the lymph hearts and thoracic ducts in the pig. Am J Anat 1:367-389.

Sacilotto, N., Monteiro, R., Fritzsche, M., Becker, P. W., Sanchez-del-Campo, L., Liu, K., Pinheiro, P., Ratnayaka, I., Davies, B., Goding, C. R., et al. 2013. Analysis of Dll4 regulation reveals a combinatorial role for Sox and Notch in arterial development. *Proc Natl Acad Sci USA* 110, 11893–11898.

Sandholzer J, Hoeth M, Piskacek M, Mayer H, de Martin R. 2007. A novel 9-amino-acid transactivation domain in the C-terminal part of Sox18. Biochem Biophys Res Commun 360:370-374.

Sakamoto, Y., K. Hara, M. Kanai-Azuma, T. Matsui, Y. Miura, N. Tsunekawa, M. Kurohmaru, Y. Saijoh, P. Koopman and Y. Kanai. 2007. "Redundant roles of Sox17 and Sox18 in early cardiovascular development of mouse embryos." Biochem Biophys Res Commun 360(3): 539-544.

Schepers GE, Teasdale RD, Koopman P. 2002. Twenty pairs of sox: extent, homology, and nomenclature of the mouse and human sox transcription factor gene families. Dev Cell 3:167-170.

Smith and Koopman 2004. " The ins and outs of transcriptional control: nucleocytoplasmic shuttling in development and disease". TRENDS in Genetics Vol.20 No.1

Siekmann AF, Lawson ND. 2007a. Notch signalling and the regulation of angiogenesis. Cell Adh Migr 1:104-106.

Siekmann AF, Lawson ND. 2007b. Notch signalling limits angiogenic cell behaviour in developing zebrafish arteries. Nature 445:781-784.

Sinner D, Rankin S, Lee M, Zorn AM. 2004. Sox17 and beta-catenin cooperate to regulate the transcription of endodermal genes. Development 131:3069-3080.

Slee. 1957. The morphology and development of Ragged-a mutant affecting the skin and hair of the house mouse. J. Genet. 55:570-584.

Stainier, D. Y., B. M. Weinstein, H. W. Detrich, 3rd, L. I. Zon and M. C. Fishman. 1995. "Cloche, an early acting zebrafish gene, is required by both the endothelial and hematopoietic lineages." Development 121(10): 3141-3150.

Stan et al. 2012. " The Diaphragms of Fenestrated Endothelia: Gatekeepers of Vascular Permeability and Blood Composition". Developmental Cell *23*, 1203–1218

Stolt, C. C., A. Schlierf, P. Lommes, S. Hillgartner, T. Werner, T. Kosian, E. Sock, N. Kessaris, W. D. Richardson, V. Lefebvre and M. Wegner. 2006. "SoxD proteins influence multiple stages of oligodendrocyte development and modulate SoxE protein function." Dev Cell 11(5): 697-709.

Strickland et al. 2005. " Plasmalemmal vesicle-associated protein (PLVAP) is expressed by tumour endothelium and is upregulated by vascular endothelial growth factor-A (VEGF)". *J Pathol* 206: 466–475

Sumanas S, Lin S. 2006. Ets1-related protein is a key regulator of vasculogenesis in zebrafish. PLoS Biol 4:e10.

Swift M. R. and B. M. Weinstein. 2009. "Arterial-venous specification during development." Circ Res 104(5): 576-588.

Tammela T, Alitalo K. 2010. Lymphangiogenesis: Molecular mechanisms and future promise. Cell 140:460-476.

Tammela T, Zarkada G, Wallgard E, Murtomaki A, Suchting S, Wirzenius M, Waltari M, Hellstrom M, Schomber T, Peltonen R, Freitas C, Duarte A, Isoniemi H, Laakkonen P, Christofori G, Yla-Herttuala S, Shibuya M, Pytowski B, Eichmann A, Betsholtz C, Alitalo K. 2008. Blocking VEGFR-3 suppresses angiogenic sprouting and vascular network formation. Nature 454:656-660.

Turchinovich G, Hayday AC. 2011. Skint-1 identifies a common molecular mechanism for the development of interferon-gamma-secreting versus interleukin-17-secreting gammadelta T cells. Immunity 35:59-68.

Umans et al. 2017. " CNS angiogenesis and barriergenesis occur simultaneously". Developmental Biology 425: 101–108.

Vaahtomeri et al. 2017. "Lymphangiogenesis guidance by paracrine and pericellular factors". GENES & DEVELOPMENT 31:1615–1634.

van Impel, A., Z. Zhao, D. M. Hermkens, M. G. Roukens, J. C. Fischer, J. Peterson-Maduro, H. Duckers, E. A. Ober, P. W. Ingham and S. Schulte-Merker. 2014. "Divergence of zebrafish and mouse lymphatic cell fate specification pathways." Development 141(6): 1228-1238.

Villani et al. 2017. " Dominant-negative Sox18 function inhibits dermal papilla maturation and differentiation in all murine hair types". Development (2017) 144, 1887-1895.

Wang HU, Chen ZF, Anderson DJ. 1998. Molecular distinction and angiogenic interaction between embryonic arteries and veins revealed by ephrin-B2 and its receptor Eph-B4. Cell 93:741-753.

Wang Y, Bagheri-Fam S, Harley VR. 2005. SOX13 is up-regulated in the developing mouse neuroepithelium and identifies a sub-population of differentiating neurons. Brain Res Dev Brain Res 157:201-208.

Wang Y, Ristevski S, Harley VR. 2006. SOX13 exhibits a distinct spatial and temporal expression pattern during chondrogenesis, neurogenesis, and limb development. J Histochem Cytochem 54:1327-1333.

Wang et al. 2014. "Plasmalemmal Vesicle Associated Protein (PLVAP) as a therapeutic target for treatment of hepatocellular carcinoma". BMC Cancer 2014, 14:815.

Watabe, T.. 2012. "Roles of transcriptional network during the formation of lymphatic vessels." J Biochem 152(3): 213-220.

Wegner M. 1999. From head to toes: the multiple facets of Sox proteins. Nucleic Acids Res 27:1409-1420.

Weinstein, B. M.. 2002. "Plumbing the mysteries of vascular development using the zebrafish." Semin Cell Dev Biol 13(6): 515-522.

Wiley DM, Kim JD, Hao J, Hong CC, Bautch VL, Jin SW. 2011. Distinct signalling pathways regulate sprouting angiogenesis from the dorsal aorta and the axial vein. Nat Cell Biol 13:686-692.

Wilson, M. and P. Koopman. 2002. "Matching SOX: partner proteins and co-factors of the SOX family of transcriptional regulators." Curr Opin Genet Dev 12(4): 441-446.

Wythe, J. D., Dang, L. T. H., Devine, W. P., Boudreau, E., Artap, S. T., He, D., Schachterle, W., Stainier, D. Y. R., Oettgen, P., Black, B. L., et al. 2013. ETS Factors Regulate Vegf-Dependent Arterial Specification. *Dev Cell* 26, 45–58.

Yaniv K, Isogai S, Castranova D, Dye L, Hitomi J, Weinstein BM. 2006. Live imaging of lymphatic development in the zebrafish. Nat Med 12:711-716.

You LR, Lin FJ, Lee CT, DeMayo FJ, Tsai MJ, Tsai SY. 2005. Suppression of Notch signalling by the COUP-TFII transcription factor regulates vein identity. Nature 435:98-104.

Zhou, Y., Williams, J., Smallwood, P. M. and Nathans, J. 2015. Sox7, Sox17, and Sox18 Cooperatively Regulate Vascular Development in the Mouse Retina. *PLoS ONE* 10, e0143650.

Part II

© 2017. Published by The Company of Biologists Ltd | Development (2017) 144, 3847-3848 doi:10.1242/dev.159715

CORRECTION

Correction: SoxF factors induce Notch1 expression via direct transcriptional regulation during early arterial development. Development doi: 10.1242/dev.146241

Ivy Kim-Ni Chiang[1,*], Martin Fritzsche[2,*], Cathy Pichol-Thievend[1], Alice Neal[2], Kelly Holmes[3], Anne Lagendijk[1], Jeroen Overman[1], Donatella D'Angelo[4], Alice Omini[4], Dorien Hermkens[5], Emmanuelle Lesieur[1], Nicolas Fossat[6], Tania Radziewic[6], Ke Liu[7], Indrika Ratnayaka[2], Monica Corada[8], George Bou-Gharios[7], Patrick P. L. Tam[6,9], Jason Carroll[3], Elisabetta Dejana[8,10], Stefan Schulte-Merker[5], Benjamin M. Hogan[1], Monica Beltrame[4], Sarah De Val[2,‡] and Mathias Francois[1,‡]

[1]Institute for Molecular Bioscience, The University of Queensland, Brisbane, Queensland 4072, Australia. [2]Ludwig Institute for Cancer Research, Nuffield Department of Clinical Medicine, The University of Oxford, Oxford OX3 7DQ, UK. [3]Cancer Research UK, The University of Cambridge, Li Ka Shing Centre, Robinson Way, Cambridge CB2 0RE, UK. [4]Dipartimento di Bioscienze, Universita' degli Studi di Milano, Via Celoria 26, 20133 Milano, Italy. [5]University of Münster, 48149 Münster, Germany Institute for Cardiovascular Organogenesis and Regeneration, Faculty of Medicine, Westfälische Wilhelms-Universität Münster (WWU), Mendelstrasse 7, 48149 Münster and CiM Cluster of Excellence, Germany. [6]Embryology Unit, Children's Medical Research Institute, Westmead NSW 2145, Australia. [7]Institute of Aging and Chronic Disease, University of Liverpool, Liverpool L69 3GA, UK. [8]IFOM, FIRC Institute of Molecular Oncology, 1620139 Milan, Italy. [9]School of Medical Sciences, Sydney Medical School, University of Sydney, Westmead NSW 2145, Australia. [10]Department of Immunology Genetics and Pathology, Uppsala University, 75185 Uppsala, Sweden.

*These authors contributed equally to this work

‡Authors for correspondence (sarah.deval@ludwig.ox.ac.uk; m.francois@imb.uq.edu.au)

There were errors published in 'SoxF factors induce Notch1 expression via direct transcriptional regulation during early arterial development' by Ivy Kim-Ni Chiang, Martin Fritzsche, Cathy Pichol-Thievend, Alice Neal, Kelly Holmes, Anne Lagendijk, Jeroen Overman, Donatella D'Angelo, Alice Omini, Dorien Hermkens, Emmanuelle Lesieur, Ke Liu, Indrika Ratnayaka, Monica Corada, George Bou-Gharios, Jason Carroll, Elisabetta Dejana, Stefan Schulte-Merker, Benjamin Hogan, Monica Beltrame, Sarah De Val and Mathias Francois (2017). *Development* **144**, 2629-2639 (doi: 10.1242/dev.146241).

The contribution of Nicolas Fossat, Tania Radziewic and Patrick P. L. Tam was inadvertently omitted. These authors generated and validated the *Sox7* knockout mouse line used to produce the *Sox7*/*Sox18* double-knockout line (Fig. 9A). An explanation of how this mouse line was generated was absent from the supplementary Materials and Methods. In addition, the middle initial of Benjamin Hogan was missing.

The corrected author list and affiliations appear above. Revised Author contributions and Funding sections, as well as a revised section of the supplementary Materials and Methods that now includes generation of the *Sox7* knockout mouse line, appear below.

The authors apologise to readers for these mistakes.

Author contributions

Conceptualization: I.K.-N.C., M.Frit., S.D.V., M.Fran.; Methodology: I.K.-N.C., M.Frit., S.D.V., M.Fran.; Formal analysis: K.H., J.C.; Investigation: I.K.-N.C., M.Frit., C.P.-T., A.N., K.H., A.L., J.O., D.D., A.O., D.H., E.L., K.L., I.R., M.C., B.M.H.; Resources: A.L., G.B.-G., J.C., S.S.-M., M.B., N.F., T.R., P.P.L.T.; Data curation: K.H., J.C.; Writing - original draft: I.K.-N.C., S.D.V., M.Fran.; Writing - review & editing: I.K.-N.C., B.M.H., M.B., S.D.V., M.Fran.; Visualization: I.K.-N.C., S.D.V., M.Fran.; Supervision: G.B.-G., J.C., E.D., B.M.H., M.B., P.P.L.T., S.D.V., M.Fran.; Project administration: S.D.V., M.Fran.; Funding acquisition: S.D.V., M.B., M.Fran.

Funding

This work was supported by the National Health and Medical Research Council of Australia (NHMRC) (APP1107643); The Cancer Council Queensland (1107631) (M.Fran.); the Australian Research Council Discovery Project (DP140100485, M.Fran.; DP1094008, P.P.L.T.); NHMRC Senior Principal Research Fellowship (APP1003100) (P.P.L.T.); University of Sydney Postdoctoral Fellowship (N.F.); NHMRC Career Development Fellowship (APP1111169) (M.Fran.); the Ludwig Institute for Cancer Research (M.Frit., A.N., I.R., S.D.V.); the Medical Research Council (MR/J007765/1) (K.L., G.B.-G., S.D.V.); the Fondazione Cariplo (2011-0555) (M.B., B.M.H., M.Fran.); and the Biotechnology and Biological Sciences Research Council (BB/L020238/1) (A.N., K.L., G.B.-G., S.D.V.). Deposited in PMC for release after 6 months.

Supplementary Materials and Methods

Generation and analysis of transgenic and mutant mice (final paragraph)

Sox7:tm1 (*Sox7*$^{+/-}$) mice were generated through germline transmission in chimaeras, using VGB6 ES cells (of C57BL/6NTac background) that contained an inactivated *Sox7* allele replaced with a ZEN-Ub1 cassette from Velocigene (*Sox7*$^{tm1(KOMP)Vlcg}$), and

Development (2017) 144, 3847-3848 doi:10.1242/dev.159715

obtained from the KOMP repository at University of California at Davis (https://www.komp.org/pdf.php?projectID=VG10649). Compound *Sox7*$^{-/-}$;*Sox18*$^{-/-}$ mouse embryos were generated on the C57BL/6 background through crossing heterozygous *Sox7*:tm1 to *Sox18*:tm1, generating *Sox7*$^{+/-}$;*Sox18*$^{+/-}$ mice which were subsequently incrossed (Pennisi et al., 2000a). Genotype was confirmed by PCR using the following primers: mSox7(F), TGTAACTTGGAGATCCATAGAGC; mSox7(R), TCATTCTCAGTATTGTTTTGCC; mSox7lacZ(R), TGGATCAGCTAAGCCAGGT; mSox18(F), CCCGACGTCCATCAGACCTC; mSox18(R), GTCGCTTGCGCTCGT-CCTTC; mSox18lacZ(R), CGCCCGTTGCACCACAGATG. All animals used were 7-24 weeks old.

© 2017. Published by The Company of Biologists Ltd | Development (2017) 144, 2629-2639 doi:10.1242/dev.146241

RESEARCH ARTICLE

SoxF factors induce Notch1 expression via direct transcriptional regulation during early arterial development

Ivy Kim-Ni Chiang[1,*], Martin Fritzsche[2,*], Cathy Pichol-Thievend[1], Alice Neal[2], Kelly Holmes[3], Anne Lagendijk[1], Jeroen Overman[1], Donatella D'Angelo[4], Alice Omini[4], Dorien Hermkens[5], Emmanuelle Lesieur[1], Ke Liu[6], Indrika Ratnayaka[2], Monica Corada[7], George Bou-Gharios[6], Jason Carroll[3], Elisabetta Dejana[7,8], Stefan Schulte-Merker[5], Benjamin Hogan[1], Monica Beltrame[4], Sarah De Val[2,‡] and Mathias Francois[1,‡]

ABSTRACT

Arterial specification and differentiation are influenced by a number of regulatory pathways. While it is known that the Vegfa-Notch cascade plays a central role, the transcriptional hierarchy controlling arterial specification has not been fully delineated. To elucidate the direct transcriptional regulators of Notch receptor expression in arterial endothelial cells, we used histone signatures, DNaseI hypersensitivity and ChIP-seq data to identify enhancers for the human *NOTCH1* and zebrafish *notch1b* genes. These enhancers were able to direct arterial endothelial cell-restricted expression in transgenic models. Genetic disruption of SoxF binding sites established a clear requirement for members of this group of transcription factors (SOX7, SOX17 and SOX18) to drive the activity of these enhancers *in vivo*. Endogenous deletion of the *notch1b* enhancer led to a significant loss of arterial connections to the dorsal aorta in Notch pathway-deficient zebrafish. Loss of SoxF function revealed that these factors are necessary for *NOTCH1* and *notch1b* enhancer activity and for correct endogenous transcription of these genes. These findings position SoxF transcription factors directly upstream of Notch receptor expression during the acquisition of arterial identity in vertebrates.

KEY WORDS: Notch1, SoxF, Artery, Arterial enhancer, Endothelial cell, Transcriptional regulation, Zebrafish, Human, Mouse

INTRODUCTION

Genetic specification of arterial fate has long been attributed to regulation downstream of the Vegfa and Notch pathways. Vegfa signalling is essential for arterial specification in both zebrafish and mammalian models, at least partially by stimulating the expression of components of the Notch pathway, while activation of Notch signalling can rescue defects in Vegfa-deficient zebrafish embryos (Lanahan et al., 2010; Lawson et al., 2002; Liu et al., 2003; Visconti et al., 2002). The Notch receptors Notch1 and Notch4 and the delta-like ligands Dll1, Dll4, Jag1 and Jag2 are expressed in endothelial cells, where they play crucial roles in both arteriogenesis and angiogenesis (Lawson et al., 2002; Liu et al., 2003; Phng and Gerhardt, 2009; Roca and Adams, 2007). Ligand binding to the Notch receptor releases the Notch intracellular domain (NICD), which translocates to the nucleus and forms a transcriptional activation complex with the otherwise repressive DNA-bound Rbpj [CSL, Su(H)] (Bray, 2006). Combined ablation of Notch1 and Notch4, which are both principally expressed in arterial endothelial cells during early vascular remodelling (Chong et al., 2011; Jahnsen et al., 2015), results in severe vascular remodelling defects (Krebs et al., 2000), as does ablation of the Notch downstream effector Rbpj or of Dll4, a Notch ligand specific within the vasculature to arteries (Duarte et al., 2004; Gale et al., 2004; Krebs et al., 2004). However, loss of Notch signalling does not fully recapitulate the arterial defects downstream of Vegfa ablation (Carmeliet et al., 1996; Krebs et al., 2000; Lawson et al., 2002), and the arterially restricted gene expression patterns of components of the Notch pathway do not fully overlap with activated Vegfa (Lawson, 2003), suggesting that additional factors are involved in the regulation of Notch-mediated arterial fate.

The SoxF group of transcription factors (Sox7, Sox17 and Sox18) are expressed in endothelial cells from early in development (Francois et al., 2010). While each SoxF member displays a subtly different endothelial expression pattern, all three factors are expressed early in arterial development (Corada et al., 2013; François et al., 2008; Zhou et al., 2015) and share considerable functional redundancy, complicating interpretation of the consequences of gene disruption (Hosking et al., 2009; Zhou et al., 2015). Combined loss of *sox7* and *sox18* in zebrafish, both by morpholino-based knockdown and genetic mutation, resulted in serious arteriovenous malformations similar to those seen after Notch ablation, suggesting that SoxF factors might genetically interact with the Notch pathway in endothelial cells (Cermenati et al., 2008; Hermkens et al., 2015; Herpers et al., 2008; Lawson et al., 2001). Further evidence was provided in mice, where endothelial-specific ablation of *Sox17* caused arterial differentiation and remodelling defects (Corada et al., 2013), and conditional deletion of SoxF factors in the adult resulted in loss of major vessel identity in the retina (Zhou et al., 2015). Inhibition of Vegfa signalling can significantly impact SoxF expression and activity in both mouse and zebrafish models (Kim et al., 2016; Pendeville et al., 2008; Duong et al., 2014; Pennisi et al., 2000b), suggesting that members of the SoxF family lie downstream of Vegfa. Further, SoxF acts in a positive feed-forward loop to maintain *Flk1*

[1]Institute for Molecular Bioscience, The University of Queensland, Brisbane, Queensland 4072, Australia. [2]Ludwig Institute for Cancer Research, Nuffield Department of Clinical Medicine, The University of Oxford, Oxford OX3 7DQ, UK. [3]Cancer Research UK, The University of Cambridge, Li Ka Shing Centre, Robinson Way, Cambridge CB2 0RE, UK. [4]Dipartimento di Bioscienze, Universita' degli Studi di Milano, Via Celoria 26, 20133 Milano, Italy. [5]University of Münster, 48149 Münster, Germany Institute for Cardiovascular Organogenesis and Regeneration, Faculty of Medicine, Westfälische Wilhelms-Universität Münster (WWU), Mendelstrasse 7, 48149 Münster and CiM Cluster of Excellence, Germany. [6]Institute of Aging and Chronic Disease, University of Liverpool, Liverpool L69 3GA, UK. [7]IFOM, FIRC Institute of Molecular Oncology, 1620139 Milan, Italy. [8]Department of Immunology Genetics and Pathology, Uppsala University, 75185 Uppsala, Sweden.
*These authors contributed equally to this work

‡Authors for correspondence (sarah.deval@ludwig.ox.ac.uk; m.francois@imb.uq.edu.au)

M.F., 0000-0002-9846-6882

Received 28 October 2016; Accepted 7 June 2017

Development (2017) 144, 2629-2639 doi:10.1242/dev.146241

(*Kdr*; *kdrl* in zebrafish) expression (Kim et al., 2016). By contrast, the ablation of Notch signalling in the vasculature does not significantly impact the expression of SoxF (Abdelilah et al., 1996; Corada et al., 2013). Different experimental models have positioned SoxF genes both upstream (Corada et al., 2013) and downstream (Lee et al., 2014) of Notch signalling in endothelial cells, suggesting a complex relationship between these two pathways.

Analysis of the only known enhancers for the Notch pathway, namely the arterial-specific *Dll4*-12 (Sacilotto et al., 2013) and *Dll4*in3 enhancers (Sacilotto et al., 2013; Wythe et al., 2013), has demonstrated a crucial role for SoxF factors in the regulation of expression of the Notch ligand *Dll4* in arteries, in combination with Rbpj/Notch binding and in the presence of Ets factors including Erg (Sacilotto et al., 2013; Wythe et al., 2013). Although this work clearly positioned the SoxF and Notch pathways as crucial regulators of arterial specification, and is supported by analysis placing Sox17 upstream of Notch signalling in mouse models (Corada et al., 2013), ablation of arterial marker expression only occurs after the removal of both SoxF factors and Notch signalling in combination (Sacilotto et al., 2013). Consequently, the precise transcriptional hierarchy of SoxF and Notch has yet to be fully established. Although studies of the Notch receptor genes *Notch1* and *Notch4* also identified SoxF binding motifs within putative promoter sequences (Corada et al., 2013; Lizama et al., 2015), a requirement for these SOX motifs in arterial-specific gene expression of Notch receptors has not been established. In this study, we have identified and characterised arterial-specific enhancers directing *NOTCH1/notch1b* gene expression *in vivo*, and used them to demonstrate a direct requirement for SoxF factors in the transcriptional regulation of Notch receptors during early arterial differentiation, positioning SoxF factors upstream of Notch in the acquisition of arterial cell identity.

RESULTS

Identification of an arterial-specific *NOTCH1* intronic enhancer

Previous studies into the transcriptional regulation of the Notch receptors have not extended to the identification or analysis of gene enhancers (cis-regulatory elements) (Corada et al., 2013; Lizama et al., 2015; Wu et al., 2005). We therefore conducted a detailed *in silico* analysis of the *NOTCH1* locus with the aim of identifying novel, arterial-specific enhancers. This analysis focused on human *NOTCH1* in order to take advantage of the wealth of publicly available information describing chromatin modifications in human endothelial cell lines. Using this information, we were able to pinpoint four regions of DNA rich in endothelial cell-specific H3K4me1 and H3K27ac histone modifications and DNaseI digital genomic footprints, all marks closely associated with enhancer activity (Heintzman and Ren, 2009; Sabo et al., 2004) (Fig. 1A, Fig. S1).

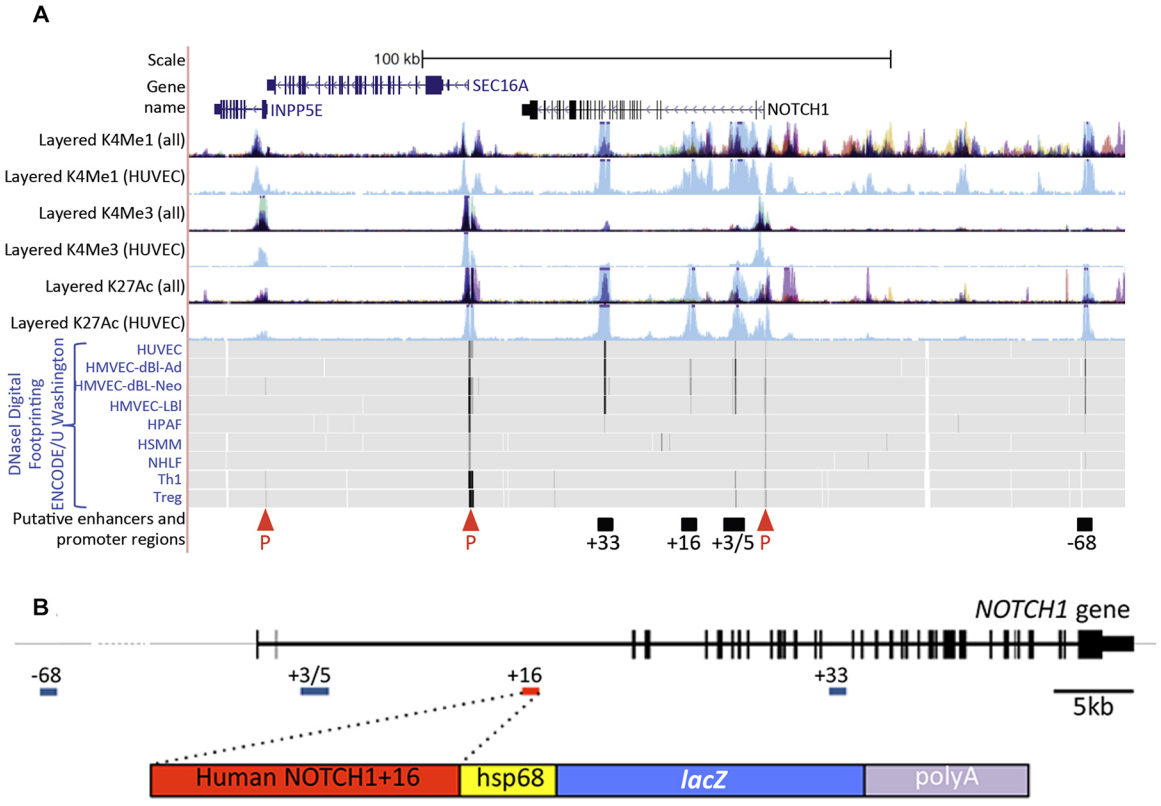

Fig. 1. The human *NOTCH1* locus contains multiple putative endothelial enhancers. (A) The human *NOTCH1* locus from UCSC ENCODE Genome Browser (http://genome.ucsc.edu). Human umbilical vein endothelial cell (HUVEC)-specific H3me1 and H3K27ac (enhancer associated) and H3K4me3 (promoter associated) peaks are indicated in light blue [both in the separate HUVEC and combined tracks (denoted as 'all')]; other colours indicate H3K4me1, H3K4me3 and H3K4ac peaks specific to non-endothelial cell lines: GM12878 cells (red), H1-hESC cells (yellow), HSMM cells (green), K562 cells (purple) NHEK cells (lilac) and NHLF cells (pink). *INPP5E* and *SEC16A* are shown (blue text) in addition to *NOTCH1* (black text). DNase I digital hypersensitive hotspots are indicated by black vertical lines on grey (HUVEC, HMVEC-dBl-Ad, HMVEC-dBl-Neo and HMVEC-LBl, which are all different endothelial cell types). The four *NOTCH1* putative enhancer regions (black bars) were identified by high levels of HUVEC-specific H3K4me1 and H3K27ac associated with endothelial cell-specific DNaseI hypersensitivity hotspots. P, putative promoters identified by H3K4me3. (B) The human *NOTCH1* gene (top, in 5′ to 3′ orientation with putative enhancers indicated) and the *NOTCH1+16hsp* transgene (bottom).

Development (2017) 144, 2629-2639 doi:10.1242/dev.146241

The putative enhancer regions were named *NOTCH1+33*, *NOTCH1+16*, *NOTCH1+3/5* and *NOTCH1−68* to reflect their distance from the transcription start site (TSS) in kb. Each enhancer region was cloned upstream of the silent *hsp68* minimal promoter and the *lacZ* reporter gene (Fig. 1B) and tested for its ability to drive reporter gene expression specifically in arterial endothelial cells of transient transgenic mice at embryonic day (E) 12-13. Although each of the four putative enhancer regions was able to drive detectable levels of *lacZ* in transgenic mice, this expression was primarily neural, an expression pattern commonly seen when using the *hsp68* minimal promoter (e.g. Becker et al., 2016; Sacilotto et al., 2013) (Table 1, Fig. S2). Only the *NOTCH1+33* and *NOTCH1+16* enhancers were able to direct expression in endothelial cells (Table 1, Fig. S2). In the case of *NOTCH1+33*, vascular expression was detected in only one of the five transgenic mice analysed. This expression was not restricted to the arterial endothelium but was pan-endothelial (Table 1, Fig. S2). This agrees with previous reports indicating that the mouse orthologue of this region, termed Notch1_enh1, also directs occasional vascular enhancer activity but did not show arterial-specific expression (Zhou et al., 2017). Conversely, the 274 bp *NOTCH1+16* enhancer was able to robustly direct expression specifically to arterial endothelial cells within the vasculature at E12 in multiple independent transgenic embryos (Table 1, Fig. 2 and Fig. S2). This indicates that the *NOTCH1+16* enhancer represents a novel, arterially restricted enhancer within the *NOTCH1* locus. Analysis of a stable mouse line expressing the *NOTCH1+16:lacZ* transgene clearly demonstrated that this enhancer is strongly active from the very early stages of vascular development, mimicking the expression of endogenous Notch by becoming restricted to the arteries by late E9.5 and then maintaining an arterial endothelial cell-restricted expression pattern throughout embryonic development (Chong et al., 2011; Jahnsen et al., 2015) (Fig. 2).

The *NOTCH1+16* enhancer is bound and regulated by SoxF factors

To identify the transcription factors that potentially regulate the *NOTCH1+16* enhancer, we performed a ClustalW analysis of orthologous mammalian sequences (Fig. 3A). This analysis clearly identified nine conserved core consensus ETS binding motifs [GGAW (Hollenhorst et al., 2011)] and two consensus SOX binding motifs [WWCAAW (Mertin et al., 1999)] (Fig. 3A) within the 274 bp *NOTCH1+16* enhancer. Because not all *in silico* consensus binding motifs are able to functionally bind the cognate protein, these motifs were then tested by electrophoretic mobility shift assay (EMSA). Both SOX motifs (termed hmSOX-a and hmSOX-b) were able to bind recombinant SOX7 and SOX18 proteins in EMSA (Fig. 3B), and three ETS motifs (termed hmETS-a, hmETS-b and hmETS-c) were able to bind the endothelial Ets protein ETV2 (Fig. 3C).

Table 1. Reporter gene expression patterns in E12 mice transgenic for each putative *NOTCH1* enhancer region and the effects of SOX motif mutation on *NOTCH1+16* enhancer activity

Transgene	*n*	Any *lacZ* expression	*lacZ* in AECs	*lacZ* in VECs
NOTCH1−68	5	3	0	0
NOTCH1+3/5	4	4	0	0
NOTCH1+16	10	9	6	0
NOTCH1+33	5	5	1	1
NOTCH1+16 WT	8	7	4	0
NOTCH1+16mutSOX-a/b	9	6	0*	0*

*Faint vascular expression was detected in section analysis but was not visible in whole-mount analysis. *n*, number of transgenic mice analysed. AECs, arterial endothelial cells; VECs, venous endothelial cells.

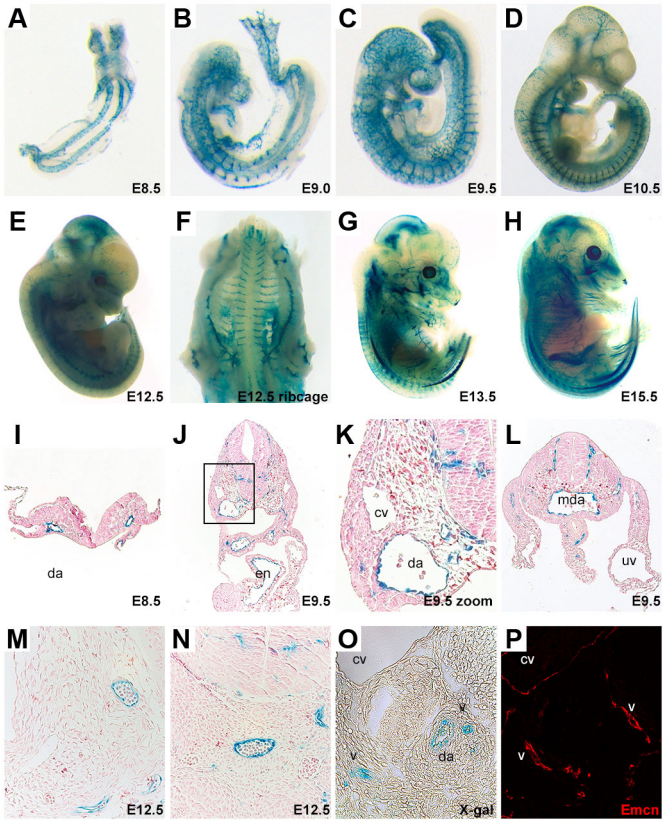

Fig. 2. The *NOTCH1+16* transgene directs arterial endothelial cell-restricted expression in transgenic mice. (A-N) Representative transgenic whole-mount embryos (A-H) and transverse sections (I-N) showing *lacZ* reporter gene expression (β-galactosidase detected by blue X-gal staining) in arterial endothelial cells throughout embryonic development. The boxed region in J is magnified in K. (O,P) E12 transverse section showing that expression of the venous marker endomucin (Emcn) does not overlap with *lacZ* reporter gene expression on the same section. cv, cardinal vein; da, dorsal aorta; Emcn, endomucin; en, endocardium; mda, midline dorsal aorta; uv,umbilical vein; v, vein.

ETS motifs are common to all endothelial-expressed gene enhancers (De Val and Black, 2009). Although the Ets factor Erg has been implicated in arterial specification (Wythe et al., 2013), previous studies have shown that ETS motifs were unable to direct expression of the arterial-specific *Dll4* and *Flk1* enhancers without additional transcription factor binding motifs (Becker et al., 2016; Sacilotto et al., 2013; Wythe et al., 2013), suggesting that Ets factors alone are unlikely to regulate the *NOTCH1+16* enhancer.

To test whether the SOX motifs play a role in *NOTCH1+16* enhancer activity, we mutated the core nucleotides of these motifs (see Materials and Methods for sequences) and tested the ability of the resultant *NOTCH1+16mutSOX-a/b* enhancer to drive reporter gene expression. Strikingly, enhancer mutation resulted in a dramatic reduction in reporter gene expression in endothelial cells in transgenic mice, although transgene expression was detected outside of the vascular system (Fig. 4, Table 1). This result differs notably from that reported for the *Dll4* enhancers, where mutations in SOX motifs, or loss of SoxF factors, resulted in no detectable decrease in *Dll4* expression unless accompanied by ablation of Notch signalling (Sacilotto et al., 2013).

Development (2017) 144, 2629-2639 doi:10.1242/dev.146241

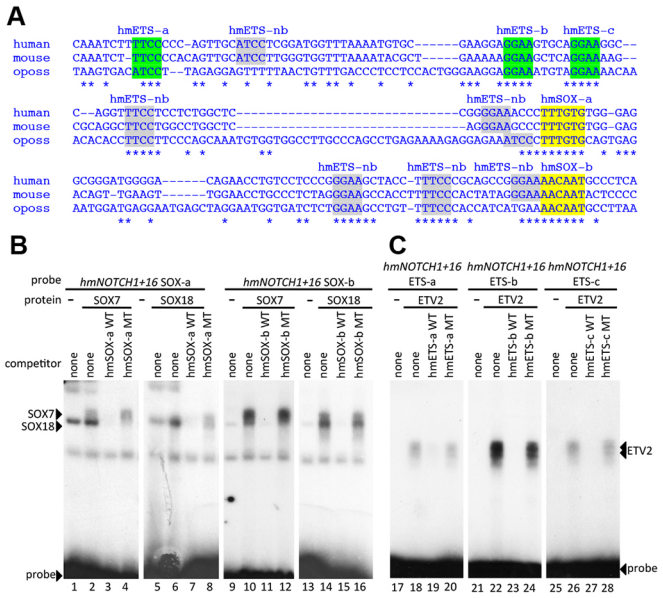

Fig. 3. The *NOTCH1+16* enhancer contains SOX and ETS binding motifs. (A) Multispecies alignment of the orthologous region of the *NOTCH1+16* enhancer from human, mouse and opossum (oposs) using ClustalW. Coloured sequences are confirmed by EMSA; grey sequences are motifs identified *in silico* that did not bind in EMSA. (B) Radiolabelled oligonucleotide probes encompassing *NOTCH1+16* hmSOX-a (lanes 1-8) and hmSOX-b (lanes 9-16) were bound to recombinant SOX7 (lanes 2-4 and 10-12) and SOX18 (lanes 6-8 and 14-16). Both proteins, which efficiently bound labelled probes (lanes 2, 6, 10 and 14), were competed by excess unlabelled self-probe (WT, lanes 3, 7, 11 and 15) but not by mutant self-probe (MT, lanes 4, 8, 12 and 16). (C) Radiolabelled oligonucleotide probes encompassing *NOTCH1+16* hmETS-a (lanes 17-20), hmETS-b (lanes 21-24) and hmETS-c (lanes 25-28) were bound to recombinant ETV2 protein. ETV2, which efficiently bound to labelled probes (lanes 18, 22 and 26), was competed by excess unlabelled self-probe (WT, lanes 19, 23 and 27) but not by mutant self-probe (MT, lanes 20, 24 and 28).

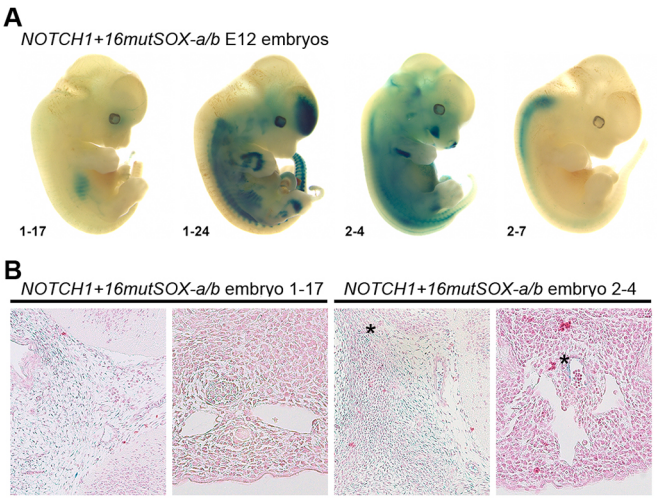

Fig. 4. SoxF factors are required for *NOTCH1+16* activity. (A) Four representative whole-mount E12 X-gal-stained embryos transgenic for the *NOTCH1+16mutSOX-a/b* construct. Numbers at the bottom left indicate the unique embryo identifier. (B) Transverse sections taken from two *NOTCH1+16mutSOX-a/b* embryos demonstrate the very limited endothelial expression detected in these embryos (asterisks). In each case, the section to the left is through the head region, the section to the right is through the upper torso region.

Zebrafish *notch1b* is directly transcriptionally regulated by SoxF factors via an evolutionarily non-conserved enhancer

The SoxF-dependent *NOTCH1+16* enhancer robustly directed arterial-restricted expression in transgenic mouse models. However, this enhancer did not exhibit sequence conservation beyond mammals (Fig. S1B), leaving it unclear how relevant these observations are to Notch signalling during arteriovenous specification in zebrafish, an extremely well-studied model system (Gore et al., 2012). We therefore investigated whether SoxF factors were able to transcriptionally regulate the zebrafish orthologue of *NOTCH1*, *notch1b*, by examining the binding patterns of the zebrafish SoxF transcription factors around the *notch1b* locus. Zebrafish SoxF are expressed in early endothelial cells and implicated in arteriovenous differentiation (Cermenati et al., 2008; Hermkens et al., 2015; Herpers et al., 2008; Pendeville et al., 2008). To probe for SoxF (Sox7, Sox17 and Sox18) genome-wide binding locations we used an endothelial-specific SOX18Ragged overexpression line. The SOX18Ragged dominant-negative protein has been shown to interfere with the endogenous function of all three SoxF transcription factors (James et al., 2003; Pennisi et al., 2000b). Using 26-28 hours post fertilisation (hpf) embryos from the *tg(fli1a:Gal4FF;10×UAS:Sox18Ragged-mCherry)* zebrafish line, in which a tagged SOX18Ragged is expressed specifically in endothelial cells (Fig. S3A), ChIP-seq analysis identified a SoxF binding event 15 kb upstream of the *notch1b* first exon (Fig. 5A). This binding peak was enriched in the enhancer-associated histone modifications H3K4me1 and H3K27ac at 24 hpf (Bogdanović et al., 2012; Kent et al., 2002) (Fig. 5A), suggesting that it might represent a novel enhancer of *notch1b*. A 1219 bp zebrafish DNA fragment corresponding to the SOX18-bound region, termed the *notch1b-15* enhancer, was cloned upstream of a silent *gata2a* promoter and *GFP* reporter gene within the zebrafish enhancer detection (ZED) vector (Bessa et al., 2009) (Fig. 5B) and used to generate the stable *tg(notch1b-15:GFP)* fish line (Fig. 5C). The *GFP* transcript was detected in the vascular cord around the midline from 19 hpf, and persisted in the vascular rod as it formed the dorsal aorta at 22 hpf (Fig. 5C). GFP expression continued to be restricted to the dorsal aorta and the segmental arteries in larvae from 24 hpf until 48 hpf. This arterial-restricted pattern of expression within the vasculature was similar to that of endogenous *notch1b* (Fig. S3B), indicating that the SOX18-bound *notch1b-15* element is a bona fide *notch1b* enhancer and suggesting that SoxF factors directly transactivate Notch receptor transcription in arterial endothelial cells in zebrafish.

ClustalW analysis comparing the orthologous enhancer sequences from fugu, stickleback and medaka revealed a remarkably similar pattern of conserved transcription factor motifs when compared with the *NOTCH1+16* enhancer (Fig. 6A), with multiple ETS and two SOX binding motifs, termed zfSOX-a and zfSOX-b, confirmed by EMSA analysis (Fig. 6B,C). To establish whether the zfSOX-a and zfSOX-b binding motifs were required for *notch1b-15* arterial enhancer function, we generated transient transgenic fish lines harbouring mutated SOX binding motifs (*notch1b-15mutSOX-a/b:GFP*) and compared the activity of the transgene with wild-type (WT) *notch1b-15:GFP* control transient transgenic animals (Fig. S4A,B). Simultaneous disruption of both zfSOX-a and zfSOX-b sites led to a reduction of arterial-specific GFP expression in endothelial cells. Although a minority of mutant fish still expressed GFP after SOX binding site mutation, the loss of expression was still much greater than that seen after SOX motif mutation in a previously published *Dll4* enhancer in transgenic zebrafish, where vascular expression rates were unaffected by

Development (2017) 144, 2629-2639 doi:10.1242/dev.146241

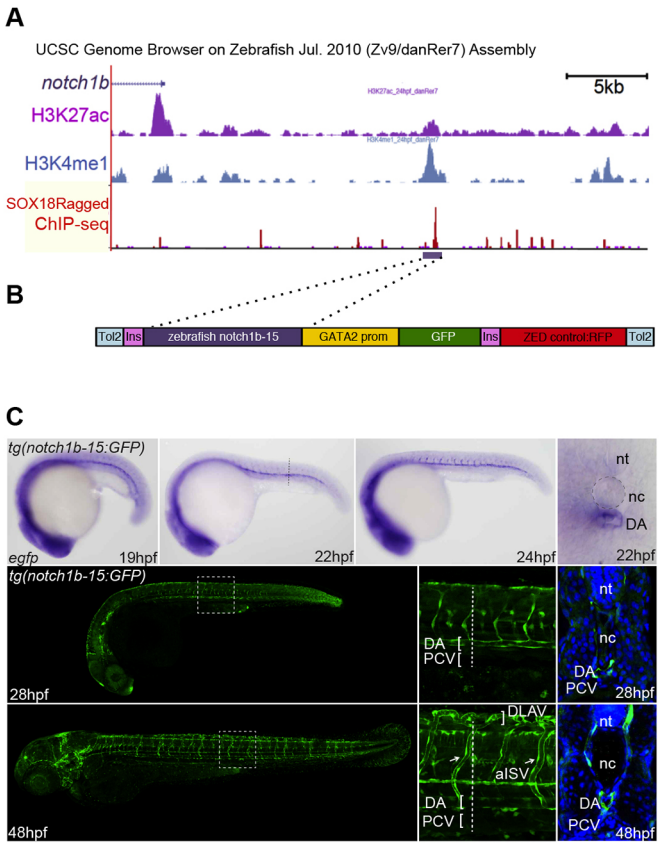

Fig. 5. A SOX18-bound region within the *notch1b* locus represents a bona fide arterial-specific enhancer. (A) Part of the zebrafish *notch1b* locus from the UCSC ENCODE Genome Browser. The *notch1b* gene is in 3′ to 5′ orientation, H3K27ac peaks at 24 hpf are in purple, H3K4me1 peaks at 24 hpf are blue, SOX18Ragged ChIP-seq peaks are red, and the region encompassing the *notch1b-15* enhancer is indicated by the purple horizontal bar. (B) The ZED *notch1b-15:GFP* transgene. Ins, insulator sequences; GATA2 prom, the silent *GATA2* promoter; ZED control:RFP, the active cardiac actin enhancer/promoter construct fused to the *RFP* gene used as a positive control in the ZED vector. (C) The *notch1b-15:GFP* transgene directs arterial endothelial cell-specific expression in the zebrafish line *tg(notch1b-15:GFP)*. Representative transgenic whole-mount embryos and transverse sections show reporter gene expression, as detected by *in situ* hybridisation (top row, blue) or GFP fluorescence (bottom rows, green) in arterial endothelial cells throughout embryonic development. nt, neural tube; nc, notochord; DA, dorsal aorta; PCV, posterior cardinal vein; aISV (arrows), arterial intersomitic vessel; DLAV, dorsal longitudinal anastomotic vessel.

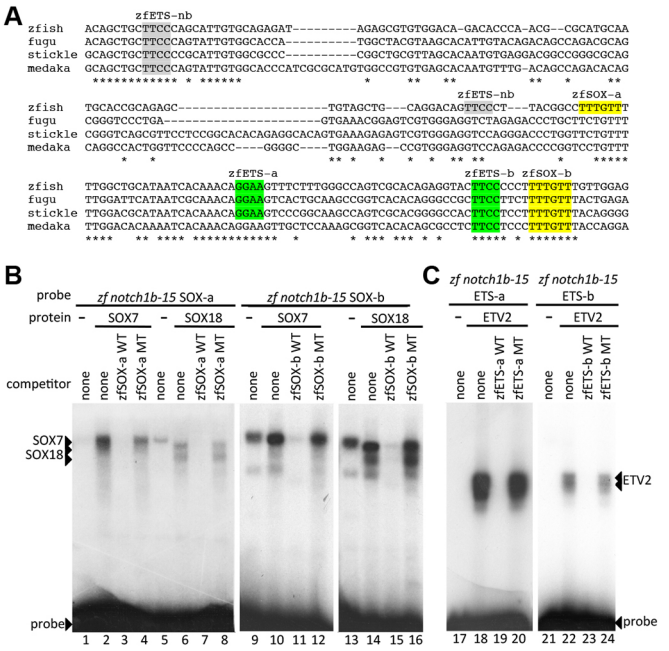

Fig. 6. The *notch1b-15* enhancer contains essential SoxF binding motifs. (A) Multispecies alignment of the orthologous regions of the *notch1b-15* enhancer from zebrafish (zfish), fugu, stickleback (stickle) and medaka using ClustalW. Coloured sequences are confirmed by EMSA; grey sequences are motifs identified *in silico* that did not bind robustly in EMSA. (B) Radiolabelled oligonucleotide probes encompassing *notch1b-15* zfSOX-a (lanes 1-8) and zfSOX-b (lanes 9-16) were bound by recombinant SOX7 (lanes 2-4 and 10-12) and SOX18 (lanes 6-8 and 14-16). Both proteins, which efficiently bound labelled probes (lanes 2, 6, 10 and 14), were competed by excess unlabelled self-probe (WT, lanes 3, 7, 11 and 15) but not by mutant self-probe (MT, lanes 4, 8, 12 and 16). (C) Radiolabelled oligonucleotide probes encompassing *notch1b-15* zfETS-a (lanes 17-20) and zfETS-b (lanes 21-24) (see A) were bound by recombinant ETV2 proteins. ETV2, which efficiently bound to labelled probes (lanes 18 and 22), was competed by excess unlabelled self-probe (WT, lanes 19 and 23) but not by mutant self-probe (MT, lanes 20 and 24).

mutations of SoxF binding motifs (Sacilotto et al., 2013), supporting a key role for SoxF factors in *notch1b* activation. To further confirm our observation, we established stable transgenic *notch1b-15mutSOX-a/b:GFP* fish lines and compared them with the established WT *notch1b-15:GFP* lines. Analysis of the stably transgenic embryos (Fig. 7A) confirmed a GFP expression pattern in the dorsal aorta and segmental arteries for the WT transgene. By contrast, the *tg(notch1b-15mutSOX-a/b:GFP)* lines showed ectopic GFP expression in neurons and a significant decrease of GFP expression in the arterial endothelium (Fig. 7A). Quantitative analysis of GFP intensity in both dorsal aorta and segmental arteries showed lower expression in most *tg(notch1b-15mutSOX-a/b:GFP)* than in WT *tg(notch1b-15:GFP)* embryos (Fig. 7B,C, Fig. S4C). Taken together, these data clearly demonstrate that the zfSOX-a/b binding sites are required to guide *notch1b-15*-specific enhancer activity *in vivo* during arterial development.

We next investigated the consequences of morpholino (MO)-based knockdown of SoxF on *tg(notch1b-15:GFP)* fish. *sox7/sox18* double morphants exhibit a severe vascular phenotype (Fig. S5), including fusions and shunts between the dorsal aorta and cardinal vein (Cermenati et al., 2008; Herpers et al., 2008; Pendeville et al., 2008), phenotypes that are shared with *sox7;sox18* double-mutant fish (Hermkens et al., 2015). MO-induced transcript depletion of *sox7* or *sox18* resulted in downregulation of *notch1b-15:GFP* expression, while *sox7/sox18* double-morphant *tg(notch1b-15:GFP)* fish demonstrated a near-complete loss of reporter gene expression (Fig. 7D,E).

Taken together, these results indicate that SoxF proteins directly modulate the activity of arterial-specific enhancers for both the mammalian NOTCH1 and zebrafish Notch1b receptors, positioning SoxF transcription factors directly upstream of Notch signalling during early arterial differentiation in both mammals and zebrafish.

Loss of endogenous *notch1b-15* enhancer activity perturbs *notch1b* transcription and causes arteriovenous defects

To assess whether the endogenous *notch1b-15* regulatory element is functionally relevant during arteriovenous differentiation *in vivo*, we deleted the endogenous *notch1b-15* enhancer in zebrafish. The resultant *notch1b-15*^{uq1mf} allele was generated using two guide RNAs to drive rapid genome editing using the CRISPR/Cas9 system (Fig. 8A), resulting in excision of a 203 bp fragment overlapping the

Development (2017) 144, 2629-2639 doi:10.1242/dev.146241

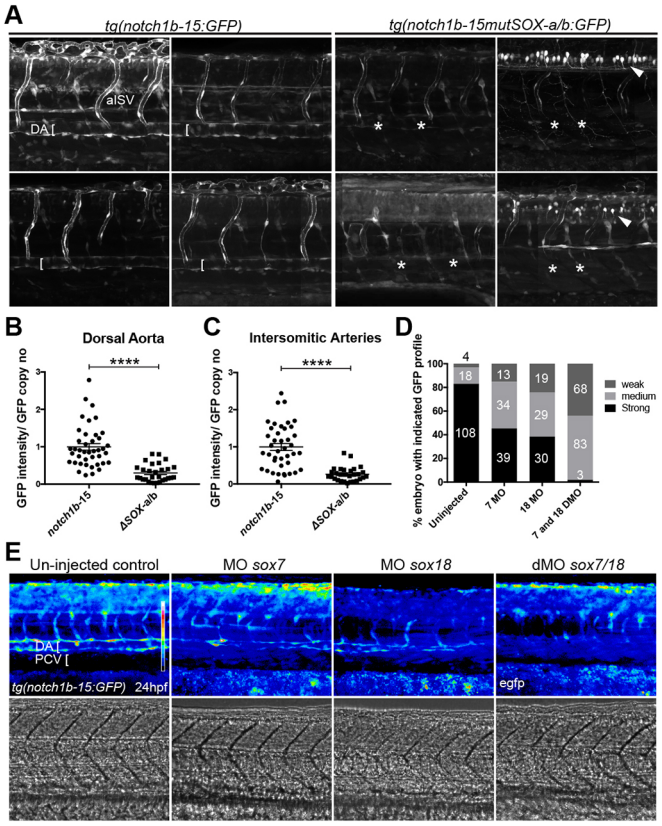

Fig. 7. SoxF factors are required for *notch1b-15* activity. (A) Confocal projection of stably transgenic WT *tg(notch1b-15:GFP)* (left) and *tg(notch1b-15mutSOX-a/b:GFP)* (right), where both zfSOX-a and zfSOX-b sites have been simultaneously mutated. Representative larvae from four independent founders are shown. Asterisks indicate the reduced GFP expression in the dorsal aorta. Arrowheads show the ectopic neuronal expression observed in *tg(notch1b-15mutSOX-a/b:GFP)*. All panels show composite images from tile scan acquisition. (B,C) The intensity of GFP expression in the dorsal aorta and arterial intersomitic vessels of the stably transgenic *tg(notch1b-15:GFP)* and *tg(notch1b-15mutSOX-a/b:GFP)* at 2 dpf. Expression is normalised to *GFP* genomic copy number. Fish were pooled from three or four separate founders. Mean±s.e.m. *tg(notch1b-15)*, *n*=41; *tg(notch1b-15mutSOX-a/b:GFP)*, *n*=29. ****P<0.0001 (Mann–Whitney *U*-test). (D) Levels of GFP expression in *tg(notch1b-15:GFP)* zebrafish embryos after MO injection. Number of fish for each condition is indicated. (E) Representative examples of *sox7/18* double-morphant *tg(notch1b-15:GFP)* zebrafish at 24 hpf as compared with uninjected controls. Double morphants (dMO) demonstrated reduced EGFP expression in the dorsal aorta and intersomitic vessels. DA, dorsal aorta; PCV, posterior cardinal vein; aISV, arterial intersomitic vessel.

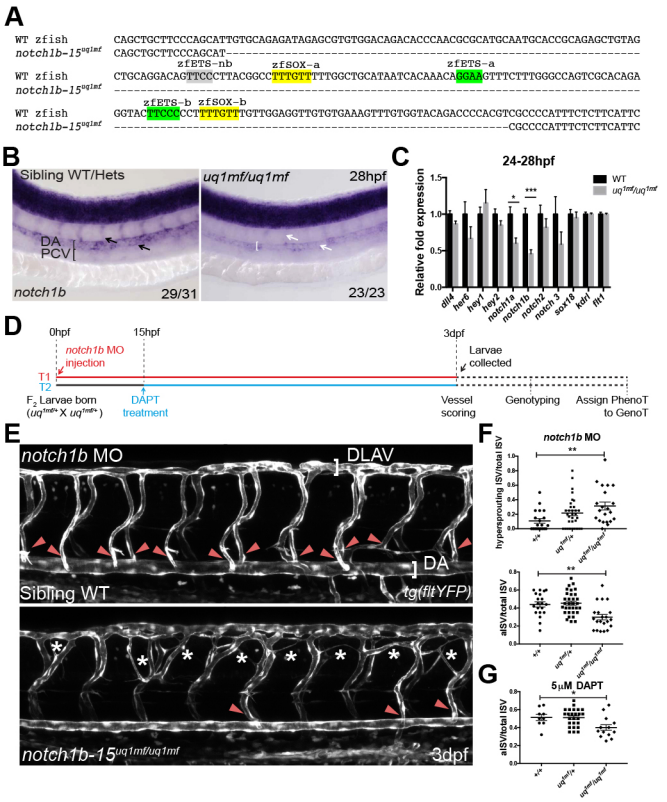

Fig. 8. Loss of endogenous *notch1b-15* compromises artery formation and reduces the endogenous *notch1b* transcript level. (A) The deleted region (dashed line) of *notch1b-15* mutant allele *uq1mf*, which includes both the zfSOX-a and zfSOX-b sites (yellow). (B) F_2 *notch1b-15*$^{uq1mf/uq1mf}$ has reduced *notch1b* expression in dorsal aorta and intersomitic vessels (white arrows) as compared with sibling WT and heterozygotes (black arrows) at 26-28 hpf. The number of embryos showing the illustrated phenotype among the total examined is indicated. (C) Quantitative PCR on FACS-sorted endothelial populations at 24-28 hpf, showing that F_3 *notch1b-15*$^{uq1mf/uq1mf}$ fish have lower *notch1b* expression than WT fish. Expression is relative to *kdrl* and *flt1*. Mean± s.e.m. *n*=6 (*uq1mf/uq1mf*) and *n*=8 (WT) independent sorts, where each sort was pooled from 60-100 larvae;. *P<0.05, ***P<0.001 (*t*-test). (D) The treatment regime conducted to characterise the vascular phenotype of the *uq1mf/+* cross. In treatment 1 (T1, red), *notch1b* MO was injected at the 1-2 cell stage. The developing vasculature of each embryo was then analysed blindly at 3 dpf. After scoring, genotypes were assigned to each larva. In treatment 2 (T2, blue), larvae from the *uq1mf/+* cross were treated with or without DAPT (5 µM) from 15-16 hpf until 3 dpf. Vessels of these treated larvae were blindly scored prior to genotyping, as reported for T1. (E) At 3 dpf, *notch1b-15*$^{uq1mf/uq1mf}$ *notch1b* morphants frequently showed ectopic sprouting in between the intersomitic vessels (asterisks) as compared with sibling WT *notch1b* morphants. Mutants also show loss of arterial connections (red arrowheads) between the dorsal longitudinal anastomotic vessel (DLAV) and dorsal aorta (DA), as indicated by the loss of YFP expression in the *tg(flt1:YFP)* background. (F) (Top) Quantification of hypersprouting ISV number in individual *notch1b* morphants labelled by *tg(flt1:YFP)* at 3 dpf. Mean±s.e.m. Sibling WT (+/+), *n*=20; heterozygote (*uq1mf/+*), *n*=32; homozygous mutant (*uq1mf/uq1mf*), *n*=21. (Bottom) Quantification of YFP-positive intersomitic vessels that connect between DLAV and DA in individual *notch1b* morphants labelled by *tg(flt1:YFP)* at 3 dpf. Mean±s.e.m. Sibling WT, *n*=20; heterozygote, *n*=32; homozygous mutant, *n*=21. **P<0.005 (Mann–Whitney *U*-test). (G) Quantification of YFP-positive intersomitic vessels that connect between DLAV and DA in individual embryos treated with 5 µM DAPT at 3 dpf. Vessels are labelled by *tg(flt1:YFP)*. Mean±s.e.m. Sibling WT, *n*=9; heterozygote, *n*=25; homozygous mutant, *n*=14. *P<0.05 (Mann–Whitney *U*-test).

notch1b-15 enhancer. Analysis of endogenous *notch1b* expression in the F_2 generation demonstrated lower *notch1b* expression levels in both dorsal aorta and arterial intersomitic vessel (aISV) of the *notch1b-15*$^{uq1mf/uq1mf}$ homozygous embryos as compared with their sibling controls, whereas no change was observed in the neural tube (Fig. 8B). Next, we assessed the *notch1b* transcript levels in purified *flt1*-positive arterial endothelial cell populations from the F_3 generation of homozygous fish (F_2 *notch1b-15*^{uq1mf} homozygous in-cross) compared with WT control larvae (F_2 *notch1b-15*$^{+/+}$ × *flt1:YFP;lyve1:dsRed*) at 24-28 hpf (Fig. 8C). As expected, *notch1b* transcripts were significantly downregulated in the homozygous animals, strongly supporting a role for the *notch1b-15* enhancer in the transcription of endogenous *notch1b* in arterial endothelial cells.

To assess the phenotypic outcome of *notch1b-15* loss of function, we took advantage of the *tg(notch1b-15*$^{uq1mf/+}$*;flt1:YFP;lyve1:dsRed)* line to analyse the developing vasculature after *notch1b-15* enhancer deletion in both the F_2 and F_3 generations. Surprisingly, given the reduced levels of *notch1b* (Fig. 8B), no overt vascular

Development (2017) 144, 2629-2639 doi:10.1242/dev.146241

phenotype was detected in F_2 *notch1b-15*$^{uq1mf/uq1mf}$ homozygous zebrafish (F_1 heterozygous *notch1b-15*$^{uq1mf/+}$ in-cross) (Fig. S6A), suggesting partial enhancer redundancy. Such redundancy, which is potentially explained by the pervasiveness of redundant, or 'shadow', enhancers around developmental genes (Cannavò et al., 2016), has previously been well documented in key endothelial genes, with examples including the *Dll4*, *Flk1* and *Tal1* loci (Cannavò et al., 2016). By contrast, we detected a subpopulation (20-30%) of larvae from the F_3 generation (F_2 homozygous *notch1b-15*$^{uq1mf/uq1mf}$ in-cross) that displayed a phenocopy of the *notch1b* loss-of-function phenotype (Fig. S6B). This increase in the phenotypic severity in the F_3 generation suggests that, in the context of the *notch1b-15*$^{uq1mf/+}$ cross, maternal mRNA deposition is likely to help compensate for the disruption of *notch1b* transcription caused by deletion of the *notch1b* enhancer, a compensation that is reduced in a purer *notch1b-15*$^{uq1mf/uq1mf}$ genetic background (Harvey et al., 2013).

To bypass potential rescue effects of shadow enhancers or maternally deposited transcripts, we also investigated arteriovenous differentiation and sprouting angiogenesis in F_2 *notch1b-15*$^{uq1mf/uq1mf}$ zebrafish after low-level depletion of *notch1b* mRNA. A splice *notch1b* MO was injected into eggs from a *notch1b-15*$^{uq1mf/+}$ in-cross in the *tg(flt1:YFP;lyve1:dsRed)* background. The *notch1b* MO was used at suboptimal concentration (5 ng/embryo), which is known to result in minimal phenotypes (Sacilotto et al., 2013). The developing vasculature of each resulting embryo was analysed blindly at 3 dpf, and genotypes were assigned to embryos after image acquisition (Fig. 8D, red). Whereas most WT siblings had normal ISV development, we observed an increased number of hypersprouting ISVs across the *notch1b-15*$^{uq1mf/+}$ and *notch1b-15*$^{uq1mf/uq1mf}$ population (Fig. 8E, asterisks; Fig. 8F, top) in a gene dosage-dependent manner, similar to the phenotype described previously in high MO concentration *notch1b* morphants and Notch signalling-deficient embryos (Geudens et al., 2010; Siekmann and Lawson, 2007). Further, mutant embryos also demonstrated loss of arterial connections between the dorsal aorta and dorsal longitudinal anastomotic vessel, similar to those described in Notch signalling-deficient zebrafish (Geudens et al., 2010; Quillien et al., 2014), while the *notch1b*-depleted *notch1b-15*$^{+/+}$ and *notch1b-15*$^{uq1mf/+}$ morphant embryos demonstrated an equal proportion of arterial and venous ISVs as previously reported (Bussmann et al., 2010) (Fig. 8E,F bottom).

To further confirm that interfering with *notch1b-15* enhancer activity is additive to *notch1b* transcript depletion, we chemically treated the *notch1b-15*$^{uq1mf/+}$ cross with DAPT, a well characterised Notch signalling inhibitor, over the course of endothelial differentiation (15- to 16-somite stage through to 3 dpf) (Fig. 8D, blue). All embryos treated with a suboptimal concentration of DAPT (5 µM) showed a straight body axis, indicating that somitogenesis (and therefore Notch activity) was not significantly compromised (Fig. S7A). Interestingly, despite this lack of morphological defects, F_2 fish homozygous for the *notch1b-15*^{uq1mf} allele displayed a lower arterial-to-total ISV ratio (Fig. 8G, Fig. S7A). By contrast, fish homozygous for the *notch1b-15*^{uq1mf} allele treated with DMSO vehicle alone had a comparable aISV ratio to both *notch1b-15*$^{+/+}$ and *notch1b-15*$^{uq1mf/+}$ siblings (Fig. S7B), similar to the untreated control. This suggests that the observed loss of aISV is specific to an additive effect of DAPT treatment and *notch1b-15* enhancer activity disruption. Overall, these data suggest a functional role of the *notch1-15* enhancer in the endothelial-specific initiation of *notch1b* transcription to promote the acquisition of arterial cell identity.

SoxF factors are required for endogenous *Notch1*/*notch1b* expression

Our results have clearly implicated SoxF factors as direct upstream regulators of arterial Notch enhancers, and therefore suggest a considerably greater role for SoxF in the regulation of the Notch receptors than of the Notch ligands. However, since the *notch1b-15* enhancer is partially redundant with other *notch1b* shadow enhancers, we wished to establish whether SoxF regulation is required for endogenous *notch1b* expression itself, not just enhancer activity. Further, our results so far do not entirely rule out the possibility of SoxF/Rbpj combinatorial regulation of *notch1b*, as was previously shown for *Dll4* enhancers (Sacilotto et al., 2013). Although neither the human *NOTCH1+16* nor the zebrafish *notch1b-15* enhancer contains conserved consensus Rbpj/Notch binding motifs, transcription factors can bind non-consensus motifs, and not all transcription factors necessarily bind conserved motifs (Wong et al., 2015). The nature of the SoxF/Notch combinatorial regulation of *Dll4*, where the SOX or RBPJ binding motifs play functionally interchangeable roles, indicates potential direct interactions between these two proteins, such that only a single SOX binding motif might be necessary for SoxF/Rbpj synergy. We therefore investigated the consequences of SoxF depletion on endogenous *Notch1*/*notch1b* expression *in vivo*.

Although *Sox17* is robustly expressed in arterial endothelial cells (Corada et al., 2013; Hosking et al., 2009), compound *Sox7;Sox18* deletion in mice resulted in a reduction of *Notch1* mRNA levels in the trunk dorsal aorta and primitive heart cavities of E8.5 embryos (Fig. 9A, Fig. S8A). These results concur with observations in the mouse retina, where the vascular phenotype after *Sox7;Sox17;Sox18* endothelial-specific triple deletion closely resembled defects caused by loss of Notch signalling (Zhou et al., 2015). Strikingly, both MO-induced gene knockdown and compound mutation of *sox7* and *sox18* in zebrafish embryos also led to a near-complete loss of *notch1b* transcript expression specifically in endothelial cells, as shown by *in situ* hybridisation analysis (Fig. 9B,C, Fig. S8B). These results further establish an essential role for SoxF transcription factors in the induction of *Notch1*/*notch1b* gene expression, and position SoxF proteins at the top of the transcriptional hierarchy regulating arterial specification.

DISCUSSION

Recent work has implicated SoxF, Ets and Rbpj, the Notch transcriptional effector, in the regulation of the Notch ligand *Dll4* and many other key arterial genes (Corada et al., 2013; Lizama et al., 2015; Sacilotto et al., 2013; Wythe et al., 2013), but has not established the hierarchical arrangement of these diverse factors in arterial specification and differentiation. In this study, we demonstrate that arterial expression of the Notch receptor *Notch1*/*notch1b*, a key player in arterial specification, is directly downstream of SoxF regulation in both fish and mouse. Unlike other key arterial specification markers, including Dll4, Efnb2a and Dlc (Sacilotto et al., 2013), ablation of Notch1/Notch1b expression after depletion of SoxF factors occurred without concurrent inhibition of Notch signalling. Therefore, this work positions SoxF factors directly above Notch signalling in the transcriptional hierarchy initiating arterial development, and suggests that SoxF factors might initiate a feed-forward loop directing arterial identity. In this model, SoxF factors would first activate Notch signalling via the transcriptional activation of Notch receptors in combination with weak activation of Notch ligands (Sacilotto et al., 2013). This early SoxF-mediated activity would then be boosted by the initiation of Notch signalling, resulting in the sustained activation

Development (2017) 144, 2629-2639 doi:10.1242/dev.146241

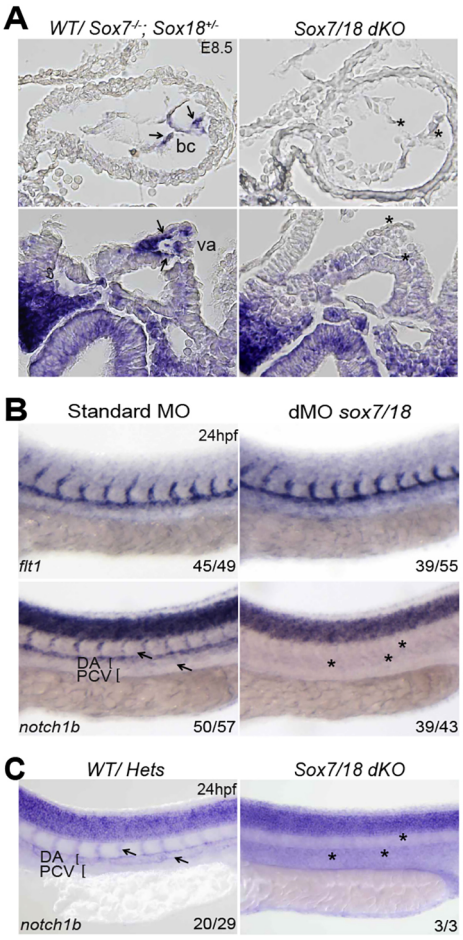

Fig. 9. Mouse and zebrafish arterial *Notch1* expression is dependent on SOX7/18 activity. (A) Transverse sections of whole-mount *in situ* hybridisation for *Notch1* transcript on E8.5 mouse embryos shows a reduction of *Notch1* expression (asterisks) in the bulbus cordis (bc) region of the primitive heart and vitelline artery (va) of *Sox7*/*Sox18* double knockouts. (B) At 24 hpf *notch1b* expression is significantly downregulated in the dorsal aorta (asterisks) of *sox7*/*sox18* double-morphant zebrafish, whereas its signal is unaffected in the neural tube. *flt1* expression is comparable between controls and *sox7*/*sox18* double morphants, indicating that the dorsal aorta is correctly formed. (C) *notch1b* was barely detectable in the dorsal aorta and ISVs of *sox7*/*18* double-knockout zebrafish (asterisks), as compared with the WT, *sox7* or *sox18* heterozygotes (arrows). The number of embryos showing the illustrated phenotype among the total examined is indicated. DA, dorsal aorta; PCV, posterior cardinal vein.

of other downstream genes, eventually activating the full cohort of genes necessary to acquire and maintain arterial endothelial cell identity.

Understanding the function of SoxF factors through mutational analysis has presented significant challenges. Strain-specific variations in mice after depletion of individual SoxF genes and varying levels of compensation from other SoxF factors have resulted in some contradictory reports (Corada et al., 2013; Lee et al., 2014), as is also the case for zebrafish morphant analysis (Cermenati et al., 2008; Herpers et al., 2008; Pendeville et al., 2008). Nonetheless, the results described here agree with an increasingly convincing body of work suggesting that SoxF factors influence Notch signalling yet are unaffected by Notch ablation. For example, overexpression of Sox17 upregulates components of the Notch pathway (Corada et al., 2013; Lizama et al., 2015), loss of functional SoxF factors results in defects similar to those observed after Notch inhibition in mice and fish (Corada et al., 2013; Sakamoto et al., 2007; Zhou et al., 2015), while Notch ablation results in little alteration to the endothelial expression of SoxF factors in mice and fish (Abdelilah et al., 1996; Corada et al., 2013). Data reported here combine with these reports to strongly support a role for SoxF factors as part of the initial transcriptional machinery that instructs arterial specification events.

However, some questions remain. In particular, it is notable that *sox7;sox18* double-mutant fish, although exhibiting severe arteriovenous defects very similar to those seen in Notch-deficient fish (Lawson et al., 2001), do not fully recapitulate the effects of Vegfa depletion on arterial specification (Lawson et al., 2002). While this difference may in part be attributed to weak expression of zebrafish *sox17*, which is expressed in some arterial endothelial cells (Hermkens et al., 2015), it is also expected that the Vegfa pathway has a wider effect on arterial endothelial cells more generally, away from SoxF-mediated activation of Notch signalling. SoxF factors are also influenced by signalling pathways beyond Vegfa. The diverse nature of Vegfa roles in the vasculature, including the regulation of both sprouting angiogenesis and arteriogenesis, processes that inevitably involve different cohorts of downstream targets, make it necessary that multiple regulatory pathways interact with Vegfa during vascular development. While recent work has shown that Vegfa signalling increases the nuclear translocation of SoxF (Duong et al., 2014), and inhibition of Vegfa results in the loss of vascular *sox7* in fish, *sox18* is still expressed in the absence of intact Vegfa signalling (Pendeville et al., 2008). Additionally, loss of the Vegf co-receptor Nrp1 has little effect on SoxF expression in mouse retinal vasculature (Zhou et al., 2015), pointing to other upstream influences on SoxF function in endothelial cells. Other upstream effectors of SoxF function are likely to include canonical Wnt signalling and Vegfd, both of which have been shown to influence SoxF nuclear localisation (Corada et al., 2013; Duong et al., 2014; Zhou et al., 2015).

Recent evidence has also implicated a role for a coordinated Vegf-Mapk-Ets pathway in the induction of Notch signalling components and early arterial differentiation (Wythe et al., 2013). Notably, in addition to SoxF motifs, both the *Notch1* and *Dll4* enhancers share a number of highly conserved consensus motifs for the Ets family of transcription factors. While ETS motifs are common to all vascular enhancer elements, including many that are not preferentially expressed in the arterial vasculature (De Val and Black, 2009), the Ets factor Erg has been specifically implicated in arterial-specific regulation of *Dll4* (Wythe et al., 2013). It is therefore likely that Vegfa-mediated activation of Ets factors may contribute to the transcriptional activity of Notch downstream effectors, and thus may influence arterial establishment independently of SoxF factors. However, it is notable that Vegfa-mediated activation of Ets transcription factors alone does not appear to be sufficient for arterial gene expression. *Dll4* enhancers lacking SOX and RBPJ motifs but retaining all ETS motifs were unable to drive any transgene expression (Sacilotto et al., 2013), nor were Notch enhancers lacking SOX motifs (Figs 2-4). Similar results were found in other delineated arterial enhancers, including the *Ece1* upstream enhancer (Robinson et al., 2014) and the *Flk1* intron 10 enhancer, where loss of Rbpj-mediated repression resulted in expansion of enhancer activity into venous cells without alterations to ETS motif binding (Becker et al., 2016). Combined with recent observations demonstrating that Erg also plays a crucial role in venous specification through activation of *Aplnr* (Lathen et al., 2014),

Development (2017) 144, 2629-2639 doi:10.1242/dev.146241

it is therefore likely that the role of Erg, and of other Ets factors, downstream of Vegfa in arterial-restricted gene expression occurs in co-operation with additional essential, arterial-specifying transcription factors. The data presented in this work, combined with the analysis of further arterial enhancers, including those of *Dll4* and *Ece1* (Robinson et al., 2014; Sacilotto et al., 2013; Wythe et al., 2013), increasingly suggest that SoxF may fulfil this role.

MATERIALS AND METHODS

Cloning

The 10×UAS:Sox18Ragged-mCherry plasmid was generated using the full-length mouse *Sox18Ragged* cDNA sequence, tagged with 10×UAS and mCherry and cloned into pDestTol2CG2 (Kwan et al., 2007). *notch1b-15:GFP* WT was generated by cloning a 1219 bp PCR fragment from zebrafish genomic DNA together with *gata2a* promoter and *GFP* reporter gene into the zebrafish enhancer detection (ZED) vector (Bessa et al., 2009). *notch1b-15mutSOX-a/b* was generated by site-directed PCR mutagenesis of the WT construct. The *NOTCH1−68*, *NOTCH1+3/5* and *NOTCH1+33* enhancers were generated by PCR from human genomic DNA, *NOTCH1+16* WT and *NOTCH1+16mutSOX-a/b* enhancers were generated as custom-made, double-stranded linear DNA fragments (GeneArt Strings, Life Technologies). All mammalian fragments were cloned into the *hsp68-lacZ* Gateway vector (provided by N. Ahituv) (De Val et al., 2004). Primers and sequences for DNA fragments are listed in the supplementary Materials and Methods.

Transgenic animals and genome editing

Animal procedures were approved by local ethical review and licensed by the UK Home Office or conformed to institutional guidelines of the University of Queensland Animal Ethics Committee. Transgenic mice were generated by oocyte microinjection and analysed as detailed in the supplementary Materials and Methods (De Val et al., 2004). Compound $Sox7^{-/-};Sox18^{-/-}$ (C57BL/6) mouse embryos were generated on the C57BL/6 background through crossing heterozygous *Sox7:tm1* to *Sox18:tm1* generating $Sox7^{+/-};Sox18^{+/-}$ mice, which were subsequently in-crossed (Pennisi et al., 2000a).

Transgenic zebrafish embryos were generated using the Tol2 system in conjunction with the ZED vector (Bessa et al., 2009). The $sox7^{hu5626};sox18^{hu10320}$ double-homozygous mutant zebrafish have been described previously (Hermkens et al., 2015). The *tg(fli1a:Gal4FF,10×UAS:Sox18Ragged-mCherry)* zebrafish line was generated by crossing *10×UAS:Sox18Ragged-mCherry* with *fli1a:Gal4FF*, *4×UAS Utrophin GFP*. MO-mediated knockdown was performed as previously described (Herpers et al., 2008). CRISPR genome editing for *notch1b-15* was performed as described by Gagnon et al. (2014) using the primers listed in the supplementary Materials and Methods to generate $notch1b\text{-}15^{uq1mf}$ (203 bp deletion) allele.

The F_2 $notch1b\text{-}15^{uq1mf/uq1mf}$ was generated by in-crossing $notch1b\text{-}15^{uq1mf/+}$, while F_3 $notch1b\text{-}15^{uq1mf/uq1mf}$ was generated from the F_2 $notch1b\text{-}15^{uq1mf/uq1mf}$ in-cross, both in the *tg(flt1:YFP;lyve1:dsRed)* background.

Chromatin immunoprecipitation (ChIP)

Positive *tg(fli1a:Gal4FF;10×UAS:Sox18Ragged-mCherry)* fish larvae were collected at 26-28 hpf and processed as described in supplementary Materials and Methods (Mohammed et al., 2013). DNA amplification was performed using the TruSeq ChIP-seq Kit (Illumina, IP-202-1012) following immunoprecipitation. The library was quantified using the KAPA library quantification kit for Illumina sequencing platforms (KAPA Biosystems, KK4824) and 50 bp single-end reads were sequenced on a HiSeq 2500 (Illumina) following the manufacturer's protocol. FASTQ files were mapped to GRCz10/danRer10 genome assembly using bowtie (Langmead, 2010), and peaks were called using MACS version 2.1.0. using input as a reference. To avoid false-positive peaks calling due to the mCherry epitope, ChIP-seq with the mCherry epitope only was performed in parallel to SOX18Ragged-mCherry ChIP-seq and peaks called in these experimental conditions were subtracted from the peaks called in the SOX18Ragged-mCherry conditions. For details, see the supplementary Materials and Methods.

Motif identification and EMSA

Sequences were analysed for consensus sequence motifs by eye and using TRANSFAC (BIOBASE; http://genexplain.com/transfac/) (Matys et al., 2006). EMSAs were performed as previously described (De Val et al., 2004), as outlined in the supplementary Materials and Methods.

Morpholinos and drug treatment

MO-mediated knockdown was performed as previously described (Duong et al., 2014; Cermenati et al., 2008). ATG MOs against *sox7* and *sox18* were injected into the *tg(notch1b-15:GFP)* stable line at the 1-2 cell stage at 5 ng/embryo (Herpers et al., 2008). To assess the effect of *sox7/18* knockdown on endogenous *notch1b* transcripts, *sox7* and *sox18* MOs were injected into WT zebrafish larvae at 1 ng/embryo in parallel with a standard control MO (std-MO) injected at 2 ng/embryo (Cermenati et al., 2008). To characterise $notch1b\text{-}15^{uq1mf}$, *notch1b* MO was injected into the $notch1b\text{-}15^{uq1mf/+}$ cross at 5 ng/embryo. For MO sequences, see the supplementary Materials and Methods.

N-[(3,5-difluorophenyl)acetyl]-L-alanyl-2-phenyl]glycine-1,1-dimethylethyl ester (DAPT; Sigma-Aldrich) was used at 5 µM dissolved in 1% DMSO. Fish were treated from the 15- to 16-somite stage to 3 dpf and the medium containing DAPT was refreshed daily.

In situ hybridisation and immunofluorescence staining

Whole-mount *in situ* hybridisation in zebrafish larvae was performed as described (Coxam et al., 2015; Duong et al., 2014). Section and whole-mount *in situ* hybridisation in mouse was performed as described (Metzis et al., 2013; Fowles et al., 2003). The *Notch1* probe was generated by PCR from mouse embryo cDNA pool at E14.5, and reverse transcribed with T7 polymerase. Whole-mount immunohistochemistry for anti-GFP was performed as described (Koltowska et al., 2015). For details, see the supplementary Materials and Methods.

Quantification and data analysis

To characterise the vasculature in Fig. 8E-G and Figs S6, S7, intersomitic vessels (20-22 ISVs) expressing *tg(flt1:YFP)* were analysed across 10-11 somites through a *z*-stack using ImageJ (NIH) after image acquisition by confocal microscopy. Intersomitic vessels connecting the dorsal longitudinal anastomotic vessel to the dorsal aorta expressing YFP were assigned as arterial ISVs. Vessels were also scored for ectopic sprouting. The proportion of aISVs or hypersprouts among the total number of ISVs was analysed by two-tailed Mann–Whitney *U*-test. To quantify the GFP intensity of *tg(notch1b-15:GFP)* and *tg(notch1b-15mutSOX-a/b:GFP)* (Fig. 7A), two to three ISVs across five to six somites in the trunk region were analysed using ImageJ. A region of interest (ROI) covering a single ISV was selected and mean pixel intensity for each ISV was quantified from each individual stack across three *z*-sections. This value was further corrected by subtracting the background value. Average ISV GFP intensity (quantified from two to three ISVs) for each fish larva was subsequently corrected for its genomic *GFP* copy number. A similar method was used to quantify GFP intensity in the endothelial lining along the dorsal aorta.

Fluorescence-activated cell sorting (FACS) and expression analysis

Flt1:YFP-positive endothelial cells were isolated from WT and F_3 $notch1b\text{-}15^{uq1mf/uq1mf}$ at 24-28 hpf. RNA was extracted, amplified and cDNA was synthesized as previously described (Coxam et al., 2014; Picelli et al., 2014). Primer sequences and details of the quantitative PCR analysis are provided in the supplementary Materials and Methods.

Acknowledgements

We thank M. Shipman for help with imaging. The ZED vector was kindly provided by F. Tessadori (Bakkers lab, Hubrecht Institute). The *notch1b* plasmid used to generate the probe was kindly provided by N. D. Lawson (University of Massachusetts Medical School).

Competing interests

The authors declare no competing or financial interests.

Author contributions

Conceptualization: I.K.-N.C., M.Frit., S.D.V., M.Fran.; Methodology: I.K.-N.C., M.Frit., S.D.V., M.Fran.; Formal analysis: K.H., J.C.; Investigation: I.K.-N.C., M.Frit., C.P.-T., A.N., K.H., A.L., J.O., D.D., A.O., D.H., E.L., K.L., I.R., M.C., B.H.; Resources: A.L., G.B.-G., J.C., S.S.-M., M.B.; Data curation: K.H., J.C.; Writing - original draft: I.K.-N.C., S.D.V., M.Fran.; Writing - review & editing: I.K.-N.C., B.H., M.B., S.D.V., M.Fran.; Visualization: I.K.-N.C., S.D.V., M.Fran.; Supervision: G.B.-G., J.C., E.D., B.H., M.B., S.D.V., M.Fran.; Project administration: S.D.V., M.Fran.; Funding acquisition: S.D.V., M.B., M.Fran.

Funding

This work was supported by the National Health and Medical Research Council of Australia (NHMRC) (APP1107643); The Cancer Council Queensland (1107631) (M.Fran.); the Australian Research Council Discovery Project (DP140100485) and a Career Development Fellowship (APP1111169) (M.Fran.); the Ludwig Institute for Cancer Research (M.Frit., A.N., I.R., S.D.V.); the Medical Research Council (MR/J007765/1) (K.L., G.B.-G., S.D.V.); the Fondazione Cariplo (2011-0555) (M.B., B.H., M.Fran.); and the Biotechnology and Biological Sciences Research Council (BB/L020238/1) (A.N., K.L., G.B.-G., S.D.V.). Deposited in PMC for release after 6 months.

Data availability

ChIP-seq data are available in the ArrayExpress database at EMBL-EBI (www.ebi.ac.uk/arrayexpress) with accession number E-MTAB-5843.

Supplementary information

Supplementary information available online at
http://dev.biologists.org/lookup/doi/10.1242/dev.146241.supplemental

References

Abdelilah, S., Mountcastle-Shah, E., Harvey, M., Solnica-Krezel, L., Schier, A. F., Stemple, D. L., Malicki, J., Neuhauss, S. C., Zwartkruis, F., Stainier, D. Y. et al. (1996). Mutations affecting neural survival in the zebrafish Danio rerio. *Development* **123**, 217-227.

Becker, P. W., Sacilotto, N., Nornes, S., Neal, A., Thomas, M. O., Liu, K., Preece, C., Ratnayaka, I., Davies, B., Bou-Gharios, G. et al. (2016). An intronic Flk1 enhancer directs arterial-specific expression via RBPJ-mediated venous repression. *Arterioscler. Thromb. Vasc. Biol.* **36**, 1209-1219.

Bessa, J., Tena, J. J., de la Calle-Mustienes, E., Fernández-Miñán, A., Naranjo, S., Fernández, A., Montoliu, L., Akalin, A., Lenhard, B., Casares, F. et al. (2009). Zebrafish enhancer detection (ZED) vector: a new tool to facilitate transgenesis and the functional analysis of cis-regulatory regions in zebrafish. *Dev. Dyn.* **238**, 2409-2417.

Bogdanović, O., Fernández-Miñán, A., Tena, J. J., de la Calle-Mustienes, E., Hidalgo, C., van Kruysbergen, I., van Heeringen, S. J., Veenstra, G. J. C. and Gómez-Skarmeta, J. L. (2012). Dynamics of enhancer chromatin signatures mark the transition from pluripotency to cell specification during embryogenesis. *Genome Res.* **22**, 2043-2053.

Bray, S. J. (2006). Notch signalling: a simple pathway becomes complex. *Nat. Rev. Mol. Cell Biol.* **7**, 678-689.

Bussmann, J., Bos, F. L., Urasaki, A., Kawakami, K., Duckers, H. J. and Schulte-Merker, S. (2010). Arteries provide essential guidance cues for lymphatic endothelial cells in the zebrafish trunk. *Development* **137**, 2653-2657.

Cannavò, E., Khoueiry, P., Garfield, D. A., Geeleher, P., Zichner, T., Gustafson, E. H., Ciglar, L., Korbel, J. O. and Furlong, E. E. M. (2016). Shadow enhancers are pervasive features of developmental regulatory networks. *Curr. Biol.* **26**, 38-51.

Carmeliet, P., Ferreira, V., Breier, G., Pollefeyt, S., Kieckens, L., Gertsenstein, M., Fahrig, M., Vandenhoeck, A., Harpal, K., Eberhardt, C. et al. (1996). Abnormal blood vessel development and lethality in embryos lacking a single VEGF allele. *Nature* **380**, 435-439.

Cermenati, S., Moleri, S., Cimbro, S., Corti, P., Del Giacco, L., Amodeo, R., Dejana, E., Koopman, P., Cotelli, F. and Beltrame, M. (2008). Sox18 and Sox7 play redundant roles in vascular development. *Blood* **111**, 2657-2666.

Chong, D. C., Koo, Y., Xu, K., Fu, S. and Cleaver, O. (2011). Stepwise arteriovenous fate acquisition during mammalian vasculogenesis. *Dev. Dyn.* **240**, 2153-2165.

Corada, M., Orsenigo, F., Morini, M. F., Pitulescu, M. E., Bhat, G., Nyqvist, D., Breviario, F., Conti, V., Briot, A., Iruela-Arispe, M. L. et al. (2013). Sox17 is indispensable for acquisition and maintenance of arterial identity. *Nat. Commun.* **4**, 2609.

Coxam, B., Sabine, A., Bower, N. I., Smith, K. A., Pichol-Thievend, C., Skoczylas, R., Astin, J. W., Frampton, E., Jaquet, M., Crosier, P. S. et al. (2014). Pkd1 regulates lymphatic vascular morphogenesis during development. *Cell Rep.* **7**, 623-633.

Coxam, B., Neyt, C., Grassini, D. R., Le Guen, L., Smith, K. A., Schulte-Merker, S. and Hogan, B. M. (2015). carbamoyl-phosphate synthetase 2, aspartate transcarbamylase, and dihydroorotase (cad) regulates Notch signaling and vascular development in zebrafish. *Dev. Dyn.* **244**, 1-9.

De Val, S. and Black, B. L. (2009). Transcriptional control of endothelial cell development. *Dev. Cell* **16**, 180-195.

De Val, S., Anderson, J. P., Heidt, A. B., Khiem, D., Xu, S.-M. and Black, B. L. (2004). Mef2c is activated directly by Ets transcription factors through an evolutionarily conserved endothelial cell-specific enhancer. *Dev. Biol.* **275**, 424-434.

Duarte, A., Hirashima, M., Benedito, R., Trindade, A., Diniz, P., Bekman, E., Costa, L., Henrique, D. and Rossant, J. (2004). Dosage-sensitive requirement for mouse Dll4 in artery development. *Genes Dev.* **18**, 2474-2478.

Duong, T., Koltowska, K., Pichol-Thievend, C., Le Guen, L., Fontaine, F., Smith, K. A., Truong, V., Skoczylas, R., Stacker, S. A., Achen, M. G. et al. (2014). VEGFD regulates blood vascular development by modulating SOX18 activity. *Blood* **123**, 1102-1112.

Fowles, L. F., Bennetts, J. S., Berkman, J. L., Williams, E., Koopman, P., Teasdale, R. D. and Wicking, C. (2003). Genomic screen for genes involved in mammalian craniofacial development. *Genesis* **35**, 73-87.

François, M., Caprini, A., Hosking, B., Orsenigo, F., Wilhelm, D., Browne, C., Paavonen, K., Karnezis, T., Shayan, R., Downes, M. et al. (2008). Sox18 induces development of the lymphatic vasculature in mice. *Nature* **456**, 643-647.

Francois, M., Koopman, P. and Beltrame, M. (2010). SoxF genes: Key players in the development of the cardio-vascular system. *Int. J. Biochem. Cell Biol.* **42**, 445-448.

Gagnon, J. A., Valen, E., Thyme, S. B., Huang, P., Akhmetova, L. Pauli, A., Montague, T. G., Zimmerman, S., Richter, C. and Schier, A. F. (2014). Efficient mutagenesis by Cas9 protein-mediated oligonucleotide insertion and large-scale assessment of single-guide RNAs. *PLoS ONE* **9**, e98186.

Gale, N. W., Dominguez, M. G., Noguera, I., Pan, L., Hughes, V., Valenzuela, D. M., Murphy, A. J., Adams, N. C., Lin, H. C., Holash, J. et al. (2004). Haploinsufficiency of delta-like 4 ligand results in embryonic lethality due to major defects in arterial and vascular development. *Proc. Natl. Acad. Sci. USA* **101**, 15949-15954.

Geudens, I., Herpers, R., Hermans, K., Segura, I., Ruiz de Almodovar, C., Bussmann, J., De Smet, F., Vandevelde, W., Hogan, B. M., Siekmann, A. et al. (2010). Role of delta-like-4/Notch in the formation and wiring of the lymphatic network in zebrafish. *Arterioscler. Thromb. Vasc. Biol.* **30**, 1695-1702.

Gore, A. V., Monzo, K., Cha, Y. R., Pan, W. and Weinstein, B. M. (2012). Vascular development in the zebrafish. *Cold Spring Harb. Perspect. Med.* **2**, a006684-a006684.

Harvey, S. A., Sealy, I., Kettleborough, R., Fényes, F., White, R., Stemple, D. and Smith, J. C. (2013). Identification of the zebrafish maternal and paternal transcriptomes. *Development* **140**, 2703-2710.

Heintzman, N. D. and Ren, B. (2009). Finding distal regulatory elements in the human genome. *Curr. Opin. Genet. Dev.* **19**, 541-549.

Hermkens, D. M. A., van Impel, A., Urasaki, A., Bussmann, J., Duckers, H. J. and Schulte-Merker, S. (2015). Sox7 controls arterial specification in conjunction with hey2 and efnb2 function. *Development* **142**, 1695-1704.

Herpers, R., van de Kamp, E., Duckers, H. J. and Schulte-Merker, S. (2008). Redundant roles for Sox7 and Sox18 in arteriovenous specification in zebrafish. *Circ. Res.* **102**, 12-15.

Hollenhorst, P. C., McIntosh, L. P. and Graves, B. J. (2011). Genomic and biochemical insights into the specificity of ETS transcription factors. *Annu. Rev. Biochem.* **80**, 437-471.

Hosking, B., François, M., Wilhelm, D., Orsenigo, F., Caprini, A., Svingen, T., Tutt, D., Davidson, T., Browne, C., Dejana, E. et al. (2009). Sox7 and Sox17 are strain-specific modifiers of the lymphangiogenic defects caused by Sox18 dysfunction in mice. *Development* **136**, 2385-2391.

Jahnsen, E. D., Trindade, A., Zaun, H. C., Lehoux, S., Duarte, A. and Jones, E. A. V. (2015). Notch1 is pan-endothelial at the onset of flow and regulated by flow. *PLoS ONE* **10**.

James, K., Hosking, B., Gardner, J., Muscat, G. E. and Koopman, P. (2003). Sox18 mutations in the ragged mouse alleles ragged-like and opossum. *Genesis* **36**, 1-6.

Kent, W. J., Sugnet, C. W., Furey, T. S., Roskin, K. M., Pringle, T. H., Zahler, A. M. and Haussler, D. (2002). The human genome browser at UCSC. *Genome Res.* **12**, 996-1006.

Kim, K., Kim, I.-K., Yang, J. M., Lee, E., Koh, B. I., Song, S., Park, J., Lee, S., Choi, C., Kim, J. W. et al. (2016). SoxF transcription factors are positive feedback regulators of VEGF signaling. *Circ. Res.* **119**, 839-852.

Koltowska, K., Paterson, S., Bower, N. I., Baillie, G. J., Lagendijk, A. K., Astin, J. W., Chen, H., François, M., Crosier, P. S., Taft, R. J. et al. (2015). mafba is a downstream transcriptional effector of Vegfc signaling essential for embryonic lymphangiogenesis in zebrafish. *Genes Dev.* **29**, 1618-1630.

Krebs, L. T., Xue, Y., Norton, C. R., Shutter, J. R., Maguire, M., Sundberg, J. P., Gallahan, D., Closson, V., Kitajewski, J., Callahan, R. et al. (2000). Notch signaling is essential for vascular morphogenesis in mice. *Genes Dev.* **14**, 1343-1352.

Krebs, L. T., Shutter, J. R., Tanigaki, K., Honjo, T., Stark, K. L. and Gridley, T. (2004). Haploinsufficient lethality and formation of arteriovenous malformations in Notch pathway mutants. *Genes Dev.* **18**, 2469-2473.

Kwan, K. M., Fujimoto, E., Grabher, C., Mangum, B. D., Hardy, M. E., Campbell, D. S., Parant, J. M., Yost, H. J., Kanki, J. P. and Chien, C. B. (2007). The Tol2kit: a multisite gateway-based construction kit for Tol2 transposon transgenesis constructs. *Dev. Dyn.* **236**, 3088-3099.

Lanahan, A. A., Hermans, K., Claes, F., Kerley-Hamilton, J. S., Zhuang, Z. W., Giordano, F. J., Carmeliet, P. and Simons, M. (2010). VEGF receptor 2 endocytic trafficking regulates arterial morphogenesis. *Dev. Cell* **18**, 713-724.

Langmead, B. (2010). Aligning short sequencing reads with Bowtie. *Curr. Protoc. Bioinformatics* **11**, 11.7.

Lathen, C., Zhang, Y., Chow, J., Singh, M., Lin, G., Nigam, V., Ashraf, Y. A., Yuan, J. X., Robbins, I. M. and Thistlethwaite, P. A. (2014). ERG-APLNR axis controls pulmonary venule endothelial proliferation in pulmonary Veno-occlusive disease. *Circulation* **130**, 1179-1191.

Lawson, N. D. (2003). phospholipase C gamma-1 is required downstream of vascular endothelial growth factor during arterial development. *Genes Dev.* **17**, 1346-1351.

Lawson, N. D., Scheer, N., Pham, V. N., Kim, C. H., Chitnis, A. B., Campos-Ortega, J. A. and Weinstein, B. M. (2001). Notch signaling is required for arterial-venous differentiation during embryonic vascular development. *Development* **128**, 3675-3683.

Lawson, N. D., Vogel, A. M. and Weinstein, B. M. (2002). sonic hedgehog and vascular endothelial growth factor act upstream of the Notch pathway during arterial endothelial differentiation. *Dev. Cell* **3**, 127-136.

Lee, S.-H., Lee, S., Yang, H., Song, S., Kim, K., Saunders, T. L., Yoon, J. K., Koh, G. Y. and Kim, I. (2014). Notch pathway targets proangiogenic regulator Sox17 to restrict angiogenesis. *Circ. Res.* **115**, 215-226.

Liu, Z.-J., Shirakawa, T., Li, Y., Soma, A., Oka, M., Dotto, G. P., Fairman, R. M., Velazquez, O. C. and Herlyn, M. (2003). Regulation of Notch1 and Dll4 by vascular endothelial growth factor in arterial endothelial cells: implications for modulating arteriogenesis and angiogenesis. *Mol. Cell. Biol.* **23**, 14-25.

Lizama, C. O., Hawkins, J. S., Schmitt, C. E., Bos, F. L., Zape, J. P., Cautivo, K. M., Borges Pinto, H., Rhyner, A. M., Yu, H., Donohoe, M. E. et al. (2015). Repression of arterial genes in hemogenic endothelium is sufficient for haematopoietic fate acquisition. *Nat. Commun.* **6**, 7739.

Matys, V., Kel-Margoulis, O. V., Fricke, E., Liebich, I., Land, S., Barre-Dirrie, A., Reuter, I., Chekmenev, D., Krull, M., Hornischer, K. et al. (2006). TRANSFAC and its module TRANSCompel: transcriptional gene regulation in eukaryotes. *Nucleic Acids Res.* **34**, D108-D110.

Mertin, S., McDowall, S. G. and Harley, V. R. (1999). The DNA-binding specificity of SOX9 and other SOX proteins. *Nucleic Acids Res.* **27**, 1359-1364.

Metzis, V., Courtney, A. D., Kerr, M. C., Ferguson, C., Rondon Galeano, M. C., Parton, R. G., Wainwright, B. J. and Wicking, C. (2013). Patched1 is required in neural crest cells for the prevention of orofacial clefts. *Hum. Mol. Genet.* **22**, 5026-5035.

Mohammed, H., D'Santos, C., Serandour, A. A., Ali, H. R., Brown, G. D., Atkins, A., Rueda, O. M., Holmes, K. A., Theodorou, V., Robinson, J. L. L. et al. (2013). Endogenous purification reveals GREB1 as a key estrogen receptor regulatory factor. *Cell Rep.* **3**, 342-349.

Pendeville, H., Winandy, M., Manfroid, I., Nivelles, O., Motte, P., Pasque, V., Peers, B., Struman, I., Martial, J. A. and Voz, M. L. (2008). Zebrafish Sox7 and Sox18 function together to control arterial-venous identity. *Dev. Biol.* **317**, 405-416.

Pennisi, D., Bowles, J., Nagy, A., Muscat, G. and Koopman, P. (2000a). Mice null for Sox18 are viable and display a mild coat defect. *Mol. Cell. Biol.* **20**, 9331-9336.

Pennisi, D., Gardner, J., Chambers, D., Hosking, B., Peters, J., Muscat, G., Abbott, C. and Koopman, P. (2000b). Mutations in Sox18 underlie cardiovascular and hair follicle defects in ragged mice. *Nat. Genet.* **24**, 434-437.

Phng, L.-K. and Gerhardt, H. (2009). Angiogenesis: a team effort coordinated by notch. *Dev. Cell* **16**, 196-208.

Picelli, S., Faridani, O. R., Björklund, A. K., Winberg, G., Sagasser, S. and Sandberg, R. (2014). Full-length RNA-seq from single cells using Smart-seq2. *Nat. Protoc.* **9**, 171-181.

Quillien, A., Moore, J. C., Shin, M., Siekmann, A. F., Smith, T., Pan, L., Moens, C. B., Parsons, M. J. and Lawson, N. D. (2014). Distinct Notch signaling outputs pattern the developing arterial system. *Development* **141**, 1544-1552.

Robinson, A. S., Materna, S. C., Barnes, R. M., De Val, S., Xu, S.-M. and Black, B. L. (2014). An arterial-specific enhancer of the human endothelin converting enzyme 1 (ECE1) gene is synergistically activated by Sox17, FoxC2, and Etv2. *Dev. Biol.* **395**, 379-389.

Roca, C. and Adams, R. H. (2007). Regulation of vascular morphogenesis by Notch signaling. *Genes Dev.* **21**, 2511-2524.

Sabo, P. J., Hawrylycz, M., Wallace, J. C., Humbert, R., Yu, M., Shafer, A., Kawamoto, J., Hall, R., Mack, J., Dorschner, M. O. et al. (2004). Discovery of functional noncoding elements by digital analysis of chromatin structure. *Proc. Natl. Acad. Sci. USA* **101**, 16837-16842.

Sacilotto, N., Monteiro, R., Fritzsche, M., Becker, P. W., Sanchez-del-Campo, L., Liu, K., Pinheiro, P., Ratnayaka, I., Davies, B., Goding, C. R. et al. (2013). Analysis of Dll4 regulation reveals a combinatorial role for Sox and Notch in arterial development. *Proc. Natl. Acad. Sci. USA* **110**, 11893-11898.

Sakamoto, Y., Hara, K., Kanai-Azuma, M., Matsui, T., Miura, Y., Tsunekawa, N., Kurohmaru, M., Saijoh, Y., Koopman, P. and Kanai, Y. (2007). Redundant roles of Sox17 and Sox18 in early cardiovascular development of mouse embryos. *Biochem. Biophys. Res. Commun.* **360**, 539-544.

Siekmann, A. F. and Lawson, N. D. (2007). Notch signalling limits angiogenic cell behaviour in developing zebrafish arteries. *Nature* **445**, 781-784.

Visconti, R. P., Richardson, C. D. and Sato, T. N. (2002). Orchestration of angiogenesis and arteriovenous contribution by angiopoietins and vascular endothelial growth factor (VEGF). *Proc. Natl. Acad. Sci. USA* **99**, 8219-8224.

Wong, E. S., Thybert, D., Schmitt, B. M., Stefflova, K., Odom, D. T. and Flicek, P. (2015). Decoupling of evolutionary changes in transcription factor binding and gene expression in mammals. *Genome Res.* **25**, 167-178.

Wu, J., Iwata, F., Grass, J. A., Osborne, C. S., Elnitski, L., Fraser, P., Ohneda, O., Yamamoto, M. and Bresnick, E. H. (2005). Molecular determinants of NOTCH4 transcription in vascular endothelium. *Mol. Cell. Biol.* **25**, 1458-1474.

Wythe, J. D., Dang, L. T. H., Devine, W. P., Boudreau, E., Artap, S. T., He, D., Schachterle, W., Stainier, D. Y. R., Oettgen, P., Black, B. L. et al. (2013). ETS factors regulate Vegf-dependent arterial specification. *Dev. Cell* **26**, 45-58.

Zhou, Y., Williams, J., Smallwood, P. M. and Nathans, J. (2015). Sox7, Sox17, and Sox18 cooperatively regulate vascular development in the mouse retina. *PLoS ONE* **10**, e0143650.

Zhou, P., Gu, F., Zhang, L., Akerberg, B. N., Ma, Q., Li, K., He, A., Lin, Z., Stevens, S. M., Zhou, B. et al. (2017). Mapping cell type-specific transcriptional enhancers using high affinity, lineage-specific Ep300 bioChIP-seq. *eLife* **6**, e22039.